University of California at San Diego
Scripps Institution of Oceanography
La Jolla, California 92093

MAGNETIC ANOMALIES OF THE OCEAN

Peter D. Young

and

Charles S. Cox

Scripps Institution of Oceanography
University of California at San Diego
La Jolla, California 92093

Contract N0014-82-K-0999

This research was sponsored by the Earth Sciences branch of the Office of Naval Research.

October 1983

Table of Contents

There are two categories of magnetic anomalies associated with the ocean. Primary anomalies are induced directly by interaction of ocean flow with the geomagnetic field, or induced by ionospheric fluctuations, or are the expression of the remnant magnetization of the ocean floor rocks. Secondary anomalies are created by interaction of electric current flow in the ocean, with irregularities of the electrical conductivity distribution within the ocean, or with irregularities of the boundaries of the ocean (seafloor ridges and troughs or ocean surface waves). Our focus in this report is on secondary anomalies, although some attention is paid to primary effects for completeness.

Large scale and relatively intense electric currents in the ocean are mainly induced by ionospheric fluctuations. The primary magnetic fields and induced electric fields in the ocean both have "red" continuum spectra in the frequency range from one cycle per day upward, which is caused by the normal unrest of the ionosphere and by bay disturbances and the principal part of magnetic storms. In addition, there is a line spectrum consisting of harmonics of 1 cpd: the solar daily variation. Typical amplitudes of electric fields induced in the ocean are of order 1 $\mu V/m$, although larger values can be found in a magnetic storm.

The spatial scale of the anomalous conductivity structures within the ocean which we shall treat are relatively small; for ocean surface waves the wavelength is typically a few hundred meters, and a comparable scale is appropriate for ocean structures such as internal waves and frontal systems. Ocean bottom hills, ridges, and troughs are typically of a few to a few tens of kilometers in size. As a consequence of the slow variation of the primary electric field in the ocean and the small spatial scale of the conductivity anomalies, the magnetic Reynold's number, $R=\omega\mu\sigma LD$, applicable to the anomalous secondary fields, is small. For example, if ω, the oscillation frequency, is $10^{-4} sec^{-1}$, the conductivity of seawater σ is 3 S/m, and the horizontal and vertical scales L and D are 40 km and 4 km respectively, then $R=0.06$. From this rough calculation it is apparent that time variations of the primary fields do not lead to appreciable self-inductance effects in the secondary fields. In the subsequent calculations we have neglected the self-inductance of secondary fields entirely, thus treating them as though they were caused by a perfectly static primary field. This approximation, valid for these secondary fields, is, of course, entirely inappropriate for the treatment of the primary fields, because their large horizontal scale ordinarily leads to magnetic Reynold's numbers of order unity or greater.

Chapter I

Magnetic Anomalies Induced by Surface Waves

1. Introduction

Here we consider magnetic anomalies associated with waves of small amplitude moving on the surface of a deep ocean. There are two principal effects in this category; that due to interaction of the surface waves with a uniform electrical current flow within the ocean (such as might be induced by electrical activity in the ionosphere), and that due to wave-associated seawater movement through the Earth's magnetic field. Section 2 of this chapter deals with the magnetic field generated by the uniform current flow alone, and section 3 derives the perturbing magnetic effects of the interaction of a surface wave with this flow. Section 4 is a note in passing that the mathematics in sections 2 and 3 is also applicable to the calculation of magnetic anomalies produced by a special class of bottom features. Section 5 discusses the interaction of the water motions that accompany surface waves with the Earth's magnetic field, summarizing previous work by others. Section 6 covers the subject of the gradients of the magnetic field vector components generated by the mechanisms explored in sections 2, 3, and 5. Finally, section 7 puts some numbers into the field expressions derived in sections 2, 3, and 5 in order to give some idea of the relative magnitudes of the different magnetic effects under various circumstances. The treatment is as general as is consistent with the small amplitude wave, deep uniform ocean model, and should lend itself to expansion to consider the effects of ocean bottom features of small aspect, should this be desired.

2. Uniform horizontal electric field in a flat-surfaced ocean

One of the consequences of magnetic field fluctuations within the volume of the ocean, such as may result from the solar daily variation of the Earth's magnetic field or from disturbances in the upper atmosphere, is the generation of an electric potential gradient within the ocean and the corresponding induction of an electrical current flow; for example, the solar daily variation typically generates a slowly oscillating electric field throughout the deep sea with an amplitude that is typically a large fraction of a microvolt per meter, and magnetic storms in the upper atmosphere can give rise to electric fields several times larger. Magnetic fluctuations of this sort are for the most part of a sufficiently low frequency that the magnetic induction number $\omega\mu\sigma l^2$ (where ω is the frequency of fluctuation, μ and σ are the magnetic permeability and electrical conductivity respectively of the material under consideration, in this case seawater, and l is the length scale of the induction effect in question, in this case the depth of the ocean) is a great deal less than unity, indicating that the magnetic fluctuations penetrate through the ocean virtually without resistance; as a result of this, in a flat-bottomed ocean the induced electric field will be essentially uniform with depth. Also, and, in this context, perhaps more to the point, the time scale of these magnetic field fluctuations is typically sufficiently large (with periods on the order of an hour and up) compared to that of water wave effects on the ocean surface that the electric fields induced by them can, for our present purposes, be considered static to excellent approximation. Accordingly, we assume a horizontal, spatially uniform, temporally static electric field $E_0\hat{x}$ within the volume of the ocean, and an induced electrical current density distribution J such that

$$J = \sigma(z)E_0\hat{x} \quad , \tag{2.1}$$

where $\sigma(z)$ is the electrical conductivity distribution of the ocean, assumed here to be a function of depth only. In the following work dealing with the magnetic effects resulting from this induced electrical current distribution, deviation of the current density from J as given by (2.1) will be considered as due to the perturbing effects of variations of the upper and/or lower boundaries of the ocean, and for a flat-surfaced, flat-bottomed ocean should be completely absent.

We consider first the magnetic field within and above a flat-surfaced, flat-bottomed ocean of depth D resulting from the induced electrical current density distribution J as given by (2.1). If this current distribution is viewed as the limit of a large number of parallel fine threads of electrical current, then one sees that the resultant magnetic field can have no component in the $\hat{x}$ direction, and consideration of the symmetry of the problem in the $\hat{y}$ direction shows that the field can have no $\hat{z}$ component, where $\hat{z}$ points vertically upward. This field can be deduced by use of the integral form of Ampere's law,

$$\int_C \vec{B}\cdot\vec{dl} = \mu_0 \int_S \vec{J}\cdot\hat{n}\, ds \quad , \tag{2.2}$$

together with some symmetry arguments, and the total magnetic field may then be inferred by adding this component to the inducing field, which can be derived by other means.

We start with a rectangular path of integration within a plane perpendicular to $\hat{x}$, its top and bottom legs parallel to $\hat{y}$ and above the surface and below the bottom respectively. From the above arguments we have that the induced magnetic induction vector $\vec{B_I}$ is everywhere parallel to $\hat{y}$, and from considerations of symmetry we have that the fields above the ocean surface and beneath the bottom should have the same magnitude but opposite directions. Since the vertical legs of the rectangle contribute nothing to the integral, we therefore have for the magnetic induction everywhere beneath the ocean floor

$$\vec{B_I} = \frac{\mu_0 E_0}{2}\,\hat{y} \int_0^D \sigma(z)\, dz \quad , \tag{2.3}$$

with the induced magnetic induction everywhere above the ocean surface being just the negative of this. We now place the lower leg of the rectangle exactly at the ocean floor, and move the upper leg down below the surface to a depth a distance z_0 above the bottom; given (2.3) for the magnetic induction along the lower leg, we have from (2.2) the magnetic induction along the upper leg

$$\vec{B_I}(z_0) = -\frac{\mu_0 E_0}{2}\,\hat{y} \left[\int_0^{z_0} \sigma(z)\, dz - \int_{z_0}^{D} \sigma(z)\, dz \right] \quad . \tag{2.4}$$

If the electrical conductivity of the seawater is constant over the depth of the ocean with a value σ_0, then this reduces to

$$\vec{B_I}(z) = -\tfrac{1}{2}\,\mu_0 J_0 D\,\hat{y} \quad , \quad z > D \tag{2.5}$$

$$\vec{B_I}(z) = +\tfrac{1}{2}\,\mu_0 J_0 (D-2z_0)\,\hat{y} \quad , \quad 0 < z < D \tag{2.6}$$

$$\vec{B_I}(z) = +\tfrac{1}{2}\,\mu_0 J_0 D\,\hat{y} \quad , \quad z < 0 \tag{2.7}$$

where

$$J_0 = \sigma_0 E_0 \tag{2.8}$$

and z=0 is at the ocean floor. Use of the differential form of Ampere's law

$$\nabla \times \vec{B} = \mu_0 \vec{J} \tag{2.9}$$

(neglecting displacement currents, a valid approximation in this context) confirms this work.

For the total magnetic induction $\vec{B_T}$ at the ocean floor we have

$$\vec{B_T} = \frac{\mu_0 E_0}{Z_E} \hat{y} \quad , \tag{2.10}$$

where Z_E is the E mode impedance of the Earth, a complex function of frequency that is dependent in ideal circumstances only on the distribution of electrical conductivity below the ocean floor (see for example Cox et al., 1970); Z_E is, technically, the ratio at the Earth's surface between the horizontal component of an oscillating electric field and the horizontal transverse component of the magnetic field that appears in response to it, and on grounds of symmetry we have in this case that this total magnetic induction $\vec{B_T}$ must be perpendicular to the induced electric field $E_0\hat{x}$ (as is usually the case in general), yielding the field direction indicated by (2.11) (arguments of scaling and symmetry suggest that if $\vec{B_T}$ has a vertical component then it must be much smaller in magnitude than the horizontal component). At a frequency of one cycle per hour, in a typical measurement Z_E might have a magnitude of 0.00025 Ω and a phase of about 45°. $\vec{B_T}$ is the sum of $\vec{B_I}$ and $\vec{B_F}$, the slowly fluctuating magnetic induction field that originally induced $\vec{B_I}$, and by the previous argument relating to the magnetic induction number we have that $\vec{B_F}$ must be essentially uniform in space throughout the ocean and for some distance above the ocean surface; accordingly, we get $\vec{B_T}$ over this altitude range simply by adding to $\vec{B_I}$ whatever is necessary to bring its value at the ocean floor up to that given by (2.10). Thus, $\vec{B_F}$ comes to

$$\vec{B_F} = \mu_0 E_0 \hat{y} \left\{ \frac{1}{Z_E} - \tfrac{1}{2} \int_0^D \sigma(z)\, dz \right\} \quad , \tag{2.11}$$

and the expression for $\vec{B_T}$ is

$$\vec{B_T}(z_0) = \mu_0 E_0 \hat{y} \left\{ \frac{1}{Z_E} - \Sigma(z_0) \right\} \quad , \tag{2.12}$$

where

$$\Sigma(z_0) = \int_0^{z_0} \sigma(z)\, dz \quad , \quad 0 \leqslant z_0 \leqslant D \tag{2.13}$$

and

$$\Sigma(z_0) = \Sigma(D) \quad , \quad z_0 > D \quad . \tag{2.14}$$

For an ocean 4 kilometers deep, for an inducing field oscillating at one cycle per hour, $\Sigma(D)$ is

smaller than $1/Z_E$ by a factor of about 3.

3. The perturbing effect of shallow waves at the surface

We now suppose the surface to be described by the expression

$$\zeta = a \exp(i\vec{k}_H \cdot \vec{x})\, e^{-i\omega t} \quad , \tag{3.1}$$

where ζ is the height of the surface above its mean level, a is the wave amplitude, $\vec{k}_H$ is the horizontal component of the wavevector, which for convenience we will express in the form

$$\vec{k}_H = k\ (\cos\theta, \sin\theta, 0) \quad , \tag{3.2}$$

where k is real and positive, $\vec{x}$ is the position vector, $\vec{x} = (x, y, z)$, and ω is the angular frequency of the wave. In practical applications the surface is considered to be given by either the real or imaginary part of expression (3.1), whichever is more convenient, and the resultant magnetic field is determined by taking the same part of the complex field expression derived from (3.1).

In order to meet the boundary condition that $\vec{J}$ at the surface should have no component normal to the surface, it is necessary to add a perturbation term to the uniform current distribution initially assumed to exist beneath the surface. Furthermore, since the current distribution within the ocean is ultimately induced by whatever electric field is present,

$$\vec{J} = \sigma \vec{E} \quad , \tag{3.3}$$

where $\vec{E}$ is the electric field and σ is the electrical conductivity of seawater (which may be considered for our purposes to be a constant, as the depth range within which the surface waves exert a noticeable electrical influence is too thin to exhibit a significant conductivity variation), $\vec{J}$ may be viewed as the gradient of a scalar function;

$$\vec{J} = \nabla\phi \quad . \tag{3.4}$$

If we make the reasonable assumption that separation of electrical charge within the body of the ocean is negligible for all ω of interest, we also have

$$\nabla \cdot \vec{J} = 0 \quad , \tag{3.5}$$

which with (3.4) implies

$$\nabla^2\phi = 0 \quad . \tag{3.6}$$

The only solutions to (3.6) that can conveniently be reconciled with (3.1) have the form

$$\phi = \{ A \exp(i\vec{k}_1 \cdot \vec{x}) + B \exp(i\vec{k}_2 \cdot \vec{x}) \} e^{-i\omega t} \quad , \tag{3.7}$$

where

$$\vec{k}_1 = k \ (\cos\theta, \sin\theta, -i) \tag{3.8}$$

and

$$\vec{k}_2 = k \ (\cos\theta, \sin\theta, i) \quad ; \tag{3.9}$$

the first term of (3.7) damps exponentially downward, and the second term grows exponentially downward. For an ocean of finite and uniform depth the coefficients A and B can be related by use of the boundary condition at the ocean floor that the electrical current flow at this interface has no vertical component, but as long as the order of magnitude of the wavelength of the surface wave is less than that of the depth of the ocean, which for our purposes will generally be the case, the second term of (3.7) is negligible compared to the first; accordingly, to simplify the calculations we will henceforth assume that B=0 and take $\vec{k}=\vec{k}_1$, giving a current distribution beneath the surface of

$$\vec{J} = J_0 \hat{x} + \vec{k} \, iA \exp(i\vec{k} \cdot \vec{x}) \, e^{-i\omega t} \quad , \tag{3.10}$$

$$\vec{k} = k \ (\cos\theta, \sin\theta, -i) \quad . \tag{3.11}$$

The value of A may be determined from the boundary condition at the surface that

$$\vec{r} \cdot \vec{J} = 0 \quad at \ z=\zeta \quad , \tag{3.12}$$

where $\vec{r}$ is a vector normal to the surface; such a vector is

$$\vec{r} = \left(-\frac{\partial \zeta}{\partial x}, -\frac{\partial \zeta}{\partial y}, 1 \right) \quad . \tag{3.13}$$

If (3.10) is substituted into (3.12) and terms of second and higher orders in (ka) are discarded, one gets

$$A = iaJ_0 \cos\theta \tag{3.14}$$

under the condition that

$$|ka| << 1 \quad . \tag{3.15}$$

This gives from (3.10)

$$\vec{J} = J_0 \{ \hat{x} - a \cos\theta \exp(i\vec{k} \cdot \vec{x}) \, e^{-i\omega t} \, \vec{k} \} \quad . \tag{3.16}$$

In general, the magnetic field $\vec{B}(\vec{x}_0)$ due to an electrical current distribution within a volume V is given by

$$\vec{B}(\vec{x}_0) = \frac{\mu_0}{4\pi} \int_V \frac{\vec{J}(\vec{x}) \times (\vec{x}_0 - \vec{x})}{|\vec{x}_0 - \vec{x}|^3} \, dV \tag{3.17}$$

(Reitz and Milford, 1967, p.154); for this problem this integral takes the form

$$\vec{B}(\vec{x}_0) = \frac{\mu_0}{4\pi} \int_{-\infty}^{\infty} dx \int_{-\infty}^{\infty} dy \int_{-D}^{\zeta} dz \, \frac{\vec{J}(\vec{x}) \times (\vec{x}_0 - \vec{x})}{|\vec{x}_0 - \vec{x}|^3} \quad , \tag{3.18}$$

where $\vec{J}(\vec{x})$ is as given by (3.16). It is convenient for purposes of calculation to express $\vec{B}$ as the sum of $\vec{B}_S$ and $\vec{B}_V$,

$$\vec{B}(\vec{x}_0) = \vec{B}_S(\vec{x}_0) + \vec{B}_V(\vec{x}_0) \quad , \tag{3.19}$$

where $\vec{B}_V$ is the field due to the part of the current distribution that is between z=-D and z=0 and $\vec{B}_S$ is the field due to the part of the current distribution between z=0 and $z=\zeta$, and to break $\vec{B}_V$ down into $\vec{B}_{VU}$ and $\vec{B}_{VP}$,

$$\vec{B}_V(\vec{x}_0) = \vec{B}_{VU}(\vec{x}_0) + \vec{B}_{VP}(\vec{x}_0) \quad , \tag{3.20}$$

where $\vec{B}_{VU}$ is due to the uniform component of the current distribution, $J_0\hat{x}$, and $\vec{B}_{VP}$ is due to the perturbation thereon which constitutes remainder of the distribution. $\vec{B}_{VU}$ has already been determined in section 2.

$\vec{B}_{VP}$ is given by

$$\vec{B}_{VP}(\vec{x}_0) = \frac{C}{4\pi} \int_{-\infty}^{\infty} dx \int_{-\infty}^{\infty} dy \int_{-\infty}^{0} dz \tag{3.21}$$

$$\times \frac{(\cos\theta, \sin\theta, -i) \times (\vec{x} - \vec{x}_0)}{|\vec{x} - \vec{x}_0|^3} \exp(i\vec{k} \cdot \vec{x})$$

$$C = \mu_0 J_0 a k \cos\theta \, e^{-i\omega t} \quad , \tag{3.22}$$

where we have simplified the integration by extending the lower limit of integration from z=-D down to $z=-\infty$; provided that the wavelength of the surface wave is somewhat less than the depth of the ocean, as has already been assumed, the error introduced by this extension should be negligible. Making the substitutions

$$u = (x - x_0)\cos\theta + (y - y_0)\sin\theta \tag{3.23}$$

$$v = (y - y_0)\cos\theta - (x - x_0)\sin\theta \tag{3.24}$$

$$w = -(z-z_0) \tag{3.25}$$

$$u_0 = x_0 \cos\theta + y_0 \sin\theta \tag{3.26}$$

$$\hat{u} = \hat{x} \cos\theta + \hat{y} \sin\theta \tag{3.27}$$

$$\hat{v} = \hat{y} \cos\theta - \hat{x} \sin\theta \tag{3.28}$$

turns (3.21) into

$$\vec{B}_{VP}(\vec{x}_0) = \frac{C\, e^{ikw_0}\, e^{kz_0}}{4\pi} \int_{-\infty}^{\infty} du \int_{-\infty}^{\infty} dv \int_{z_0}^{\infty} dw \tag{3.29}$$

$$\times \frac{(i\hat{u}+\hat{z})\,v + \hat{v}\,(w-iu)}{(u^2+v^2+w^2)^{3/2}}\, e^{iku}\, e^{-kw} \quad ,$$

where z_0 is the altitude of the observation point relative to the ocean surface. The term in $(i\hat{u}+\hat{z})$ does not contribute to the integral, as it gives an integrand antisymmetric in v. Further reduction of the integral is aided by the identity

$$\int_{-\infty}^{\infty} \frac{dx}{(x^2+c)^{3/2}} = \frac{2}{c} \tag{3.30}$$

(Grobner, sec. 213, eq. 1, p. 34); use of this identity in the integration over v gives from (3.29)

$$\vec{B}_{VP}(\vec{x}_0) = \frac{C\, e^{ikw_0}\, e^{kz_0}\, \hat{v}}{2\pi} \int_{-\infty}^{\infty} du \int_{z_0}^{\infty} dw\, \frac{e^{iku}\, e^{kw}}{w+iu} \quad , \tag{3.31}$$

which yields easily to contour integration in u (over the upper half plane) followed by standard integration in w, to give

$$\vec{B}_{VP}(\vec{x}_0) = \tfrac{1}{2}\,\mu_0\, J_0\, a\, \cos\theta\, e^{ikw_0}\, e^{-|kz_0|}\, e^{-i\omega t} \tag{3.32}$$

$$\times\, (-\sin\theta,\, \cos\theta,\, 0) \quad .$$

In the computation of $\vec{B}_S$ the perturbation part of the current distribution contributes only in second order in (ka), and thus can be ignored, leaving only the uniform component of the current distribution to be considered. The appropriate integral expression is then

$$\vec{B}_S(\vec{x}_0) = \frac{\mu_0\, J_0}{4\pi} \int_{-\infty}^{\infty} dx \int_{-\infty}^{\infty} dy \int_{0}^{\zeta} dz\, \frac{\hat{x} \times (\vec{x_0}-\vec{x'})}{|\vec{x}_0-\vec{x}|^3} \quad , \tag{3.33}$$

or

$$\vec{B}_S(\vec{x}_0) = \frac{\mu_0 J_0}{4\pi} \int_{-\infty}^{\infty} dx \int_{-\infty}^{\infty} dy \int_0 dz \qquad (3.34)$$

$$\times \frac{\{0, (z-z_0), -(y-y_0)\}}{|\vec{x}-\vec{x}_0|^3} \ .$$

The small range of integration of z in this integral suggests a Taylor expansion of the integrand over this variable; if this is done, only the first term (the constant term) contributes to $\vec{B}_S$ in first order in ka. Doing this, we get

$$\vec{B}_S(\vec{x}_0) = -\frac{\mu_0 J_0}{4\pi} \int_{-\infty}^{\infty} dx \int_{-\infty}^{\infty} dy \qquad (3.35)$$

$$\times \frac{\{0, z_0, (y-y_0)\}}{\{(x-x_0)^2+(y-y_0)^2+z_0^2\}^{3/2}} \zeta(x,y) \ .$$

Using the expression (3.1) for ζ and making the variable changes (3.23), (3.24), and (3.26) gives from this

$$\vec{B}_S(\vec{x}_0) = -\frac{\mu_0 J_0 a\, e^{ikau_0} e^{-i\omega t}}{4\pi} \int_{-\infty}^{\infty} du \int_{-\infty}^{\infty} dv \qquad (3.36)$$

$$\times \frac{(0, z_0, u\sin\theta + v\cos\theta)}{(u^2+v^2+z_0^2)^{3/2}} e^{ikau} \ ,$$

from which the integration over v gives

$$\vec{B}_S(\vec{x}_0) = -\frac{\mu_0 J_0 a\, e^{ikau_0} e^{-i\omega t}}{2\pi} \int_{-\infty}^{\infty} du \frac{(0, z_0, u\sin\theta)\, e^{ikau}}{(u+iz_0)(u-iz_0)} \ , \qquad (3.37)$$

which yields to contour integration in u, closing the contour in the upper half plane, to give

$$\vec{B}_S(\vec{x}_0) = -\tfrac{1}{2}\mu_0 J_0 a\, e^{ikau_0} e^{-|kz_0|} e^{-i\omega t} \vec{\epsilon}(z_0) \qquad (3.38)$$

$$\vec{\epsilon}(z_0) = \begin{cases} (0, 1, i\sin\theta) & , \ z_0 > 0 \\ (0, -1, i\sin\theta) & , \ z_0 < 0 \end{cases} \ . \qquad (3.39)$$

Combining this with (3.31) gives for $\vec{B}_W$, the field due to the perturbing effects of the surface wave,

$$\vec{B}_W(\vec{x}_0) = -\tfrac{1}{2}\mu_0 J_0 a\, e^{ikau_0} e^{-|kz_0|} e^{-i\omega t} \vec{\epsilon}(z_0) \qquad (3.40)$$

$$\vec{e}(z_0) = \begin{cases} \sin\theta\ (\cos\theta, \sin\theta, i) & , z_0 > 0 \\ \sin\theta\ (\cos\theta, \sin\theta, i) - (0, 2, 0) & , z_0 < 0 \end{cases} , \tag{3.41}$$

to which the field computed in section 2 for a uniform current distribution within a flat-surfaced ocean must be added to give the complete magnetic field to first order in (ka). As a check, (3.40) and (3.41) have been verified by use of the curl expression (2.5). Note, as a special case, that when the wave crests are perpendicular to the $\hat{x}$ direction there is no wave-induced contribution to the field above the surface. This is reasonable on physical grounds, as in this case the total vertically integrated horizontal electric current flow within the ocean is unchanged from the flat surface condition and unchanging with position everywhere in the ocean; therefore, by Ampere's law, the difference ΔB between the magnitudes of the horizontal component of the magnetic field above the ocean surface and beneath the ocean floor is unchanged from the flat ocean case, and considerations of symmetry rule out a vertical field component for this geometry. By contrast, when the wave crests are parallel to $\hat{x}$ there is more total electrical current flow through the water beneath a crest than beneath an adjacent trough, and hence ΔB is variable from place to place.

4. Application to fields induced by bottom topography

The work in the previous section can be applied, with minor modifications, to the calculation of magnetic anomalies produced by certain types of bottom features. Any reasonably smooth bottom feature can be described by a series of terms of the form of (3.1) with ω set to zero, and the problem is then reduced to that of the previous section turned upside-down. The usefulness of this approach is limited in that the lateral dimension of the feature to be investigated must be somewhat greater than its vertical dimension in order to meet the small-scale approximation (3.15) used in developing the mathematics. This application is discussed in detail in section 6 of chapter 2.

In the event that the lateral dimension of the feature is on the order of the depth of the ocean, both terms of the general solution (3.7) for the electrical current potential, that which increases exponentially with depth and that which decreases exponentially with depth, must be used, and the subsequent steps of the derivation altered to suit. Since the vertical scale of the bottom feature will generally be much greater than the amplitudes of whatever waves there are on the ocean surface, it is a reasonable simplifying assumption in this development to consider the ocean surface to be completely flat.

5. Surface waves moving through the Earth's magnetic field

Surface waves will be accompanied by motion of the seawater beneath the surface, and the movement of charge-carrying fluid through the Earth's magnetic field will result in an induced electrical current distribution; this current distribution will in turn give rise to a magnetic field modifying the Earth's field. This subject has been covered by Crews and Futterman (1962), Warburton and Caminiti (1964), and Weaver (1965), but for the sake of completeness an abbreviated derivation of the effect is given here in the mathematical framework developed in sections 2 and 3 of this chapter.

The current distribution induced by the water movement is given by

$$\vec{J} = \sigma\, \vec{v}\times\vec{F} + \vec{J}_C \quad , \tag{5.1}$$

where σ is the electrical conductivity of the water, taken here to be constant, $\vec{v}$ is the water velocity distribution, and $\vec{F}$ is the Earth's magnetic field, which may be taken to be locally uniform. $\vec{J}_C$ is a correction term whose purpose is to insure that the boundary condition is met that there be no electrical current flow through the surface. If we assume the water flow to be irrotational (for a discussion of the validity of this assumption see Lamb, 1945, sec. 33, pp. 35-37), then the condition

$$\nabla\cdot\vec{J} = 0 \tag{5.2}$$

is automatically satisfied provided that the same condition holds for $\vec{J}_C$;

$$\begin{aligned}\nabla\cdot\vec{J} &= \sigma\, \nabla\cdot(\vec{v}\times\vec{F}) + \nabla\cdot\vec{J}_C \\ &= \sigma\, \{\vec{F}\cdot(\nabla\times\vec{v}) - \vec{v}\cdot(\nabla\times\vec{F})\} + \nabla\cdot\vec{J}_C \\ &= 0 \quad .\end{aligned} \tag{5.3}$$

Another consequence of the assumption of irrotational water flow is that the velocity field may be viewed as the gradient of a scalar function, and if we also suppose that the seawater is incompressible, which is safe enough, we have

$$\nabla\cdot\vec{v} = 0 \quad . \tag{5.4}$$

If ϕ is the scalar function, then

$$\vec{v} = \nabla\phi \tag{5.5}$$

$$\nabla^2\phi = 0 \quad . \tag{5.6}$$

The solution of (5.6) that most conveniently fits with the surface equation (3.1) has the form

$$\phi(\vec{x}) = A \exp(i\vec{k}\cdot\vec{x})\, e^{-i\omega t} \quad , \tag{5.7}$$

where $\vec{k}$ is as given in (3.11), and if we make the constraint that

$$\frac{\partial \zeta}{\partial t} = v_z = \frac{\partial \phi}{\partial z} \quad at\ z=\zeta \quad , \tag{5.8}$$

an approximation that is correct to first order in (ka), we find that

$$A = -i \left[\frac{\omega}{k}\right] a \tag{5.9}$$

$$\vec{v} = (\cos\theta, \sin\theta, -i)\, \omega\, a\, \exp(i\vec{k}\cdot\vec{x})\, e^{-i\omega t} \quad . \tag{5.10}$$

$\vec{J}$ is then given by

$$\vec{J} = \sigma\, \omega\, a\, \exp(i\vec{k}\cdot\vec{x})\, e^{-i\omega t}\, (\cos\theta, \sin\theta, -i) \times \vec{F} \tag{5.11}$$

$$+ \vec{J}_C \quad .$$

$\vec{J}_C$ will have zero divergence as required if it is proportional to $\vec{k}$, and the boundary condition that there be no electrical current flow through the surface, given by (3.12), is satisfied to first order in (ka) if $J_z=0$; the result is

$$\vec{J}_C = -i\, (\cos\theta, \sin\theta, -i)\, \sigma\, \omega\, a\, [(\cos\theta, \sin\theta, -i) \times \vec{F}]_z \tag{5.12}$$

$$\times \exp(i\vec{k}\cdot\vec{x})\, e^{-i\omega t}$$

$$\vec{J} = \sigma\, \omega\, a\, \chi\, (\sin\theta, -\cos\theta, 0)\, \exp(i\vec{k}\cdot\vec{x})\, e^{-i\omega t} \tag{5.13}$$

$$\chi = i\, (\cos\theta, \sin\theta, -i)\cdot\vec{F} \quad . \tag{5.14}$$

The magnetic field arising from this current distribution may be found by inserting (5.13) into (3.18). As in section 3, we find it convenient to divide the integral into an integral over the volume below z=0 and an integral covering the complementary region between z=0 and the surface at $z=\zeta$; upon doing this, we find by inspection that the second integral contributes nothing below the second order in (ka) to the magnetic field, leaving only the first integral to evaluate. Making the substitutions (3.23) through (3.26) and simplifying the integration by assuming infinite depth for the ocean as in section 3 gives the integral

$$\vec{B}(\vec{x}_0) = -\frac{C}{4\pi} \int_{-\infty}^{\infty} du \int_{-\infty}^{\infty} dv \int_{z_0}^{\infty} dw \tag{5.15}$$

$$\times \frac{(w\cos\theta,\ w\sin\theta,\ u)}{(u^2+v^2+w^2)^{3/2}}\, e^{iku}\, e^{-kw}$$

$$C = \mu_0 \sigma \omega a \chi e^{ikx_0} e^{kz_0} e^{-i\omega t} \quad . \tag{5.16}$$

Integration over v gives from this

$$\vec{B}(\vec{x}_0) = -\frac{C}{2\pi} \int_{-\infty}^{\infty} du \int_{z_0}^{\infty} dw \, \frac{(w\cos\theta,\, w\sin\theta,\, u)}{u^2+v^2} \, e^{ikx_0} \, e^{-kw} \quad , \tag{5.17}$$

from which contour integration in u (closing the contour in the upper half plane) followed by integration over w gives

$$\vec{B}(\vec{x}_0) = -\tfrac{1}{4} \mu_0 \sigma a \chi e^{ikx_0} e^{-|kz_0|} e^{-i\omega t} \vec{e}(z_0) \tag{5.18}$$

$$\vec{e}(z_0) = \begin{cases} \left(\frac{\omega}{k}\right)(\cos\theta, \sin\theta, i) & , z_0 > 0 \\ \left(\frac{\omega}{k}\right)(\cos\theta, \sin\theta, i) + 2\omega z_0 (\cos\theta, \sin\theta, -i) & , z_0 < 0 \end{cases} . \tag{5.19}$$

This has been verified with the curl expression (2.5).

6. Gradients of the field components

Above the surface, the field derived in section 2 for a uniform electric current flow, given by (2.2) through (2.4), is completely uniform itself, and therefore has a zero gradient. Below water, though, the field magnitude decreases linearly with increasing depth; the gradient of the y-component of the field, the only nonzero component, is given by

$$\nabla B_y = -\mu_0 J_0 \hat{z} \quad . \tag{6.1}$$

The calculation of the tensor gradients of the magnetic field derived in section 3, and given by (3.37) and (3.38), is made easy by the fact that all of the field components have the same spatial dependence,

$$f(\vec{x}) = exp(i\vec{k}\cdot\vec{x}) \quad , \tag{6.2}$$

where $\vec{k}$ is given by (3.8) where $z<0$ and by (3.9) where $z>0$; the gradient of this expression is given by

$$\nabla f(\vec{x}) = i\,\vec{k}\,f(\vec{x}) \quad , \tag{6.3}$$

where $\vec{k}$ is defined as above. Accordingly, the appropriate component gradients may be derived just by multiplying the individual field components by $i\vec{k}$ with $\vec{k}$ given by

$$\vec{k} = \begin{cases} k\ (cos\theta, sin\theta, i) & , z > 0 \\ k\ (cos\theta, sin\theta, -i) & , z < 0 \end{cases} . \tag{6.4}$$

Examining (5.18) and (5.19), the field expression derived in section 5, we see that the field above the surface has the spatial dependence (6.2), and the gradients of its vector components are found in the same way as those for the field derived in section 3. Beneath the surface the field expression has two terms; one of these has the spatial dependence (6.2), but the other has the spatial dependence

$$g(\vec{x}) = z\ exp(i\vec{k}\cdot\vec{x}) \quad , \tag{6.5}$$

whose gradient is

$$\nabla g(\vec{x}) = \left(i\vec{k} + \frac{\hat{z}}{z} \right) g(\vec{x}) \quad , \tag{6.6}$$

where $\vec{k}$ is defined as in (6.4) for $z<0$. In order to calculate the gradient of a given underwater field component, one multiplies the appropriate component of the first term of the field expression by $i\vec{k}$, then multiplies the corresponding component in the second term by $(i\vec{k}+\hat{z}/z)$, and

finally adds together the resulting vectors.

7. Discussion

In the open ocean, the ionospherically induced electric fields that one might expect to find on an electromagnetically quiet day will have fluctuations on the order of $1\ \mu V/m$, induced mainly by the solar daily variation, whose amplitude will be roughly 2×10^{-8} tesla, whereas during an intense magnetic storm the field intensity might go as high as $10\ \mu V/m$; in the neighborhood of a coastline, where there are boundary effects, the field intensities will typically be larger than those of the open ocean by a factor of 2 to 3. Assuming a uniform electrical conductivity for the ocean of 3.3 S/m, this implies induced electrical current densities in the open ocean of from 3.3 $\mu A/m^2$ up to 33 $\mu A/m^2$, with larger values near a coastline. Use of this range of current density values in equation (2.5), assuming an ocean depth of 5.0 kilometers, gives for $\vec{B}_I$, the magnetic induction in the air over the ocean due to induced electrical current flow within it, a magnitude ranging from 1.0×10^{-8} tesla to 1.0×10^{-7} tesla and a direction horizontally perpendicular to the subsurface electrical current flow. By comparison, the Earth's magnetic field over the open ocean off of La Jolla, California, is roughly 6×10^{-5} tesla in intensity and has a tilt of about 60° from the horizontal.

The magnitude of the magnetic induction generated by the interaction of an ocean wave with the uniform current density varies with the angle that the wave crest makes with the uniform flow, but a root mean square average of (3.39) over time, lateral position, and this angle gives for $z>0$

$$|\vec{B}| = \tfrac{1}{2}\,\mu_0 J_0\, a\, \exp(-2\pi z/\lambda) \quad , \tag{7.1}$$

where a is the wave's amplitude and λ is its wavelength. A typical wave amplitude on a calm day is roughly 1 meter, and during a storm one might see a typical wave amplitude on the order of 5 meters. Assuming a wave amplitude of 1.0 meter and using the current density range of from 3.3 $\mu A/m^2$ to 33 $\mu A/m^2$ gives at just above the surface a magnetic induction magnitude range of from 2.1×10^{-12} tesla to 2.1×10^{-11} tesla, assuming that the wave crests are parallel to the electric current flow.

Performing the same averaging process on (5.18), we get for the mean magnitude in the air of the magnetic induction of surface waves moving through the Earth's field

$$|\vec{B}| = \tfrac{1}{2}\,\mu_0\,\sigma\, a\, (\omega/k)\, G\, \exp(-2\pi z/\lambda) \tag{7.2}$$

$$G = \sqrt{(F_z^2 + \tfrac{1}{2}F_h^2)} \quad , \tag{7.3}$$

where F_z is the vertical component of the Earth's field and F_h is the magnitude of the horizontal component. Most of the surface wave energy in the open ocean off of La Jolla falls in the

range of wave periods from 5 seconds to 15 seconds, equivalent to an angular frequency range of from 0.42 sec^{-1} to 1.26 sec^{-1}; using the dispersion relation for surface waves on a deep ocean,

$$\omega^2 = gk \tag{7.4}$$

(Sommerfeld, pp.168-173), where g is the gravitational acceleration and has a value of about 9.81 m/sec^2, we calculate a range of phase velocities (ω/k) of from 7.8 m/sec to 23.4 m/sec. The value for G in the vicinity of La Jolla comes to about 6×10^{-5} tesla, and if we again assume a wave amplitude of 1.0 meter and an electrical conductivity for the ocean of 3.3 S/m we get a range of magnitudes for the magnetic induction at just above the ocean surface of from 6×10^{-10} tesla to 2×10^{-9} tesla.

The uniform field discussed in the first paragraph, that is produced by the ionospherically induced current flow, is at the weaker calculated extreme a little less than four orders of magnitude down from the Earth's field, and will generally not be detectable. The two wave interaction effects are roughly five orders of magnitude down from the Earth's field, but their periodic nature, both spatially and temporally, should allow them also to be detected. Except in the presence of a powerful magnetic storm the wave-magnetic field interaction effect discussed in the previous paragraph will typically be roughly two orders of magnitude stronger than the wave-current interaction effect discussed in the second paragraph, making the latter difficult to resolve from the former, as above the surface they have the same spatial dependence. Although these effects both scale linearly with the wave amplitude, making their ratio independent of this quantity, the wave-magnetic field interaction effect is also directly proportional to the phase velocity of the wave in question, which increases linearly with the wave's period as long as the deep water approximation is valid. The two wave interaction effects are seen from rough calculations to have comparable magnitudes in the extreme case of a surface wave with a period of 0.16 second or less in the presence of a strong magnetic storm.

Chapter II

Magnetic Anomalies Induced by Bottom Features

1. Introduction

We consider in this chapter magnetic anomalies associated with the presence of rocky projections from and depressions in an otherwise level ocean floor. Only magnetic effects due to electrical current flow within the water of the ocean are considered; magnetic effects due to magnetization of the ocean floor, to the magnetic properties of large projections of magnetic minerals from the ocean floor, and to irregularities of magnetization of the seafloor rocks are covered in other works (see for example Larson et al., 1974, or Vacquier, 1972). In this treatment, a large scale, horizontal uniform electric current flow driven by sources of EMF outside of the ocean is assumed, and the local distortion of this flow by the presence of a bottom feature (treated as an insulator), is determined; then, by means discussed in section 2, the magnetic field perturbation associated with this electrical current flow distortion is calculated. As the scale of the bottom feature in question will typically be several orders of magnitude greater than the amplitudes of any waves on the ocean surface, the simplifying assumption of a completely flat ocean surface will be made.

In section 3, in order to give some feeling for orders of magnitude, numerical calculations are made of magnetic fields and the tensor gradients thereof associated with a submerged hemisphere with a radius half the depth of the ocean and resting on a level ocean floor. In section 4, the problem of a localized bottom feature of arbitrary shape is considered, and section 5 gives a quick algorithm for approximating the electrical current flow deflection by bottom features of small aspect. Section 6 covers in detail the magnetic effects of small features of low aspect on the ocean floor (such as a low ridge or shallow trough), a subject touched lightly upon in section 4 of chapter 1. Finally, section 7 briefly discusses the problem of the magnetic effects due to the interaction of seawater current flow over a bottom feature with the Earth's magnetic field.

2. Mathematical methods

2.1 The basic integration formula

The basic formula for computing the magnetic field $\vec{B}$ due to an electrical current density distribution $\vec{J}$ within the ocean is the law of Biot and Savart as applied to a continuous electrical current density distribution,

$$\vec{B}(\vec{x_0}) = \frac{\mu_0}{4\pi} \int_V \frac{\vec{J}(x) \times (x_0 - x)}{|x_0 - x|^3} \, d\vec{x} \quad ; \tag{2.1}$$

$\vec{J}(x)$ is assumed to have already been adequately determined for practical purposes, and may be taken as a given.

In practical calculations, the selected volume of integration is broken down into rectangular boxes, and the electrical current density vector $\vec{J}(x_c)$ and its tensor gradient at the geometrical center $\vec{x_c}$ of each box are determined; the current density distribution throughout the box is then assumed to be given by the formula

$$J_i(\vec{x}) = J_i(\vec{x_c}) + (\vec{x} - \vec{x_c}) \cdot \nabla J_i(\vec{x_c}) \quad . \tag{2.2}$$

Also, it is assumed that the distance between $\vec{x_0}$ and $\vec{x_c}$ is much greater than the maximum dimension of the box, allowing the expansion of the denominator of the integrand of (2.1) in a binomial series. Given these assumptions, one can write an algebraic expression for the contribution to the integral (2.1) and its tensor gradient of any given box in terms of the box dimensions, the position $\vec{x_c}$ of the center of the box, and the electrical current density and its tensor gradient at $\vec{x_c}$.

We start with a variation of (2.1),

$$\vec{B}(\vec{x_0} + \vec{x_1}) = \frac{\mu_0}{4\pi} \int_R \frac{\vec{J}(\vec{x_c} + \vec{v}) \times |\vec{r_0} + (\vec{x_1} - \vec{v})|}{|\vec{r_0} + (\vec{x_1} - \vec{v})|^3} \, d\vec{v} \quad , \tag{2.3}$$

where

$$\vec{r_0} = \vec{x_0} - \vec{x_c} \quad , \tag{2.4}$$

$$\vec{x} = \vec{x_c} + \vec{v} \quad , \tag{2.5}$$

and R denotes the rectangular volume of integration centered on the position $\vec{x_c}$; the vector $\vec{x_1}$ is a small offset from $\vec{x_0}$ in an arbitrary direction, and is used to find the tensor gradient of $\vec{B}$ at $\vec{x_0}$. For the current density distribution in the numerator of the integrand we write

$$\vec{J}(\vec{x}_c+\vec{v}) = \vec{J}_0 + \bar{M}\vec{v} \quad , \tag{2.6}$$

or

$$J_i(\vec{x}_c+\vec{v}) = J_{0i} + \sum_{j=1}^{3} M_{ij}\, v_j \quad , \tag{2.7}$$

and expansion of the denominator gives

$$\frac{1}{|\vec{r}_0+(\vec{x}_1-\vec{v})|^3} = \frac{(1+z)^{-3/2}}{r_0^3} \tag{2.8}$$

$$= \frac{1}{r_0^3}\left[1 - \frac{3}{2}z + \frac{15}{8}z^2 - \frac{35}{16}z^3 + \cdots\right] \quad ,$$

where

$$z = 2\,\frac{\vec{r}_0\cdot(\vec{x}_1-\vec{v})}{r_0^2} + \frac{(\vec{x}_1-\vec{v})\cdot(\vec{x}_1-\vec{v})}{r_0^2} \quad . \tag{2.9}$$

Insertion of (2.6) and (2.8) into (2.3) gives a series expansion in $\vec{r}_0$, $\vec{x}_1$, and $\vec{v}$ for the integrand, only a few terms of which are of practical interest to us. The terms in this series that are linear in $\vec{x}_1$ are sufficient for the determination of the tensor gradient of the magnetic field, and so terms quadratic or higher in $\vec{x}_1$ may be ignored; also, due to the symmetry of the volume of integration about $\vec{x}_c$, the integrals of terms linear or cubic in $\vec{v}$ vanish, and those of terms quartic or of higher powers in $\vec{v}$ will in general be small enough in comparison to the integrals of terms quadratic or constant in $\vec{v}$ to be safely disregarded in practical calculations. These two conditions together eliminate all terms in the expansion (2.8) derived from terms quartic or higher in z, and most of the terms in smaller powers of z in this expansion. When all terms of interest are taken into account, we have from (2.3)

$$\vec{B}(\vec{x}_0) = \frac{\mu_0}{4\pi}\,\frac{V_0}{r_0^3}\left[(\vec{J}_0\times\vec{r}_0)\left\{1 - \frac{3}{2}C_1 + \frac{15}{2}C_2\right\}\right. \tag{2.10}$$

$$\left. - 3r_0(\vec{J}_0\times\vec{U}_1) + 3r_0(\bar{M}\vec{U}_1\times\vec{r}_0) - r_0^2\vec{U}_3\right]$$

and

$$\vec{B}(\vec{x}_0+\vec{x}_1) = \vec{B}(\vec{x}_0) + \frac{\mu_0}{4\pi}\,\frac{V_0}{r_0^3}\left[(\vec{J}_0\times\vec{r}_0)\left\{-3\,\frac{\vec{W}\cdot\vec{x}_1}{r_0} - \frac{105}{2}\,\frac{\vec{W}\cdot\vec{x}_1}{r_0}C_2 + 15C_3\right\}\right. \tag{2.11}$$

$$\left. + (\vec{J}_0\times\vec{x}_1)\left\{1 - \frac{3}{2}C_1 + \frac{15}{2}C_2\right\} - \vec{J}_0\times\{3r_0\vec{U}_2 - 15(\vec{W}\cdot\vec{x}_1)\vec{U}_1\}\right.$$

$$+\{3r_0\bar{M}\vec{U}_2 - 15(\vec{W}\cdot\vec{x}_1)\bar{M}\vec{U}_1\}\times\vec{r}_0 + 3r_0(\bar{M}\vec{U}_1\times\vec{x}_1) + 3r_0(\vec{W}\cdot\vec{x}_1)\vec{U}_3\Big] \quad ,$$

where

$$\vec{U}_1 = \frac{1}{r_0^3 V_0}\int_R \vec{v}(\vec{r}_0\cdot\vec{v})\,d\vec{v} \tag{2.12}$$

$$= (S_1W_1, S_2W_2, S_3W_3) \quad ,$$

$$\vec{U}_2 = \frac{1}{r_0^3 V_0}\int_R \vec{v}(\vec{x}_1\cdot\vec{v})\,d\vec{v} \tag{2.13}$$

$$= r_0^{-1}\,(S_1x_{11}, S_2x_{12}, S_3x_{13}) \quad ,$$

$$\vec{U}_3 = \frac{1}{r_0^2 V_0}\int_R (\bar{M}\vec{v}\times\vec{v})\,d\vec{v} \tag{2.14}$$

$$= \bar{P}\,\vec{S} \quad ,$$

$$\bar{P} = \begin{bmatrix} 0 & -M_{32} & M_{23} \\ M_{31} & 0 & -M_{13} \\ -M_{21} & M_{12} & 0 \end{bmatrix} \tag{2.15}$$

where

$$\bar{M} = \begin{bmatrix} M_{11} & M_{12} & M_{13} \\ M_{21} & M_{22} & M_{23} \\ M_{31} & M_{32} & M_{33} \end{bmatrix} \quad , \tag{2.16}$$

$$\vec{S} = (S_1, S_2, S_3) \quad , \tag{2.17}$$

$$C_1 = \frac{1}{r_0^2 V_0}\int_R \vec{v}\cdot\vec{v}\,d\vec{v} \tag{2.18}$$

$$= S_1 + S_2 + S_3 \quad ,$$

$$C_2 = \frac{1}{r_0^4 V_0}\int_R (\vec{r}_0\cdot\vec{v})^2\,d\vec{v} \tag{2.19}$$

$$= U_1\cdot\vec{W} \quad ,$$

$$C_3 = \frac{1}{r_0^4 V_0} \int_R (\vec{x}_1 \cdot \vec{v})(\vec{r}_0 \cdot \vec{v})\, d\vec{v} \tag{2.20}$$

$$= \frac{\vec{U}_1 \cdot \vec{x}_1}{r_0} = \vec{U}_2 \cdot \vec{W} \quad ,$$

where

$$V_0 = \int_R d\vec{v} = d_1 d_2 d_3 \quad , \tag{2.21}$$

$$\vec{W} = \frac{\vec{r}_0}{r_0} \quad , \tag{2.22}$$

and

$$S_i = \frac{1}{12} \frac{d_i^2}{r_0^2} \quad , \quad i=1,2,3 \quad , \tag{2.23}$$

d_i being the dimension of the volume of integration in the direction $\hat{x}_i$. The basic relation used for the evaluation of the above integrals is

$$\int_R v_i v_j \, d\vec{v} = r_0^2 V_0 \, \delta_{ij} \, S_i \quad , \tag{2.24}$$

where δ_{ij} is the Kronecker delta. Expression (2.11) may be rewritten in the form

$$\vec{B}(\vec{x}_0 + \vec{x}_1) = \vec{B}(\vec{x}_0) + \overline{T}\vec{x}_1 \quad , \tag{2.25}$$

where the construction of the tensor $\overline{T}$ is just a matter of sorting the coefficients of the vector elements of $\vec{x}_1$ in (2.11) into the proper tensor elements of $\overline{T}$. When the field $\vec{B}$ is expressed in this form, it is apparent that $\overline{T}$ is the tensor gradient of $\vec{B}$ at the point $\vec{x}_0$.

2.2 Correction for edge effect errors

One difficulty in the practical use of (2.1) is that it makes the implicit assumption that the entire electrical current density distribution is contained within the volume of integration, and use of a volume of integration that has a current flow through any part of its surface results in the appearance of nonphysical elements in the results of the integration. As an example of this effect we consider the case of a semi-infinite wire extending from the origin in the positive $\hat{x}$ direction out to infinity and carrying an electrical current in that direction. In this case (2.1) becomes

$$\vec{B}(\vec{x_0}) = \frac{\mu_0 I_0}{4\pi} \hat{x} \int_0^\infty \frac{(x_0 - x, y_0, z_0)}{[(x_0-x)^2+\rho_0^2]^{3/2}} dx \quad , \tag{2.26}$$

$$\vec{x_0} = (x_0, y_0, z_0) \quad , \tag{2.27}$$

$$\rho_0^2 = y_0^2 + z_0^2 \quad . \tag{2.28}$$

this reduces to

$$\vec{B}(\vec{x_0}) = \frac{\mu_0 I_0}{4\pi} (\hat{x} \times \vec{x_0}) K_1(\vec{x_0}) \quad , \tag{2.29}$$

or,

$$\vec{B}(\vec{x_0}) = \frac{\mu_0 I_0}{4\pi} \rho_0 \hat{\phi} K_1(\vec{x_0}) \quad , \tag{2.30}$$

where

$$K_1(\vec{x_0}) = \int_0^\infty \frac{dx}{[(x_0-x)^2+\rho_0^2]^{3/2}} \tag{2.31}$$

$$= \frac{1}{\rho_0^2} \left[1 + \frac{x_0}{r_0} \right] ,$$

$$r_0^2 = x_0^2 + \rho_0^2 \tag{2.32}$$

(CRC, p. 322, eq. 196). For large distances from the origin and relatively much smaller distances from the origin this gives

$$\lim_{x_0 \to \infty} \vec{B}(\vec{x_0}) = \frac{\mu_0 I_0}{2\pi \rho_0} \hat{\phi} \quad , \tag{2.33}$$

the field around an infinitely long wire, as one would expect on physical grounds. However, if we use Ampere's law to compute from (2.29) the electrical current density outside of the wire,

which on physical grounds should be zero, we get

$$\vec{J}(\vec{x}) = \frac{1}{\mu_0} \nabla \times \vec{B}(\vec{x}) \qquad (2.34)$$

$$= -\frac{I_0}{4\pi} \frac{\hat{r}}{r^2} \quad , \quad r^2 = \vec{x} \cdot \vec{x} \quad ;$$

the physical interpretation of this expression indicates a current density distribution converging on the end of the wire at the origin in such a way as to feed a total current I_0 into the wire end. In general, it seems that assuming a source or sink of electrical current in the postulated electrical current density distribution results in a mathematical artifact that, if taken at face value, cancels out the source or fills in the sink.

In the calculation of magnetic fields associated with localized bottom features, one will typically be dealing with an electrical current density distribution anomaly the bulk of whose magnetic effects are produced by the part of the distribution in the immediate neighborhood of the bottom feature, but which gives minor contributions to the magnetic field at substantial distances from the feature; in numerical calculations of the magnetic field the approach that first suggests itself is to consider only the volume immediately about the bottom feature, tolerating errors of perhaps a few percent in the field values of interest in order to avoid expensive integration over large volumes of seawater. On the basis of the example of the semi-infinite wire, it appears that if this approach is used it must be used with care, as neglecting the extended part of the current density distribution not only results in errors of omission, but may also contaminate the calculated values with mathematical artifacts.

A method for dealing with the artifact problem may be derived by viewing an infinitely long, straight, current carrying wire, for which there is an artifact-free solution for the magnetic field and its tensor gradients, as being composed of two semi-infinite wires pointing outward from the origin in opposite directions and carrying currents of equal magnitude and opposite sign. From the observation that the artifacts associated with the two wire segments must exactly cancel, we deduce that any terms in the magnetic field expression for a semi-infinite wire that contribute to the artifact must be asymmetric with respect to simultaneous reversal of wire direction and current direction, and we infer from symmetry arguments that any singularities in the artifact terms must be at the origin. Given that these constraints are sufficient to uniquely identify those terms contributing to the artifact, once an artifact correction expression for a semi-infinite wire has been derived it may be use as a Green's function for a general current density flow through a surface.

To derive an expression for a semi-infinite current carrying wire pointing from the origin in an arbitrary direction, we start with a binomial expansion of (2.1), after the manner of (2.3);

$$\lim_{|\bar{y}|\to 0} \bar{B}(\bar{x_0}+\bar{y}) = \bar{B}(\bar{x_0}) + \bar{B_1}(\bar{x_0},\bar{y}) - \bar{B_2}(x_0,\bar{y}) \quad , \tag{2.35}$$

$$\bar{B_1}(\bar{x_0},\bar{y}) = \frac{\mu_0}{4\pi} \int_v \frac{\bar{J}(\bar{x})\times\bar{y}}{|\bar{x_0}-\bar{x}|^3}\, d\bar{x} \quad , \tag{2.36}$$

$$\bar{B_2}(\bar{x_0},\bar{y}) = \frac{3\mu_0}{4\pi} \int_v \frac{[\bar{J}(\bar{x})\times(\bar{x_0}-\bar{x})](\bar{x_0}-\bar{x})\cdot\bar{y}}{|\bar{x_0}-\bar{x}|^5}\, d\bar{x} \quad . \tag{2.37}$$

We let $\hat{w}$ be the unit vector of the direction in which the wire points outward from the origin, and we let I_0 be the current flow out of the origin. Then (2.36) and (2.37) become

$$\bar{B_1}(\bar{x_0},\bar{y}) = \frac{\mu_0 I_0}{4\pi} (\hat{w}\times\bar{y})\, L_1(\bar{x_0}) \quad , \tag{2.38}$$

$$L_1(\bar{x_0}) = \int_0^\infty \frac{dt}{|\bar{x_0}-\hat{w}t|^3} \tag{2.39}$$

and

$$B_2(\bar{x_0},\bar{y}) = \frac{\mu_0 I_0}{4\pi} (\hat{w}\times\bar{x_0})\{\bar{x_0}L_2(\bar{x_0}) - \hat{w}L_3(\bar{x_0})\}\cdot\bar{y} \quad , \tag{2.40}$$

$$L_2(\bar{x_0}) = 3\int_0^\infty \frac{dt}{|\bar{x_0}-\hat{w}t|^5} \quad , \tag{2.41}$$

$$L_3(\bar{x_0}) = 3\int_0^\infty \frac{t\,dt}{|\bar{x_0}-\hat{w}t|^5} \quad . \tag{2.42}$$

It is seen that $L_1(\bar{x_0})$ is a generalization of $K_1(\bar{x_0})$ as defined by (2.31); if we define

$$x_0 = \hat{w}\cdot\bar{x_0} \tag{2.43}$$

$$\bar{\rho_0} = \bar{x_0} - \hat{w}x_0 \tag{2.44}$$

$$\rho_0^2 = \bar{\rho_0}\cdot\bar{\rho_0} \tag{2.45}$$

$$= r_0^2 - x_0^2$$

$$\rho_0^2 = \bar{x_0}\cdot\bar{x_0} \quad , \tag{2.46}$$

then (2.39) becomes

$$L_1(\vec{x_0}) = \int_0^\infty \frac{dt}{|(x_0-t)\hat{w}+\vec{\rho_0}|^3} \quad , \tag{2.47}$$

which, since by (2.43) and by (2.44)

$$\hat{w}\cdot\vec{\rho_0} = 0 \quad , \tag{2.48}$$

becomes

$$L_1(\vec{x_0}) = \int_0^\infty \frac{dt}{[(x_0-t)^2+\rho_0^2]^{3/2}} \quad . \tag{2.49}$$

This is the same integral as in expression (2.31), and its solution in this context is

$$L_1(\vec{x_0}) = \frac{1}{\rho_0^2}\left[1+\frac{\hat{w}\cdot\vec{x_0}}{r_0}\right] \quad , \tag{2.50}$$

where ρ_0 and r_0 are as defined by (2.45) and (2.46) respectively. a similar process gives for L_2 and L_3

$$L_2(\vec{x_0}) = \frac{1}{\rho_0^2}\left[2L_1(\vec{x_0}) + \frac{\hat{w}\cdot\vec{x_0}}{r_0^3}\right] \tag{2.51}$$

and

$$L_3(\vec{x_0}) = (\hat{w}\cdot\vec{x_0})L_2(\vec{x_0}) + \frac{1}{r_0^3} \quad . \tag{2.53}$$

By (2.44) and (2.53), (2.40) becomes

$$\vec{B_2}(\vec{x_0},\vec{y}) = \frac{\mu_0 I_0}{4\pi}(\hat{w}\times\vec{x_0})\left[\vec{\rho_0}L_2(\vec{x_0}) - \frac{\hat{w}}{r_0^3}\right]\cdot\vec{y} \quad , \tag{2.54}$$

which by (2.51) becomes

$$\vec{B_2}(\vec{x_0},\vec{y}) = \frac{\mu_0 I_0}{4\pi}(\hat{w}\times\vec{x_0})\left[\frac{1}{r_0^3}\left\{\vec{\rho_0}\frac{\hat{w}\cdot\vec{x_0}}{\rho_0^2} - \hat{w}\right\} + 2\vec{\rho_0}\frac{L_1(\vec{x_0})}{\rho_0^2}\right]\cdot\vec{y} \quad . \tag{2.55}$$

Finally, we have for $\vec{B}(\vec{x_0})$

$$\vec{B}(\vec{x_0}) = \frac{\mu_0 I_0}{4\pi}(\hat{w}\times\vec{x_0})\,L_1(\vec{x_0}) \quad , \tag{2.56}$$

or, in a cylindrical coordinate system centered about the wire and with its axis in the $\hat{w}$ direction,

$$\vec{B}(\vec{x_0}) = \frac{\mu_0 I_0}{4\pi} \rho_0 \hat{\phi}\, L_1(\vec{x_0}) \quad . \tag{2.57}$$

Reexpressing (2.35) with an eye toward symmetry, we have

$$\lim_{|\vec{y}|\to 0} \vec{B}(\vec{x_0}+\vec{y}) = \vec{B}(\vec{x_0}) + \vec{B_S}(\vec{x_0},\vec{y}) + \vec{B_{A1}}(\vec{x_0},\vec{y}) + \vec{B_{A2}}(\vec{x_0},\vec{y}) \quad , \tag{2.58}$$

where the perturbation terms symmetric with respect to simultaneous reversal of I_0 and $\hat{w}$ are

$$\vec{B_S}(\vec{x_0},\vec{y}) = \frac{\mu_0 I_0}{4\pi} \left[\frac{\hat{w}\times\vec{y}}{\rho_0^2} - \frac{2(\hat{w}\times\vec{x_0})(\vec{\rho_0}\cdot\vec{y})}{\rho_0^4} \right] \quad , \tag{2.59}$$

and those that are antisymmetric are

$$\vec{B_{A1}}(\vec{x_0},\vec{y}) = \frac{\mu_0 I_0}{4\pi} \frac{(\hat{w}\times\vec{x_0})}{r_0^3} \left[\hat{w} - \vec{\rho_0}\frac{\hat{w}\cdot\vec{x_0}}{\rho_0^2} \right]\cdot\vec{y} \tag{2.60}$$

and

$$\vec{B_{A2}}(\vec{x_0},\vec{y}) = \frac{\hat{w}\cdot\vec{x_0}}{r_0} \vec{B_S}(\vec{x_0},\vec{y}) \quad . \tag{2.61}$$

Taking derivatives, we find that

$$\nabla\times\vec{B_{A1}} = -\frac{\mu_0 I_0}{4\pi} \frac{\hat{\rho}}{\rho^2} \quad , \tag{2.62}$$

whereas

$$\nabla\times\vec{B_S} = \nabla\times\vec{B_{A2}} = 0 \quad . \tag{2.63}$$

It is apparent that the field derivatives associated with $\vec{B_{A1}}$ are artifact-contributed. On the other hand, $\vec{B_{A2}}$ is not implicated as artifact-producing by the curl test, and is eliminated on the grounds that, like B_S and unlike B_{A1}, it becomes singular everywhere along the axis of the wire. Hence, in (2.60) we have an expression that can be used for the correction of artifact effects in the elements of the tensor gradient of the magnetic field. It is undesirable to make an artifact correction to the magnetic field itself, since in the nonphysical truncation of a current flow one just loses the field contribution from the truncated section of the current flow without also gaining a nonphysical field component in its place; it is essentially the absence of a field component where one would expect it on physical grounds to be that is responsible for the nonphysical behavior of the field derivatives in the case of the semi-infinite wire.

2.3 Streamline tracing

In numerical exploration work it is frequently desirable to trace streamlines of electrical current flow, perhaps to check for peculiarities in the flow distribution that might require special programming to handle. The simplest approach to streamline tracing is to pick a starting point, find the current density vector at this point, extrapolate in the direction of the vector from the starting point over some convenient interval of distance to a new point, and, using this new point as a starting point, repeat the process for as long along the streamline as on wishes to trace; however, in problems where there is some region in which the direction of the current density vector changes rapidly with position (a characteristic of most problems of practical interest), this method can lead to large cumulative errors unless the step size is kept expensively small. To deal with this difficulty, a more complicated method of the predictor-corrector type was developed, and was found to be satisfactory.

We assume two parallel planes separated by a distance d and a streamline passing through them both, intersecting the first plane at the point $\vec{x_0}$ and then the second plane at the point $\vec{x_*}$; the electrical current density is given for everywhere between the planes. The basic idea of the method is that if the direction of the current density vector $\vec{v_m}$ at the point $\vec{x_m}$ along the streamline midway between the two planes is determined and a line is extended from $\vec{x_0}$ in the direction of $\vec{v_m}$ until it intersects the second plane, then the point of intersection will be very close to $\vec{x_*}$, provided that the curve of the streamline is roughly uniform and reasonably gentle. To approximate the position of this midpoint, we first determine the current density vector $\vec{v_0}$ at the point $\vec{x_0}$, then draw a line from $\vec{x_0}$ in the direction of $\vec{v_0}$ until it intersects the second plane at the point $\vec{x_1}$;

$$\vec{x_1} = d\,\frac{\vec{v_0}}{\hat{n}\cdot\vec{v_0}} + \vec{x_0} \quad , \tag{2.64}$$

where $\hat{n}$ is a unit vector perpendicular to the planes and pointing from the first plane toward the second. This line will miss $\vec{x_*}$ on the convex side of the streamline. We then find the point $\vec{x_2}$ midway between $\vec{x_0}$ and $\vec{x_1}$,

$$\vec{x_2} = \tfrac{1}{2}\,(\vec{x_1}-\vec{x_0}) + \vec{x_0} \tag{2.65}$$

$$= \frac{d}{2}\,\frac{\vec{v_0}}{\hat{n}\cdot\vec{v_0}} + \vec{x_0} \quad ,$$

and find $\vec{v_2}$ the current density vector at $\vec{x_2}$; this vector should be a somewhat better approximation to $\vec{v_m}$ than is $\vec{v_0}$. We then draw a line from $\vec{x_0}$ in the direction of $\vec{v_2}$ until it intersects the second plane at the point $\vec{x_3}$;

$$\vec{x_3} = d\,\frac{\vec{v_2}}{\hat{n}\cdot\vec{v_2}} + \vec{x_0} \quad . \tag{2.66}$$

This line should miss $\vec{x_2}$ on the concave side of the streamline. The point $\vec{x_4}$ midway between $\vec{x_3}$ and $\vec{x_0}$ is given by

$$\vec{x_4} = \tfrac{1}{2}\,(\vec{x_3}-\vec{x_0}) + \vec{x_0} \tag{2.67}$$

$$= \frac{d}{2}\,\frac{\vec{v_2}}{\hat{n}\cdot\vec{v_2}} + \vec{x_0} \quad .$$

The point $\vec{x_5}$ midway between $\vec{x_2}$ and $\vec{x_4}$,

$$\vec{x_5} = \tfrac{1}{2}\,(\vec{x_4}-\vec{x_2}) + \vec{x_2} \tag{2.68}$$

$$= \tfrac{1}{2}\,(\vec{x_4}+\vec{x_2}) \quad ,$$

should then be fairly close to $\vec{x_m}$, and the current density vector $\vec{v_5}$ at $\vec{x_5}$ should be a good approximation to $\vec{v_m}$. Finally, we draw a line from $\vec{x_0}$ in the direction of $\vec{v_5}$ until it intersects the second plane at the point $\vec{x_6}$;

$$\vec{x_6} = d\,\frac{\vec{v_5}}{\hat{n}\cdot\vec{v_5}} + \vec{x_0} \quad . \tag{6.69}$$

The point $\vec{x_6}$ within the second plane should then lie very close to $\vec{x_2}$. Although this method requires considerably more calculation per step than does the simple extrapolation from $\vec{x_0}$ along the direction of $\vec{v_0}$, it permits one to safely increase the step size to the point where the total amount of calculation needed to trace a given length of streamline is much less than that required by the simple extrapolation method.

For problems in which a streamline may double back upon itself, giving rise to the possibility of denominators going to zero in some of the expressions given above, this method may be modified to suit. In this case, we picture a sphere of radius d centered at the point $\vec{x_0}$, and postulate a streamline passing through $\vec{x_0}$ and emerging through the surface of the sphere at the point $\vec{x_2}$. The formulas corresponding to (2.64) through (2.69) are

$$\vec{x_1} = d\,\frac{\vec{v_0}}{|\vec{v_0}|} + \vec{x_0} \tag{2.70}$$

$$\vec{x_2} = \frac{d}{2}\,\frac{\vec{v_0}}{|\vec{v_0}|} + \vec{x_0} \tag{2.71}$$

$$\vec{x_3} = d\,\frac{\vec{v_2}}{|\vec{v_2}|} + \vec{x_0} \tag{2.72}$$

$$\vec{x_4} = \frac{d}{2}\frac{\vec{v_2}}{|\vec{v_2}|} + \vec{x_0} \tag{2.73}$$

$$\vec{x_5} = \frac{d}{2}\frac{(\vec{x_4}-\vec{x_0})+(\vec{x_2}-\vec{x_0})}{|(\vec{x_4}-\vec{x_0})+(\vec{x_2}-\vec{x_0})|} + \vec{x_0} \tag{2.74}$$

$$\vec{x_6} = d\frac{\vec{v_5}}{|\vec{v_5}|} + \vec{x_0} \quad , \tag{2.75}$$

where $\vec{x_6}$ is the method's approximation to $\vec{x_0}$. Note that, due to scaling opportunities not present in the previous case, $\vec{x_2}$ and $\vec{x_4}$ in (2.74) may be replaced with $\vec{x_1}$ and $\vec{x_3}$ respectively, thereby eliminating the need to calculate $\vec{x_4}$.

3. Magnetic anomalies in the air above a submerged hemisphere

In order to gain some feel for the orders of magnitude of the magnetic field values associated with a localized bottom feature, we consider the case of a hemisphere with its base resting on an otherwise level ocean floor and with its radius equal to half of the ocean depth. An electrical current density field, uniform at large lateral distances from the hemisphere, is induced within the ocean by an outside source of EMF, and the anomalous magnetic effects associated with the bottom feature are defined to be those arising from the perturbation on the uniform electrical current field caused by the feature.

The calculation of the electrical current field is based on the placement of current dipoles in such a way as to satisfy the boundary conditions of the problem, these being that there should be no current flow through either the ocean floor or the ocean surface. The basic formulae for the estimation of the appropriate dipole strengths are those for the electrical current density distribution about and within a sphere of radius a suspended in an infinite ocean within which the electrical current density field approaches $J_0\hat{x}$ at large distances from the sphere,

$$\vec{J}(r,\theta) = J_0\left[\hat{x} - \frac{a^3}{r^3}(\hat{r}\cos\theta + \tfrac{1}{2}\hat{\theta}\sin\theta)\right] \quad , \quad r \geq a \tag{3.1}$$

$$\vec{J}(r,\theta) = 0 \quad , \quad r < a \quad , \tag{3.2}$$

where r is the distance from the center of the sphere and the direction of $\theta=0$ is parallel to $\hat{x}$; expression (3.1) is the gradient of the potential

$$\phi(r,\theta) = J_0\left[r + \frac{a^3}{2r^2}\right]\cos\theta \quad , \tag{3.3}$$

which is a solution to Laplace's equation, and (3.2) derives from a trivial solution to Laplace's equation. It may be verified that on the spherical surface defined by $r=a$ the curren density field component $\vec{J}\cdot\hat{r}$ normal to the surface is equal to zero. Expression (3.1) is seen to be the superposition of a uniform field $J_0\hat{x}$ and a dipole field having a strength of $(J_0a^3/2)$ and a direction antiparallel to the uniform component. These expressions also apply to the case of a hemisphere of radius a resting on the floor of an ocean of arbitrarily great depth, as the cylindrical symmetry of the sphere problem about the x-axis guarantees that no streamline will intersect a plane containing the x-axis. The case of a hemisphere resting on the floor of an ocean of finite depth may be approximately dealt with by setting up an array of many dipoles of equal strength and a common orientation antiparallel to the uniform field $J_0\hat{x}$, equally spaced along a line perpendicular to $\hat{x}$ with a spacing equal to twice the depth of the ocean. If the

ocean floor is taken to correspond to the plane bisecting this line at the central dipole of this array, and the ocean surface to the parallel plane midway between this dipole and the dipole immediately above it, then by symmetry there is no current flow through either ocean bottom or ocean surface; however, due to the effects of the dipoles on either side of the central dipole, the surface about this dipole on which $\vec{J}\cdot\hat{r}=0$ is no longer a perfect sphere, but an oblate spheroid. The degree of this hemispherical distortion was examined by use of a streamline tracing program with graphical output, and it was found for an array of five dipoles that if the value of a is no more than half of the ocean depth then the deviation of the surface about the central dipole from a hemispherical shape is difficult to see with the unaided eye, implying a distortion of no more than about 5% of a.

Granted that this method adequately gives the electrical current density distribution within the ocean, the next step in the magnetic anomaly calculations is to use expressions (2.10) and (2.11), giving the magnetic effects due to the current density distribution within a rectangular box, for incremental integration over the current density field to estimate the total magnetic field and its spatial derivatives at various points of interest. The procedure that was constructed to do this starts with the selection of a volume of integration having a rectangular horizontal cross-section and reaching vertically from the ocean floor to the surface, covering a substantial area of the ocean floor about the bottom feature; this volume is oriented so that its vertical faces are either parallel or perpendicular to the $\hat{x}$ direction. The volume is then sectioned by a set of equally spaced planes perpendicular to the $\hat{x}$ direction, and also by another set of equally spaced planes (not necessarily the same spacing as the first set) both vertical and perpendicular to the first set, thus breaking the horizontal cross-section of the volume up into a regular rectangular grid. Then, one goes to the bottom edge of the upcurrent face of the volume of integration, and draws a horizontal line along the face slightly above the edge, marking the points along this line that intersect the sectioning planes parallel to $\hat{x}$; these points serve as starting points for the tracing of a streamline surface, the algorithm for which is given in the next paragraph. The objective of this part of the procedure is to trace out a streamline surface running very close to the ocean bottom, and use this surface in subsequent calculations as the base of the volume of integration; this is substantially less cumbersome than numerically specifying the shape of the ocean bottom, and the error introduced into the calculations by this approximation may be made negligible by starting the streamline surface tracing algorithm sufficiently close to the actual bottom. The tracing algorithm yields the points of intersection between the streamline surface and the regular array of vertical lines which are defined by the intersection of the two perpendicular sets of sectioning planes. One constructs a rectangular volume about each one of these vertical lines from the point where it intersects the ocean

bottom to the point where it intersects the ocean surface, and then then divides this into small rectangular boxes, to each of which the expressions (2.10) and (2.11) are applied and the magnetic field contributions therefrom summed; the lateral dimensions of the rectangular volume taken to be about each line are determined by the spacing of the lines, and chosen so that the vertical faces of these volumes meet, thereby covering the whole volume of integration. The current density distribution used with these expressions is the anomalous current density distribution, which is the total field with the uniform component $J_0\hat{x}$ subtracted off; the current density field between the ocean surface and the streamline surface is then only the superposition of the individual dipole fields, and the field below the streamline surface and above the ocean floor is just $-J_0\hat{x}$, with the field everywhere else being equal to zero.

The algorithm used for tracing a streamline surface is partly based on the first streamline tracing algorithm discussed in section 2.2. We suppose that the sectioning planes perpendicular to $\hat{x}$ are separated from each other by a distance d, and that on one of them we have a set of points along the intersection curve of the plane with the streamline surface, these points being the points of intersection between this curve and the vertical lines defined by the intersection of the plane and the perpendicular set of sectioning planes. Using a single step of the streamline tracing algorithm for each one of these points taken as a starting point, we get another set of points on the next plane over in the $\hat{x}$ direction, to which we can fit another, slightly different, curve; in general, these points will not lie on the vertical lines of intersection in this plane. Finally, we go in turn to each of the vertical lines of intersection of the second plane, and fit a cubic polynomial curve through the four points nearest it (these usually being the two nearest points on either side of the line), and and record the point where the fitted curve crosses the line. This last set of points may be used to start another step of this algorithm, which may be used recursively to trace the points of the entire streamline surface. As a final check of accuracy, one may note whether or not the streamline surface tends toward a flat sheet slightly above the level ocean floor as it is extended past the localized bottom feature. Note that it is unnecessary to trace out and store the points for the entire streamline surface before proceeding with the integration; it is possible to perform the integration for a given plane after computing the streamline surface points of that plane from those of the previous plane, add the results of the integration to an accumulated sum, throw away the points of the previous plane, and then go on to the next plane, and so on, with considerable savings in program array storage space.

In dealing with the electrical current density distribution truncation error problem discussed in section 2.3, a method that has proved reasonably effective in practice is to examine, in the course of integration, each of the rectangular boxes that constitute the basic unit of

integration to see if it has one or more faces on the outside of the volume of integration; if an outside face is detected, then the current density vector at its center is multiplied by the area of the face in order to estimate the total current flow through the face, and then equation (2.60) from section 2.3 is used with this information to calculate corrections to the elements of the tensor gradient of the magnetic field. Failure to make such corrections will result in nonzero values for the curl of the magnetic field in places, such as empty air, where there is no electrical current; practical experience has shown that these tensor element corrections can be comparable in magnitude to the elements of the corrected tensor. A further problem exists in that the current density field on the faces of a box is estimated by the imperfect method of extrapolation from its value and tensor gradient at the center of the box, and that therefore one can expect slight discontinuities in the current density field as one passes from one box to the next; properly, the effects of these discontinuities should be corrected for with further applications of (2.60). Also, there will be minor errors from the use of (2.60) on the outside box faces with what amounts to face-averaged current densities, rather than the more correct procedure of integrating (2.60) over the surfaces of the faces in question. However, both of these additional sources of error can be reduced by cutting down on the size of the basic unit of integration, and, with the primary source of error allowed for as described, practical calculations imply that accuracy to two significant places seems feasible.

The actual calculations were done for a roughly hemispherical shape of radius 4.0 meters at its base on the bottom of an ocean 4.5 meters deep (see figure 2.1), assuming a uniform electrical current density field component of 1.0 $ampere/meter^2$ in the $\hat{x}$ direction; scaling relationships may be used with the fields and their tensor gradients calculated for this model to estimate the corresponding values for a somewhat larger system with a different uniform current density field component. The flattening shown in the figure near the top of the projection from the seafloor is the result of the use of only five dipoles to simulate the electrical current flow about a hemisphere in the close vicinity of the plane of symmetry which in this representation stands for the ocean surface. Had a much larger number of dipoles been used in the simulation, this flattening effect could have been greatly reduced, yielding the flow pattern about a nearly perfect hemispherical surface; however, such a flattening at the top is in fact a characteristic of some oceanic features of interest, such as seamounts, and accordingly is more realistic for features of this sort. The basic unit of integration was a cubical box 10 centimeters on a side, and the grid spacing of the vertical lines of intersection of the sectioning planes was 10 centimeters by 10 centimeters. At each one of these vertical lines, cubes were stacked from the ocean floor upward until a cube extended beyond the streamline surface, at which point this cube was truncated level with the streamline surface; expressions (2.10) and (2.11) were then

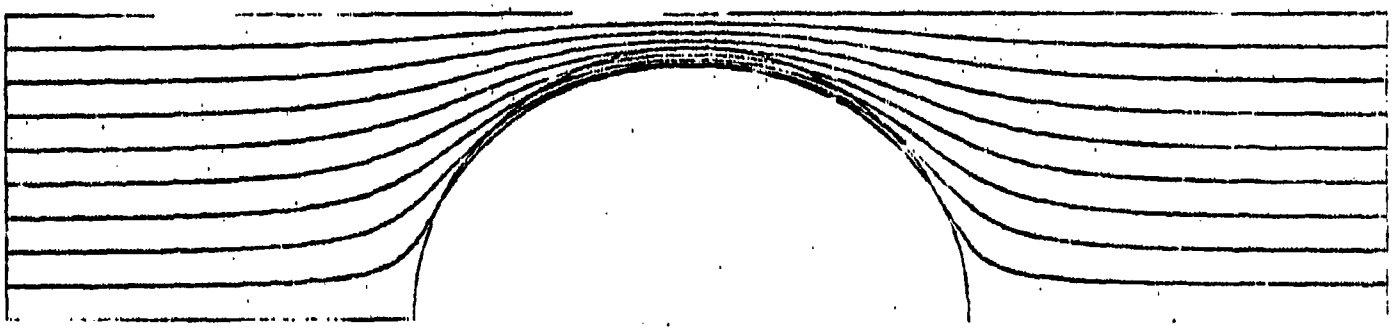

FIGURE 2.1

Streamline flow over the roughly hemispherical bottom feature in the vertical plane parallel to the flow at a distance from the feature and passing through the centerline of the feature; to point up the extent of the deformation from the flow pattern over a perfect hemisphere, a hemisphere of the appropriate radius is superposed over the streamline pattern.

used, assuming a uniform current density field of -1.0 *ampere/meter*^{2} $\hat{x}$ within all of the integration units. Then, cubes were stacked from the top of the truncated cube until one extended above the ocean surface, at which point this cube was truncated level with the surface; the current density fields and their tensor gradients used in expressions (2.10) and (2.11) are generated by the five dipoles making up the vertical dipole array for this problem. The total volume of integration was 20 meters by 20 meters laterally by 4.5 meters vertically, with the hemisphere located at its bottom center. Tracing of the streamline surface was started 15 centimeters over the ocean bottom at the upcurrent edge of the volume of integration, and its extrapolation at the downcurrent edge of this volume differed no more than 5 centimeters from this height at any point along the upcurrent side, verifying that the extrapolation had been properly done. Calculations were done for various points of interest in the air over the ocean surface, and the results are presented in table 2.1. The x-axis of the coordinate system points in the direction of the uniform component of the electrical current flow, and the z-axis points upward; the origin of the coordinate system is on the ocean bottom, at the center of the hemisphere.

We make this work useful in practice by developing scaling relations for the magnetic field and its tensor gradients in going from one system with one length scale to another system with a different length scale but with the same ratios between its various length parameters as the first system. Referring to equation (2.1), we see that the magnetic field is linear with respect to the electrical current density. Further work with this equation, experimenting with changes of length variables by multiplicative factors, indicate that if we have two systems, identical except as to scale, and B_1, J_1, and d_1 are magnetic field, electrical current density, and length parameters of the first system whereas B_2, J_2, and d_2 are the corresponding parameters of the second system, then we have

$$\frac{B_2}{B_1} = \frac{J_2}{J_1}\,\frac{d_2}{d_1} \quad ; \tag{3.4}$$

the same process applied to spatial derivatives of equation (2.1) shows that if B_1' and B_2' are corresponding magnetic field gradients for the two systems, then

$$\frac{B_2'}{B_1'} = \frac{J_2}{J_1} \quad , \tag{3.5}$$

which is to be expected, as the larger system will show a smaller percentage change in a field value than the smaller system for a given change in position.

As an example, suppose that we wish to find the magnetic field and its tensor gradients at a point 1.0 kilometer in the air over the surface of an ocean 4.5 kilometers deep, with a

$y = 4.0$ *meters*	$x = 0.0$ *meters*	$x = 4.0$ *meters*
B_x	0.000	-0.111
B_y	0.132	0.137
B_z	-0.338	-0.194
B_{xx}	-0.048	0.002
B_{xy}	0.000	-0.001
B_{xz}	0.000	0.048
B_{yy}	-0.084	-0.055
B_{yz}	0.016	-0.007
B_{zz}	0.132	0.053

$y = 0.0$ *meters*	$x = 0.0$ *meters*	$x = 4.0$ *meters*
B_x	0.000	0.000
B_y	0.473	0.325
B_z	0.000	0.000
B_{xx}	0.000	0.000
B_{xy}	0.000	-0.050
B_{xz}	0.000	0.000
B_{yy}	0.000	0.000
B_{yz}	-0.181	-0.088
B_{zz}	0.000	0.000

TABLE 2.1

Field and field gradient values at selected points in a horizontal plane 1.0 meter above the surface of an ocean 4.5 meters deep with a hemispherical bulge of radius 4.0 meters resting on the bottom, as described in the text on page 36. The field values are in units of 10^{-6} *tesla*, and the field gradient values are in units of 10^{-6} *tesla/meter*. The origin of the plane is on the axis of the bulge. In the absence of the bulge the field would be a uniform $\vec{B} = -2.82 \times 10^{-6} \hat{y}$ *tesla*.

shape such as illustrated in figure 2.1, having a radius at its base of 4.0 kilometers, resting on the ocean floor directly below the point; we assume a uniform electrical conductivity of 3.3 S/m for the ocean, and suppose that sources of EMF outside of the ocean induce an essentially constant electric field within it that is a uniform 1.0 $\mu V/m$ in the $\hat{x}$ direction at great distances from the distorting effects of the hemisphere. The system described is that of table 2.1 scaled up in size by a factor of 1000, with an electrical current density at large distances from the hemisphere of 3.3×10^{-6} *ampere/meter*^{2} in the $\hat{x}$ direction, as opposed to 1.0 *ampere/meter*^{2} for the smaller system. From equation (3.4) we then have for the field values that $B_2 = 3.3\times10^{-3}\, B_1$, and from equation (3.5) we have for the field value gradients that $B_2' = 3.3\times10^{-6}\, B_1'$. Referring to table 2.1 to get the field values directly above the center of the bottom feature, we therefore have for B_y, the only nonzero field component, a value of 1.6×10^{-9} tesla, and for B_{yx} and B_{zy}, the only nonzero tensor gradient elements, a common value of -6.0×10^{-13} tesla per meter. Using this procedure, we scale up the contents of table 2.1, giving the results in table 2.2.

As there are no electrical currents in the air above the ocean surface, the magnetic field in this region can be expressed as the gradient of a scalar potential which is a solution to Laplace's equation. The principle restriction on the practical use of the method of magnetic field computation discussed in the text above, that the points at which the field is computed must be a distance above the ocean surface that is on the order of many times the largest linear dimension of the basic unit volume of integration, can in principle be circumvented by fitting a general series expansion solution to Laplace's equation to the values computed by this method, and then using the resulting potential expression to compute the magnetic field and its tensor derivatives at points elsewhere; probably the best such solution to Laplace's equation for this purpose is an expansion in the spherical harmonics about the center of the base of the hemispherical shape, using only those terms which vanish at arbitrarily large radial distances from this point. However, one should bear in mind that downward continuations of this sort tend to be numerically unstable, in that small errors in the determination of the field values at the 1.0 kilometer altitude above the ocean surface can easily be multiplied to large errors in the values computed at the surface from the potential expression, and that the field gradients computed by the method of this section are mildly prone to distortion by the effects of those mathematical artifacts which cannot be completely compensated (principally those introduced at the faces of the basic rectangular volumes of integration making up the simulation volume, and in particular those faces which are on the outer surface of this volume); it could easily happen in many cases that the continuation error exceeds the magnitude of the value being computed, and it is recommended that in fitting the potential expression to the values numerically determined at

$y = 4.0\,km$	$x = 0.0\,km$	$x = 4.0\,km$
B_x	0.00	-0.37
B_y	0.44	0.45
B_z	-1.1	-0.64
B_{xx}	-0.16	0.005
B_{xy}	0.00	-0.003
B_{xz}	0.00	0.16
B_{yy}	-0.28	-0.18
B_{yz}	0.05	-0.02
B_{zz}	0.44	0.18

$y = 0.0\,km$	$x = 0.0\,km$	$x = 4.0\,km$
B_x	0.00	0.00
B_y	1.6	0.11
B_z	0.00	0.00
B_{xx}	0.00	0.00
B_{xy}	0.00	-0.15
B_{xz}	0.00	0.00
B_{yy}	0.00	0.00
B_{yz}	-0.60	-0.29
B_{zz}	0.00	0.00

TABLE 2.2

Field and field gradient values at selected points in a horizontal plane 1.0 kilometer above the surface of an ocean 4.5 kilometers deep with a hemispherical bulge of radius 4.0 kilometers resting on the bottom, as described in the text on pages 38 and 40. The field values are in units of 10^{-9} *tesla*, and the field gradient values are in units of 10^{-12} *tesla/meter*. The origin of the plane is on the axis of the bulge. In the absence of the bulge the field would be a uniform $\vec{B} = -9.3\times 10^{-9}\,\hat{y}$ *tesla*.

moderate to large distances above the ocean surface one relies heavily on the magnetic field vector elements, which should be somewhat less contaminated by mathematical artifacts than the tensor gradient elements.

4. Solution for the electrical current density distribution in an ocean with arbitrary bottom features

Given the methods of section 2, the magnetic anomalies resulting from a given bottom feature may be computed provided that the electrical current disturbances associated with that feature are known. In this section an algorithm is given for finding the electrical current distribution about a localized bottom feature of arbitrary shape.

The construction process starts with a level-surfaced ocean of indefinite depth, within which there is a horizontal electric field presumed to be induced by sources in the upper atmosphere. This primary electric field $\vec{E}_0$ is taken to be the gradient of the potential ϕ_0, and is assumed to induce an electrical current distribution $\vec{J}_0$ according to the relation

$$\vec{J}_0 = \sigma \nabla \phi_0 \quad , \tag{4.1}$$

where σ is the electrical conductivity distribution for the ocean.

A pillbox-shaped closed surface is then postulated, whose top is the level ocean surface and whose bottom has the shape of a hypothetical ocean floor profile; this profile is taken to be level and parallel to $\vec{J}_0$ except for a region close to the axis of the pillbox, where the profile is allowed to take any shape that does not intersect the top of the pillbox. We now assume a potential ϕ_1 and an electrical current density distribution $\vec{J}$ such that

$$\vec{J} = \sigma \nabla (\phi_0 + \phi_1) \quad , \tag{4.2}$$

and require as boundary conditions on $\vec{J}$ that its component normal to the pillbox surface should be zero at all points of the top and bottom of the box (indicating the absence of current flow through either boundary), and that the pillbox sides should be far enough removed from the central disturbance that $\vec{J}$ may safely be assumed to be equal to $\vec{J}_0$.

The boundary condition on $\vec{J}$ at the top of the box is already met by $\vec{J}_0$, so we have for ϕ_1 there that

$$\hat{z} \cdot \nabla \phi_1 = 0 \quad , \tag{4.3}$$

and at the bottom of the box we immediately have from (4.2) that

$$\hat{n} \cdot \nabla \phi_1 = - \hat{n} \cdot \nabla \phi_0 \quad , \tag{4.4}$$

where $\hat{n}$ is the inward-pointing unit vector normal to the box surface; since by hypothesis $\vec{J}_0$ is parallel to the bottom except near the axis of the box, this reduces to (4.3) over most of the box's bottom. On the box sides, the condition that $\vec{J} = \vec{J}_0$ implies by (4.1) and (4.2) that

$$\nabla\phi_1 = 0 \quad . \tag{4.5}$$

The normal derivative of ϕ_1 is therefore specified over the entire closed surface of the pillbox, thereby constituting Neuman boundary conditions, which are sufficient to define a solution for ϕ_1 unique to within an additive constant. We thus have $\vec{J}$ everywhere within the box; as $\vec{J}$ meets the boundary conditions appropriate to an electrical current density distribution within an ocean having the specified bottom topography, the problem is solved. For methods to compute ϕ_1 given Neuman boundary conditions, see Forsythe and Wasow, 1960.

5. A quick, inexact method for approximation of the electrical current density distribution due to a localized bottom feature

For situations where the aspect of the bottom feature is small, a quick if inexact method for estimating the associated electrical current flow disturbance is outlined. As in the previous section, one assumes a horizontal electric field $\vec{E}_0$ such as would exist in the absence of an ocean bottom, constructs a hypothetical surface within the ocean having the shape of the actual bottom topography, then calculates at each point on this sheet the component of $\vec{E}_0$ parallel to the surface normal. A surface charge distribution over the bottom sheet is then estimated that will give rise to an electric field whose normal component at each point on the sheet exactly cancels the corresponding normal component of $\vec{E}_0$. The supplementary condition that there be no electrical current flow through the ocean surface (which is assumed for convenience to be level) may be met by constructing a system of image reflections of the estimated surface charge distribution through the planes of the ocean surface and the level ocean bottom from which the bottom features are taken to protrude. This method is suggested by the physical observation that an electrical current flow over a bottom irregularity will in fact deposit charges on the irregularity's surface in a fashion tending to divert the flow away from the irregularity.

There appears to be no rapid, straightforward algorithm for deriving a surface charge distribution that will exactly solve the above problem. However, an approximate method exists which should serve adequately in many cases of practical interest. Suppose that we have an infinite plane surface with a uniform surface charge density ρ_u, which is embedded in an infinite uniform dielectric medium with a dielectric constant ϵ_u; then by Gauss' law we have that the electric field $\vec{E}_u$ in the medium is given by the relation

$$\vec{E}_u = \frac{\rho_u}{2\epsilon_u}\,\hat{n} \quad , \tag{5.1}$$

where $\hat{n}$ is the normal unit vector outward from the plane. If the plane suffers a local deformation of small aspect, then this should still be a reasonably good approximation for the electric field at distances from the surface small compared to the lateral extent of the deformation.

Similarly, if the surface charge is allowed to vary gradually from one point to another on the surface, then for our purposes the approximation should remain serviceable for distances from the surface small with respect to the scale of variation; such a charge variation would produce a horizontal electric field component close to the surface, but the local field indicated by (5.1) should nevertheless be a fairly good estimate of the normal component of the field at small distances from the surface. The seawater medium with which we are in practice

concerned is not a dielectric material, but, as it is only weakly conducting and in principle the distribution of free charges in the problem is maintained in a steady state by outside sources of EMF (upper atmospheric sources, etc.), it may be considered to be a dielectric material for the purposes of these calculations. The effective dielectric constant of this medium is difficult to estimate, and it is fortunate that its value has no effect on the end results of the calculations. In calculations deriving the surface charge ρ from the field $\vec{E}_0$ within a medium of dielectric constant ϵ it is the ratio (ρ/ϵ) that is solved for, and it is this ratio that is used in turn to compute the correction field to $\vec{E}_0$; provided that the surface charge is used only as an intermediate calculational device, rather than being given any physical significance, any value of ϵ will do provided that it is consistently used. A value of $90\,\epsilon_0$, roughly the value for distilled water at 0°C, would be a good choice if one wishes ρ to have a physically reasonable range of values.

The recommended approximation is, then, given by

$$\rho = -2\epsilon_s \vec{E}_0 \cdot \hat{n} \quad , \tag{5.2}$$

where $\hat{n}$ is the normal unit vector directed outward from the charged surface at a given point, $\vec{E}_0$ is the uncorrected field vector at that point, and ϵ_s is the chosen value for the effective dielectric constant of the seawater. For calculation of the correction field $\vec{E}_1$ one might sweep the surface charge distribution into a number of small piles and use the formula

$$\vec{E}_1(\vec{x}) = \frac{1}{4\pi\epsilon_s} \sum_{i=1}^{N} q_i \frac{\vec{x}-\vec{x_i}}{|\vec{x}-\vec{x_i}|^3} \quad , \tag{5.3}$$

where N is the number of piles, q_i is the accumulated charge in each pile, and $\vec{x_i}$ is the position of each pile. If the surface charge distribution derived from (5.2) is divided sufficiently finely, the resultant error in the field calculations will be smaller than the error of approximation in using (5.2) to get the surface charge distribution. In any case, it is strongly advised to use a streamline tracing program such as is described in section 2 to verify that the above procedure has given an answer acceptable for one's purposes. In the event that the approximate solution falls short of adequacy, it may still usefully serve as a starting point for a charge-redistributing variation program leading to a more exact solution. The electric current density distribution $\vec{J}$ within the ocean is given by

$$\vec{J} = \sigma(\vec{E}_0 + \vec{E}_1) \quad , \tag{5.4}$$

where σ is the electrical conductivity distribution within the ocean.

6. Shallow features on the ocean floor

6.1 Basic mathematics

The shape of any reasonably smooth bottom feature can be described by the superposition of terms of the form

$$\zeta(x,y) = a\ exp(i\vec{k_H}\cdot\vec{x}) \quad , \tag{6.1}$$

$$\vec{k_H} = k\ (cos\theta, sin\theta, 0) \quad , \quad k>0 \quad , \tag{6.2}$$

where ζ is altitude relative to the mean depth of the ocean floor, and the magnetic effects of a single such term may be computed by means of a variation of the mathematics developed in section 3 of chapter 1 for finding the magnetic effects of a shallow wave on the ocean surface. Provided that the relation between bottom profile and associated magnetic effect is linear, the magnetic field due to a bottom profile given by the superposition of a number of terms of the form (6.1) is just the superposition of the fields calculated for the individual terms. It will be seen that, for this linearity to be safely assumed, the amplitude of each term must be somewhat smaller than its wavelength and somewhat smaller than the depth of the ocean, and the electrical conductivity of the seawater at the ocean bottom must be essentially constant over the term's amplitude range.

The ocean bottom feature problem differs from the surface wave problem discussed in section 3 of chapter 1 in that the scale of the induced electrical current density distribution perturbations could reasonably be a significant fraction of the depth of the ocean, and the electrical conductivity of the ocean cannot automatically be considered uniform throughout the ocean. Keeping this in mind in the adaptation of the surface wave mathematics to the present problem, we write for the electrical current density distribution $\vec{J}$

$$\vec{J} = \sigma\ \vec{E} \tag{6.3}$$

$$\vec{E} = -\nabla\phi \quad ; \tag{6.4}$$

the divergence condition

$$\nabla\cdot\vec{E} = 0 \tag{6.5}$$

then gives us from (6.4)

$$\nabla^2\phi = 0 \quad . \tag{6.6}$$

We assume an electric field $\vec{E_0}$, induced by sources of EMF outside of the ocean, that would be

the field within the ocean in the absence of bottom features; it is taken to be horizontal and uniform within the ocean, with the form

$$\vec{E}_0 = E_0\hat{x} \quad . \tag{6.7}$$

We then have for the general solution to (6.6)

$$\phi = E_0 x + A\ exp(i\vec{k}_1\cdot\vec{x}) + B\ exp(i\vec{k}_2\cdot\vec{x}) \tag{6.8}$$

$$\vec{k}_1 = k\ (cos\theta, sin\theta, -i) \tag{6.9}$$

$$\vec{k}_2 = k\ (cos\theta, sin\theta, i) \quad , \tag{6.10}$$

and hence

$$\vec{E} = E_0\hat{x} + \vec{k}_1\, i\ A\ exp(i\vec{k}_1\cdot\vec{x}) + \vec{k}_2\, i\ B\ exp(i\vec{k}_2\cdot\vec{x}) \quad . \tag{6.11}$$

The term in A represents a field component that grows exponentially upward, and the term in B represents a component that damps exponentially upward; if the ocean were assumed to be infinitely deep, then the term in A would vanish.

Let us define the vertical coordinate so that the mean level of the ocean floor is at $z=0$ and the level of the ocean surface is at $z=d$. The boundary condition at the surface, that there be no electrical current flow through the level surface, is

$$\vec{J}\cdot\hat{z} = 0 \quad at \quad z=d \quad , \tag{6.12}$$

which implies through (6.3) that

$$\vec{E}\cdot\hat{z} = 0 \quad at \quad z=d \quad ; \tag{6.13}$$

from this condition and (6.11) we have that

$$A = B\ exp(-2kd) \quad . \tag{6.14}$$

The corresponding boundary condition at the bottom is

$$\vec{J}\cdot\vec{\tau} = 0 \quad at \quad z=\zeta(x,y) \quad , \tag{6.15}$$

$$\vec{\tau} = \left[-\frac{\partial\zeta}{\partial x}\ ,\ -\frac{\partial\zeta}{\partial y}\ ,\ 1 \right] \quad , \tag{6.16}$$

where $\vec{\tau}$ is a vector normal to the ocean floor at $z=\zeta(x,y)$ as defined by (6.1). Once again, from (6.3) we have

$$\vec{E}\cdot\vec{r} = 0 \quad at \quad z=\zeta \quad ; \tag{6.17}$$

using (6.11) for $\vec{E}$, assuming that

$$|ka| << 1 \quad , \tag{6.18}$$

and discarding terms quadratic or higher in (ka), we get from (6.17)

$$B = -i\, a\, E_0 \chi \cos\theta \quad , \tag{6.19}$$

where

$$\chi = \frac{1}{1 - exp(-2kd)} \quad . \tag{6.20}$$

We then have from (6.11) for the electric field within the ocean subject to (6.18)

$$\vec{E} = E_0 \{\hat{x} + a\, \vec{k_1} \chi \cos\theta\, exp(-2kd)\, exp(i\vec{k_1}\cdot\vec{x}) + a\, \vec{k_2} \chi \cos\theta\, exp(i\vec{k_2}\cdot\vec{x})\} \quad . \tag{6.21}$$

In the course of this derivation one finds that, in order for the discarding of the terms higher than linear in (ka) to be valid, one must also assume that $d >> |\zeta|$. In particular, if $a \geq \frac{1}{2}d$ then the result (6.19) becomes grossly invalid.

From equations (2.1) and (6.3) we have for the magnetic field $\vec{B}(\vec{x_0})$ at the position $\vec{x_0}$

$$\vec{B}(\vec{x_0}) = \frac{\mu_0}{4\pi} \int_{-\infty}^{\infty} dx \int_{-\infty}^{\infty} dy \int_{\zeta}^{d} dz\, \sigma(z) \frac{\vec{E}(\vec{x}) \times (\vec{x_0}-\vec{x})}{|\vec{x_0}-\vec{x}|^3} \quad , \tag{6.22}$$

where the electrical conductivity of the seawater is assumed not to vary laterally. For purposes of calculation we find it expedient to separate (6.22) into two parts;

$$\vec{B}(\vec{x_0}) = \vec{B_S}(\vec{x_0}) + \vec{B_V}(\vec{x_0}) \tag{6.23}$$

$$\vec{B_S} = \frac{\mu_0}{4\pi} \int_{-\infty}^{\infty} dx \int_{-\infty}^{\infty} dy \int_{\zeta}^{0} dz\, \sigma(z) \frac{\vec{E}(\vec{x}) \times (\vec{x_0}-\vec{x})}{|\vec{x_0}-\vec{x}|^3} \tag{6.24}$$

$$\vec{B_V}(\vec{x_0}) = \frac{\mu_0}{4\pi} \int_{-\infty}^{\infty} dx \int_{-\infty}^{\infty} dy \int_{0}^{d} dz\, \sigma(z) \frac{\vec{E}(\vec{x}) \times (\vec{x_0}-\vec{x})}{|\vec{x_0}-\vec{x}|^3} \quad . \tag{6.25}$$

If we expand the integrand of (6.24) in powers of z about z=0, we find that only the term constant with respect to z contributes to $\vec{B_S}(\vec{x_0})$ less than quadratically in powers of (ka). Accordingly, retaining only this term and letting σ_B be the value of $\sigma(z)$ at z=0, we have for (6.24) to first order

$$\vec{B_S}(\vec{x_0}) = \frac{\mu_0 \sigma_B E_0}{4\pi} \int_{-\infty}^{\infty} dx \int_{-\infty}^{\infty} dy \frac{\{0, z_0, (y-y_0)\}}{\{(x-x_0)^2 + (y-y_0)^2 + z_0^2\}^{3/2}} \zeta(x,y) \quad . \tag{6.26}$$

Note that retaining only terms up to first order in (ka) requires us to disregard the effects of variation of $\sigma(z)$ over the amplitude range of the bottom feature. Making then the substitutions

$$u = (x-x_0)\cos\theta + (y-y_0)\sin\theta \tag{6.27}$$

$$v = (y-y_0)\cos\theta - (x-x_0)\sin\theta \tag{6.28}$$

$$u_0 = x_0\cos\theta + y_0\sin\theta \quad , \tag{6.29}$$

we get from (6.26)

$$\vec{B_S}(\vec{x_0}) = \frac{\mu_0\sigma_B E_0 a}{4\pi}\exp(iku_0)\int_{-\infty}^{\infty} du \int_{-\infty}^{\infty} dv \frac{(0,z_0,u\sin\theta + v\cos\theta)}{(u^2+v^2+z_0^2)^{3/2}}\exp(iku) \quad , \tag{6.30}$$

from which integration over v gives, by use of symmetry and equation (3.30) of chapter 1,

$$\vec{B_S}(\vec{x_0}) = \frac{\mu_0\sigma_B E_0 a}{2\pi}\exp(iku_0)\int_{-\infty}^{\infty} du \frac{(0,z_0,u\sin\theta)}{u^2+z_0^2}\exp(iku) \quad . \tag{6.31}$$

This integral yields easily to contour integration, giving for $z_0>0$ (the only region of practical interest)

$$\vec{B_S}(\vec{x_0}) = \tfrac{1}{2}\mu_0\sigma_B E_0 a \exp(iku_0)\exp(-kz_0)(0,1,i\sin\theta) \quad . \tag{6.32}$$

We find it convenient also to further separate $\vec{B_V}$ into the parts

$$\vec{B_V}(\vec{x_0}) = \vec{B_{VU}}(\vec{x_0}) + \vec{B_{VP1}}(\vec{x_0}) + \vec{B_{VP2}}(\vec{x_0}) \quad , \tag{6.33}$$

where $\vec{B_{VU}}$ is concerned with the uniform component of (6.21), $\vec{B_{VP1}}$ with the perturbation term in $\vec{k_1}$, and $\vec{B_{VP2}}$ with the perturbation term in $\vec{k_2}$. $\vec{B_{VU}}$ has already been evaluated in section 2 of chapter 1. For $\vec{B_{VP1}}$ we have

$$\vec{B_{VP1}}(\vec{x_0}) = \frac{\mu_0 E_0 a\ k\ \chi\cos\theta}{4\pi}\exp(-2kd)\int_{-\infty}^{\infty} dx \int_{-\infty}^{\infty} dy \int_0^d dz \tag{6.34}$$

$$\times\,\sigma(z)\exp(i\vec{k_H}\cdot\vec{x})\exp(kz)\frac{(\cos\theta,\sin\theta,-i)\times(\vec{x_0}-\vec{x})}{|\vec{x_0}-\vec{x}|^3} \quad .$$

Using the substitutions (6.27) through (6.29) together with the definitions

$$\hat{u} = \hat{x}\cos\theta + \hat{y}\sin\theta \tag{6.35}$$

$$\hat{v} = \hat{y}\cos\theta - \hat{x}\sin\theta \quad , \tag{6.36}$$

this becomes

$$\vec{B}_{VP1}(\vec{x}_0) = \frac{i\mu_0 E_0 a\ k\ \chi\ \cos\theta}{4\pi} \exp(-2kd)\ \exp(iku_0) \int_{-\infty}^{\infty} du \int_{-\infty}^{\infty} dv \int_0^d dz \tag{6.37}$$

$$\times\ \sigma(z)\ \exp(iku)\ \exp(kz)\ \frac{\hat{v}\{u - i(z-z_0)\} - v(\hat{u} - i\hat{z})}{\{u^2+v^2+(z-z_0)^2\}^{3/2}}$$

Integration over v then gives

$$\vec{B}_{VP1}(\vec{x}_0) = \frac{i\mu_0 E_0 a\ k\ \chi\ \cos\theta}{2\pi} \exp(-2kd)\ \exp(iku_0)\ \hat{v} \tag{6.38}$$

$$\times \int_{-\infty}^{\infty} du \int_0^d dz\ \frac{\sigma(z)\exp(iku)\exp(kz)}{u + i(z-z_0)} \quad ,$$

which yields readily to contour integration over u to give

$$\vec{B}_{VP1}(x_0) = -\mu_0 E_0 a\ k\ \chi\ \cos\theta\ \exp(iku_0)\ \exp(-kz_0)\ \hat{v} \tag{6.39}$$

$$\times \int_0^{\min(z_0,d)} \sigma(z)\ \exp\{-2k(d-z)\}\ dz \quad .$$

For $\vec{B}_{VP2}$ we have

$$\vec{B}_{VP2}(\vec{x}_0) = \frac{\mu_0 E_0 a\ k\ \chi\ \cos\theta}{4\pi} \int_{-\infty}^{\infty} dx \int_{-\infty}^{\infty} dy \int_0^d dz \tag{6.40}$$

$$\times\ \sigma(z)\ \exp(i\vec{k}_H \cdot \vec{x})\ \exp(-kz)\ \frac{(\cos\theta, \sin\theta, i) \times (\vec{x}_0 - \vec{x})}{|\vec{x}_0 - \vec{x}|^3} \quad ,$$

which by a similar process reduces to

$$\vec{B}_{VP2}(\vec{x}_0) = \mu_0 E_0 a\ k\ \chi\ \cos\theta\ \exp(iku_0)\ \exp(-kz_0)\ \hat{v} \tag{6.41}$$

$$\times \int_{\min(z_0,d)}^d \sigma(z)\ \exp\{-2k(z-z_0)\}\ dz \quad .$$

For the special case in which the electrical conductivity of the seawater has the constant value σ_0 throughout the ocean, over the depth range $0 < z_0 < d$ the expressions (6.39) and (6.41) for $\vec{B}_{VP1}$ and $\vec{B}_{VP2}$ respectively become

$$\vec{B}_{VP1}(x_0) = -\mu_0\sigma_0 E_0 a\ \chi\ \cos\theta\ \exp(-2kd)\ \exp(iku_0)\ \sinh(kz_0)\ \hat{v} \tag{6.42}$$

$$\vec{B}_{VP2}(x_0) = \mu_0\sigma_0 E_0 a\ \chi\ \cos\theta\ \exp(-kd)\ \exp(iku_0)\ \sinh\{k(d-z_0)\}\ \hat{v} \quad , \tag{6.43}$$

and over the depth range $z_0 > d$ they become

$$\vec{B_{VP1}}(\vec{x_0}) = -\tfrac{1}{2}\,\mu_0\sigma_0 E_0 a\,\cos\theta\,\exp(iku_0)\,\exp(-kz_0)\,\hat{v} \tag{6.44}$$

$$\vec{B_{VP2}}(\vec{x_0}) = 0 \quad . \tag{6.45}$$

For $z_0 > d$, the total field minus the uniform component $\vec{B_{VU}}$, derived by adding together (6.32) and (6.44), is given for a single term by

$$\vec{B_T}(\vec{x_0}) = \tfrac{1}{2}\,\mu_0\sigma_0 E_0 a\,\exp(iku_0)\,\exp(-kz_0)\,\sin\theta\,(\cos\theta, \sin\theta, i) \quad . \tag{6.46}$$

6.2 Application to two-dimensional bottom features

If we represent a two-dimensional bottom feature in the form

$$\zeta(u_0) = \int_{-\infty}^{\infty} a(k)\, exp(iku_0)\, dk \quad , \tag{6.47}$$

where the a(k) for positive values of k are the coefficients for terms for which $-\frac{\pi}{2} \leqslant \theta \leqslant \frac{\pi}{2}$, and the a(k) for negative values of k are the coefficients for terms for which θ is in the opposite direction, we then have for $\vec{B_S}$ for $z_0>0$

$$\vec{B_S}(x_0) = \tfrac{1}{2}\mu_0\sigma_0 E_0 \{ \hat{y} \int_0^{\infty} [a(k)exp(iku_0)+a(-k)exp(-iku_0)]\, exp(-kz_0)\, dk \tag{6.48}$$

$$+ i \sin\theta\, \hat{z} \int_0^{\infty} [a(k)exp(iku_0)-a(-k)exp(-iku_0)]exp(-kz_0)\, dk \} \quad .$$

For $0<d<z_0$ we have for $\vec{B_{VP1}}$ and $\vec{B_{VP2}}$

$$\vec{B_{VP1}}(\vec{x_0}) = -\mu_0\sigma_0 E_0 \cos\theta\ (-\sin\theta,\cos\theta,0) \int_0^{\infty} [a(k)exp(iku_0)+a(-k)exp(-iku_0)] \tag{6.49}$$

$$\times \frac{exp(-2kd)sinh(kz_0)}{1-exp(-2kd)}\, dk$$

$$\vec{B_{VP2}}(\vec{x_0}) = \mu_0\sigma_0 E_0 \cos\theta\ (-\sin\theta,\cos\theta,0) \int_0^{\infty} [a(k)exp(iku_0)+a(-k)exp(-iku_0)] \tag{6.50}$$

$$\times \frac{exp(-kd)\sinh\{k(d-z_0)\}}{1-exp(-2kd)}\, dk \quad ,$$

and for $z_0>d$ we have for $\vec{B_{VP}}$

$$\vec{B_{VP}}(\vec{x_0}) = \vec{B_{VP1}}(\vec{x_0}) = -\tfrac{1}{2}\mu_0\sigma_0 E_0 \cos\theta\ (-\sin\theta,\cos\theta,0) \int_0^{\infty} \tag{6.51}$$

$$\times [a(k)exp(iku_0)+a(-k)exp(-iku_0)]\, exp(-kz_0)\, dk \quad .$$

The bottom features to which this method is most easily applied are low ridges and shallow trenches, which may be roughly approximated by a Gaussian profile of the form

$$\zeta(u_0) = A\ \exp\left[-\frac{u_0^2}{2\alpha^2} \right] \quad , \tag{6.52}$$

where A is positive for a ridge and negative for a trough, and α is the effective half-width of the feature (see figure 2.2); to properly satisfy the condition (6.18), α should be somewhat larger than A. If (6.52) is expressed in the form (6.47), then we have for a(k)

$$a(k) = \frac{A\alpha}{\sqrt{2\pi}} \exp\left(-\frac{\alpha^2 k^2}{2} \right) \quad . \tag{6.53}$$

When expression (6.46) is adapted to bottom features expressed in the form (6.47), it becomes

$$\vec{B_T}(\vec{x_0}) = \tfrac{1}{2}\,\mu_0\sigma_0 E_0 A\ \{\sin\theta\ (\cos\theta,\sin\theta,0)\ I_1(\vec{x_0},\alpha) - \sin\theta\ \hat{z}\ I_2(\vec{x_0},\alpha)\} \tag{6.54}$$

$$I_1(\vec{x_0},\alpha) = A^{-1} \int_0^\infty \{a(k)\exp(iku_0) + a(-k)\exp(-iku_0)\}\ \exp(-kz_0)\ dk \tag{6.55}$$

$$I_2(\vec{x_0},\alpha) = i\,A^{-1} \int_0^\infty \{a(k)\exp(iku_0) - a(-k)\exp(-iku_0)\}\ \exp(-kz_0)\ dk \quad . \tag{6.56}$$

Substitution of (6.53) gives for I_1 and I_2

$$I_1(\vec{x_0},\alpha) = \frac{2\alpha}{\sqrt{2\pi}} \int_0^\infty \exp\left(-\frac{\alpha^2 k^2}{2} - z_0 k \right) \cos(ku_0)\ dk \tag{6.57}$$

$$I_2(\vec{x_0},\alpha) = \frac{2\alpha}{\sqrt{2\pi}} \int_0^\infty \exp\left(-\frac{\alpha^2 k^2}{2} - z_0 k \right) \sin(ku_0)\ dk \quad . \tag{6.58}$$

These integrals are dealt with as Fourier cosine and sine transforms in Erde'lyi et al., 1954, v. 1 (sec. 1.4, eq. 16, p. 15 and sec. 2.4, eq. 27, p. 74), and have the solutions

$$I_1(\vec{x_0},\alpha) = \tfrac{1}{2}\{f_+(\vec{x_0},\alpha) + f_-(\vec{x_0},\alpha)\} \tag{6.59}$$

$$I_2(\vec{x_0},\alpha) = i/2\,\{f_+(\vec{x_0},\alpha) - f_-(\vec{x_0},\alpha)\} \quad , \tag{6.60}$$

where

$$f_+(\vec{x_0},\alpha) = \exp(s_+^2)\ erfc(s_+) \tag{6.61}$$

$$s_+ = \frac{z_0 + iu_0}{\sqrt{2}\alpha} \quad , \quad \alpha > 0 \quad , \quad z_0 > d \tag{6.62}$$

$$f_-(\vec{x_0},\alpha) = \exp(s_-^2)\ erfc(s_-) \tag{6.63}$$

$$s_- = \frac{z_0 - iu_0}{\sqrt{2}\alpha} \quad , \quad \alpha > 0 \quad , \quad z_0 > d \quad , \tag{6.64}$$

with the function $erfc(x)$ being defined such that on the positive real axis

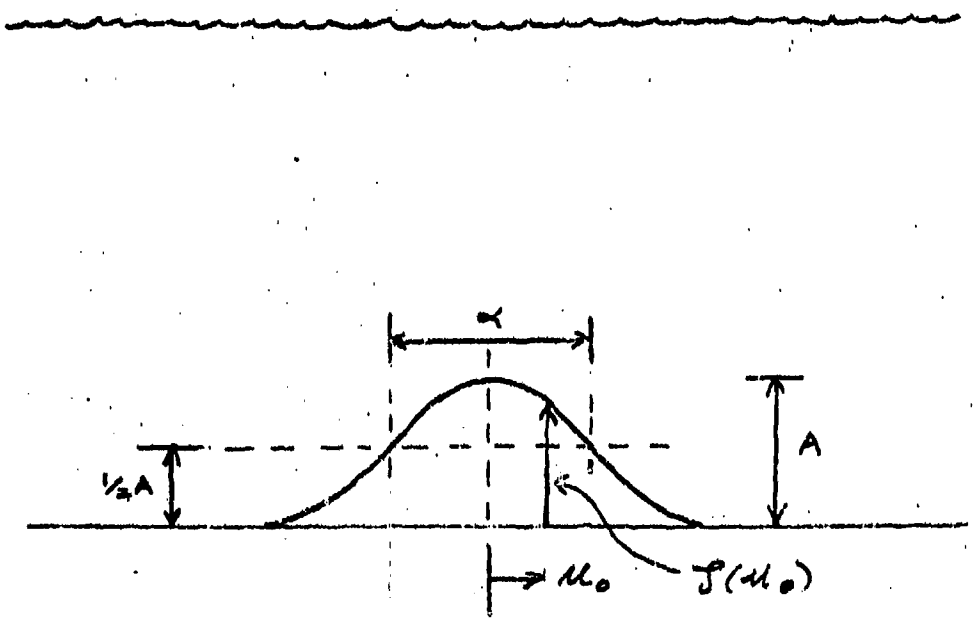

FIGURE 2.2

Illustration of the parameters describing a Gaussian ridge or trough on the ocean floor, as used in equation (6.52). A is the ridge height (positive for a ridge, negative for a trough), α is the half-width of the ridge, u_0 is the perpendicular distance from the ridge axis, and ζ is the vertical coordinate of the ridge surface as a function of u_0.

$$erfc(x) = \frac{2}{\sqrt{\pi}} \int_x^\infty exp(-t^2)\, dt \quad . \tag{6.65}$$

Note that f_+ and f_- are complex conjugates of each other, and that therefore both (6.59) and (6.60) will always be real-valued. The integrals I_1 and I_2 are plotted in figure 2.3 for the special cases of (α/z_0) equal to 0.2, 0.4, and 0.8, for values of (u_0/α) ranging from 0.0 to 6.0; I_1 is symmetric with respect to u_0, and I_2 is antisymmetric with respect to u_0. Expressions found useful for the evaluation of (6.61) and (6.63) were the formulas 7.1.5 on page 297 of Abramowitz and Stegun and 7.1.23 on page 298 of same, the former being appropriate for small absolute values of the argument and the latter for large values; it was found that if 10 terms were retained in the latter expansion then there was a region of overlap of satisfactory size in the z-plane where neither of the corresponding expressions for $\exp(z^2)erfc(z)$ diverged and both gave the same value to several significant places.

As a practical example, we consider the case of a submarine canyon on the continental shelf. We assume an electrical conductivity for the ocean of 3.3 S/m, and as a calculational convenience we consider the special case in which the feature is parallel to the inducing EMF (such a feature running perpendicular to the inducing EMF yields a zero anomalous magnetic field above the ocean surface, although an anomalous field is present below the surface). Also, in order to satisfy the approximations made in deriving this method, the feature must be somewhat broader than it is deep and somewhat less in vertical dimension than the depth of the ocean. We take the value of the inducing EMF to be 1.0 $\mu V/m$, a reasonable value for an electromagnetically quiet day. The submarine canyon extends to a depth 20 meters below an otherwise level ocean floor at a depth of 100 meters beneath the ocean surface, and has a Gaussian shape with a standard deviation of 80 meters. The anomalous magnetic field due to the undersea canyon is plotted in figure 2.4, normalized against the spatially uniform magnetic field calculated from equation (2.5) for such an ocean and such an inducing EMF in the absence of any bottom feature; this field is $-2.07\times10^{-10}\wp$ tesla. Note that while the anomalous field is, at its strongest, no more than about a tenth the strength of the uniform field upon which it is superposed, the spatial gradient properties of the anomalous field should make it easy to distinguish from the uniform background.

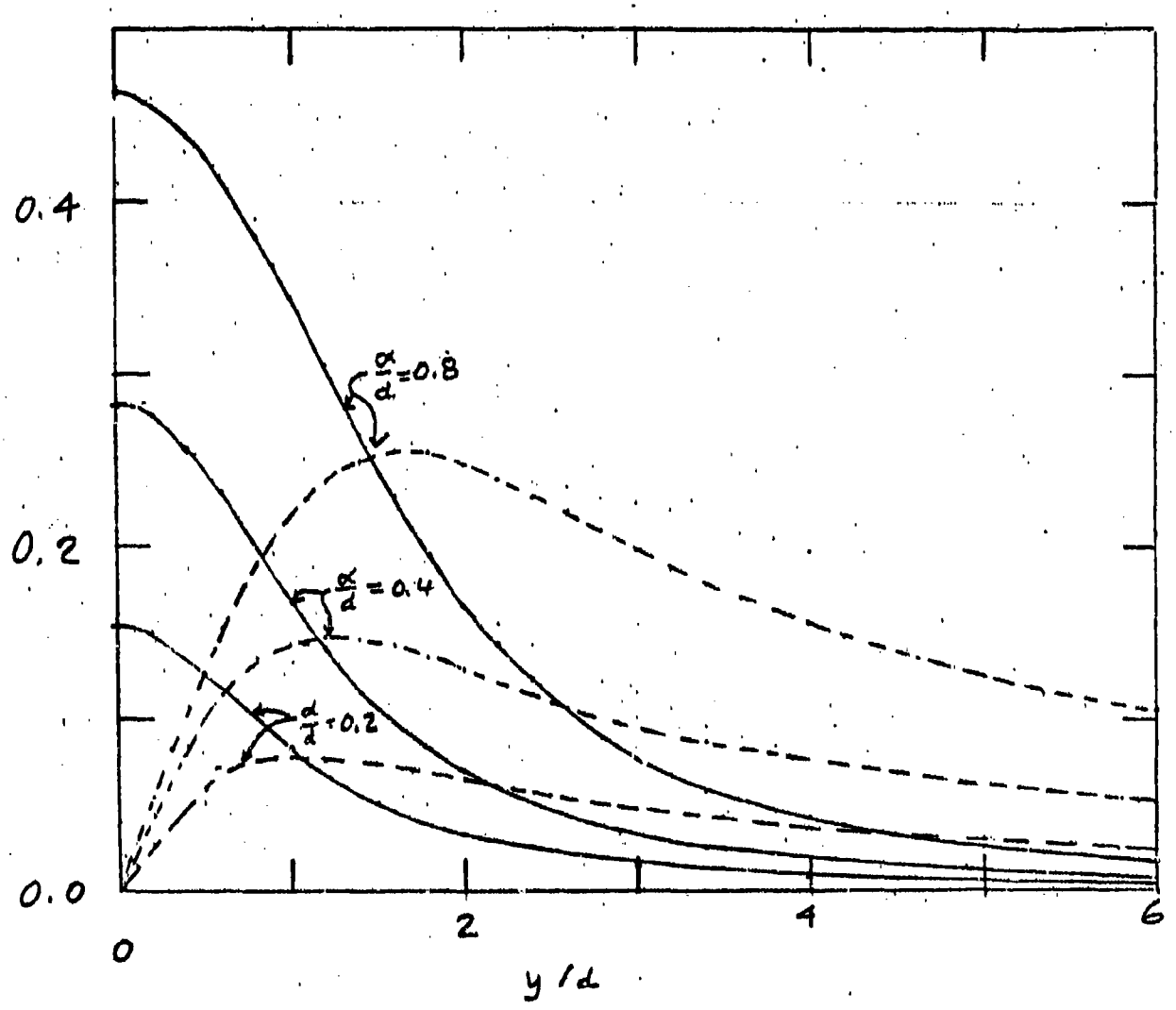

FIGURE 2.3

The integrals I_1 (solid line) and I_2 (dashed line) according to equations (6.57) and (6.58), for three different ridge widths. Notations are α = ridge half-width, d = depth of ocean, and y = lateral distance from center of ridge.

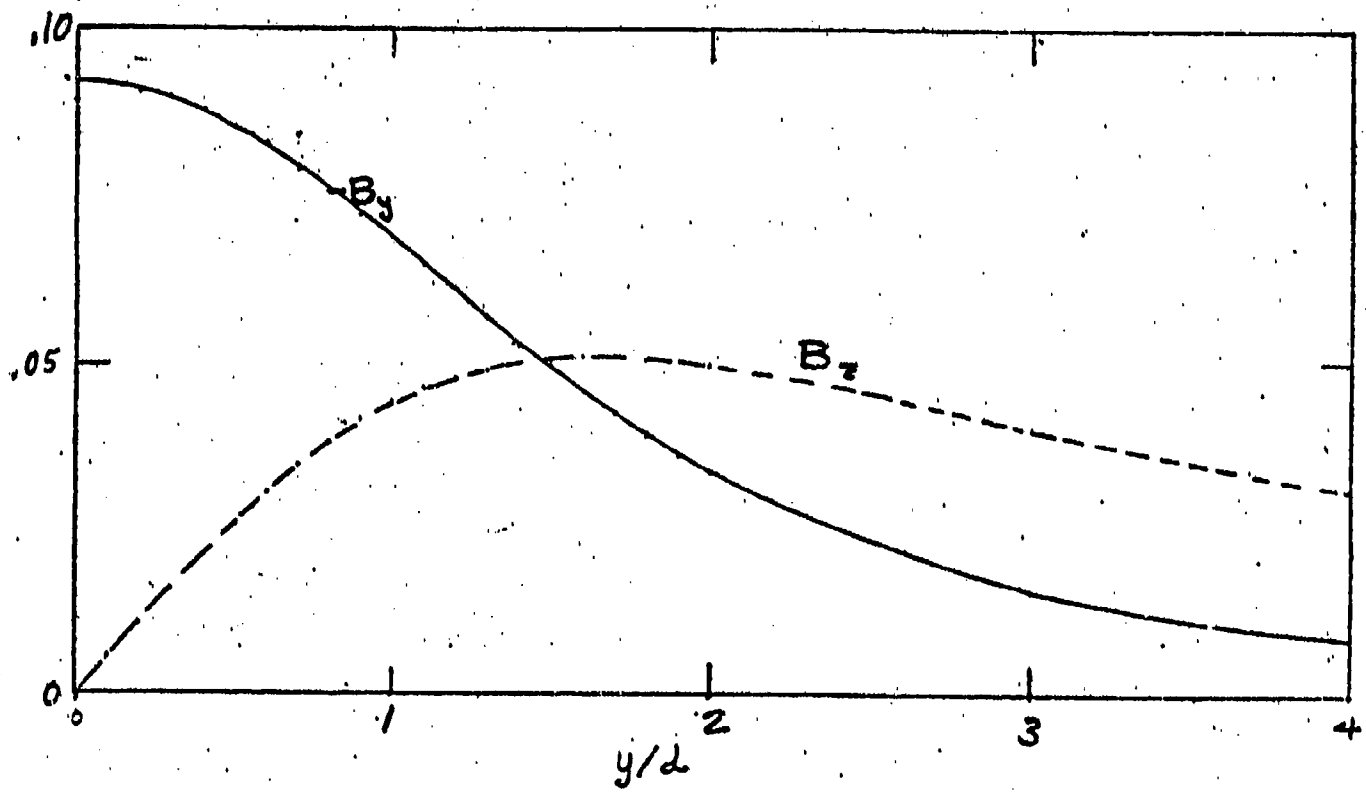

FIGURE 2.4

The anomalous magnetic field components B_y and B_z induced, at the sea surface over a submarine canyon incised parallel to the x-axis into a level seafloor, by an electric field running parallel to the axis of the canyon, as given by equation (6.53). The field components are normalized against the reference B_y field which would be induced by the primary electric field in the absence of the canyon, with a completely level seafloor. For this example the ratio of α, the canyon half-width, to d, the depth on the level part of the ocean floor, is $\alpha/d = 0.8$, and the ratio of canyon depth to water depth is 0.2. The distance y is the lateral distance from the axis of the canyon.

6.3 Application to three-dimensional bottom features

Let us now suppose that we have a three-dimensional bottom feature whose shape is given by the function $\zeta(x,y)$, which we write as a Fourier transform;

$$\zeta(x,y) = \int_{-\infty}^{\infty} dk_x \int_{-\infty}^{\infty} dk_y \; a(k_x,k_y) \exp[i(k_x x + k_y y)] \quad . \tag{6.66}$$

If the direction of positive x is chosen to be parallel to the uniform current-inducing electric field within the ocean, then we can write

$$k_x = k\cos\theta \quad , \quad k_y = k\sin\theta \quad , \quad k^2 = k_x^2 + k_y^2 \quad , \tag{6.67}$$

where k is a positive real scalar, which will transform the Cartesian coordinate frame in which (6.66) is expressed into the cylindrical coordinate system in which (6.46) is expressed. Equation (6.46) is the expression for the anomalous magnetic field $\vec{B_T}(\vec{x_0})$ above the ocean surface due to a bottom feature given, in Cartesian coordinates, by $a\exp[i(k_x x_0 + k_y y_0)]$; as (6.66) is a superposition of such terms, we thus have for $\vec{B_A}(\vec{x})$ the anomalous field above the ocean surface due to the bottom feature $\zeta(x,y)$

$$\vec{B_A}(\vec{x}) = \frac{\mu_0\sigma_0 E_0}{2} \int_{-\infty}^{\infty} dk_x \int_{-\infty}^{\infty} dk_y \; A(k_x,k_y) \exp[i(k_x x + k_y y)] \exp(-kz) \tag{6.68}$$

$$\times \frac{k_y(k_x,k_y,i)}{k^2} \quad ,$$

or, in cylindrical coordinates,

$$\vec{B_A}(\vec{x}) = \frac{\mu_0\sigma_0 E_0}{2} \int_0^{\infty} k\,dk \int_0^{2\pi} d\theta \; a(k\cos\theta, k\sin\theta) \tag{6.69}$$

$$\times \exp[ik(x\cos\theta + y\sin\theta)] \exp(-kz) \sin\theta(\cos\theta,\sin\theta,i) \quad .$$

In cases where $\zeta(x,y)$ is cylindrically symmetric, $a(k\cos\theta, k\sin\theta)$ is a function of k only, and judicious use of the identity

$$2\pi J_0(k\rho) = \int_0^{2\pi} d\theta \exp[ik(x\cos\theta + y\sin\theta)] \quad , \quad \rho^2 = x^2 + y^2 \tag{6.70}$$

allows (6.69) to be written in the form

$$\vec{B}_A(\vec{r}) = -\pi\mu_0\sigma_0 E_0 \int_0^\infty k\, a(k)\, \exp(-kz) \left[\frac{1}{k^2}\frac{\partial^2}{\partial x \partial y}\,,\ \frac{1}{k^2}\frac{\partial^2}{\partial y^2}\,,\ \frac{-1}{k}\frac{\partial}{\partial y} \right] \tag{6.71}$$

$$\times J_0(k\rho)\, dk \quad ;$$

from here, use of the standard Bessel function recurrence relations gives

$$\vec{B}_A(\vec{r}) = -\pi\mu_0\sigma_0 E_0 \int_0^\infty k\, a(k)\, \exp(-kz) \left[\frac{xy}{\rho^2} J_2(k\rho)\,,\ \frac{y^2}{\rho^2} J_2(k\rho) - \frac{1}{k\rho} J_1(k\rho) \right. \tag{6.72}$$

$$\left. \frac{y}{\rho} J_1(k\rho) \right] dk \quad .$$

If the bottom feature has the Gaussian form

$$\zeta(x,y) = A\, \exp\left\{ \frac{-(x^2+y^2)}{2\alpha^2} \right\} \quad , \tag{6.73}$$

then we have for its Fourier transform

$$a(k_x,k_y) = \frac{A\alpha^2}{2\pi} \exp\left\{ \frac{-(k_x^2+k_y^2)}{2} \right\} = \frac{A\alpha^2}{2\pi} \exp\left\{ \frac{\alpha^2 k^2}{2} \right\} = a(k) \quad , \tag{6.74}$$

and (6.72) becomes

$$\vec{B}_A(\vec{r}) = -\frac{\mu_0\sigma_0 E_0 A\alpha^2}{2} \int_0^\infty k\, \exp\left\{ -\frac{\alpha^2 k^2}{2} \right\} \exp(-kz) \tag{6.75}$$

$$\times \left[\frac{xy}{\rho^2} J_2(k\rho)\,,\ \frac{y^2}{\rho^2} J_2(k\rho) - \frac{1}{k\rho} J_1(k\rho)\,,\ \frac{y}{\rho} J_1(k\rho) \right] dk \quad ,$$

which with the substitution

$$\nu = k\rho \tag{6.76}$$

turns into

$$\vec{B}_A(\vec{r}) = -\frac{\mu_0\sigma_0 E_0 A\alpha^2}{2\rho^2} \left[\frac{xy}{\rho^2} I_3(\vec{r},\alpha)\,,\ \frac{y^2}{\rho^2} I_3(\vec{r},\alpha) - I_1(\vec{r},\alpha)\,,\ \frac{y}{\rho} I_2(\vec{r},\alpha) \right] \quad , \tag{6.77}$$

where

$$I_1(\vec{r},\alpha) = \int_0^\infty \exp\left\{ -\frac{\alpha^2}{\rho^2}\frac{\nu^2}{2} \right\} \exp\left\{ -\frac{z}{\rho}\nu \right\} J_1(\nu)\, d\nu \quad , \tag{6.78}$$

$$I_2(\mathcal{R},\alpha) = \int_0^\infty \nu \exp\left[-\frac{\alpha^2}{\rho^2}\frac{\nu^2}{2} \right] \exp\left[-\frac{z}{\rho}\nu \right] J_1(\nu)\, d\nu \quad , \tag{6.79}$$

and

$$I_3(\mathcal{R},\alpha) = \int_0^\infty \nu \exp\left[-\frac{\alpha^2}{\rho^2}\frac{\nu^2}{2} \right] \exp\left[-\frac{z}{\rho}\nu \right] J_2(\nu)\, d\nu \quad . \tag{6.80}$$

These integrals may be straightforwardly evaluated in the two regimes $\rho \ll \alpha$ and $\rho \gg \alpha$. In the first case, the Gaussian in the integrands has gone to virtually zero while ν is still very small; accordingly, if the Bessel functions in the integrands are expressed as power series expansions, only a small number of terms from each expansion are required to adequately approximate the values of the integrals. The basic integral for these calculations is

$$S_n(\mathcal{R},\alpha) = \int_0^\infty \nu^n \exp\left[-\frac{\alpha^2}{\rho^2}\frac{\nu^2}{2} \right] \exp\left[-\frac{z}{\rho}\nu \right] d\nu \tag{6.81}$$

$$= (n!) \left(\frac{\rho}{\alpha} \right)^{n+1} \exp\left[\frac{z^2}{4\alpha^2} \right] D_{-(n+1)}(z/\alpha)$$

(Erde'lyi et al., 1954, v. 1, sec. 4.5, eq. 24, p. 146), where n is a nonnegative integer and the $D_n(x)$ are parabolic cylinder functions (see Erde'lyi et al., 1955, v. 2, sec. 8, p. 115), and the appropriate power series expansion for Bessel functions of integer order is

$$J_n(x) = \sum_{k=0}^{\infty} \frac{(-1)^k}{(k!)[(n+k)!]} \left(\frac{x}{2} \right)^{n+2k} \quad . \tag{6.82}$$

Accordingly, from the integral representations I_1, I_2, and I_3 we have

$$I_1(\mathcal{R},\alpha) = \sum_{k=0}^{\infty} \frac{(-1)^k}{2^{2k+1}(k!)[(k+1)!]} S_{2k+1}(\mathcal{R},\alpha) \quad , \tag{6.83}$$

$$I_2(\mathcal{R},\alpha) = \sum_{k=0}^{\infty} \frac{(-1)^k}{2^{2k+1}(k!)[(k+1)!]} S_{2k+2}(\mathcal{R},\alpha) \quad , \tag{6.84}$$

and

$$I_3(\mathcal{R},\alpha) = \sum_{k=0}^{\infty} \frac{(-1)^k}{2^{2k+2}(k!)[(k+2)!]} S_{2k+3}(\mathcal{R},\alpha) \quad . \tag{6.85}$$

To generate the necessary parabolic cylinder functions, we have the recurrence relation

$$D_{n+1}(x) - x\, D_n(x) + n\, D_{n-1}(x) = 0 \tag{6.86}$$

(ibid., sec. 8.3, eq. 14, p. 119), and the functions

$$D_{-1}(x) = \sqrt{\frac{\pi}{2}}\,\exp\left[\frac{x^2}{4}\right]\,erfc\left(\frac{x}{\sqrt{2}}\right) \quad , \tag{6.87}$$

and

$$D_{-2}(x) = \exp\left[-\frac{x^2}{4}\right]\left\{1 - \sqrt{\frac{\pi}{2}}\,x\,\exp\left[\frac{x^2}{2}\right]\,erfc\left(\frac{x}{\sqrt{2}}\right)\right\} \tag{6.88}$$

$$= \exp\left[-\frac{x^2}{4}\right] - x\,D_{-1}(x) \quad ,$$

where $erfc\,(x)$, the complementary error function, is as given in equation (6.65) of the last section. Expressions (6.87) and (6.88) were found by comparison of (6.81) for the cases $n=0$ and $n=1$ with the equivalent expressions in Grobner (sec. 312, eqs. 10(a) and 10(b), p. 57).

From (6.81) and (6.86) we have the recurrence relation

$$S_n(\rho,z,\alpha) = (n-1)\left(\frac{\rho}{\alpha}\right)^2 S_{n-2}(\rho,z,\alpha) - \left(\frac{\rho z}{\alpha^2}\right) S_{n-1}(\rho,z,\alpha) \quad , \tag{6.89}$$

and from (6.81) and (6.87) and (6.88) respectively we have

$$S_0(\rho,z,\alpha) = \left[\frac{\rho}{\alpha}\right]\sqrt{\frac{\pi}{2}}\,\exp\left[\frac{z^2}{2\alpha^2}\right]\,erfc\left[\frac{z}{\sqrt{2}\alpha}\right] \tag{6.90}$$

and

$$S_1(\rho,z,\alpha) = \left[\frac{\rho}{\alpha}\right]^2\left\{1 - \sqrt{\frac{\pi}{2}}\left[\frac{z}{\alpha}\right]\exp\left[\frac{z^2}{2\alpha^2}\right]\,erfc\left[\frac{z}{\sqrt{2}\alpha}\right]\right\} \tag{6.91}$$

$$= \left[\frac{\rho}{\alpha}\right]^2 - \left[\frac{\rho z}{\alpha^2}\right] S_0(\rho,z,\alpha) \quad .$$

In evaluating the complementary error function, the approximate expression (7.1.26) on page 299 of Abramowitz and Stegun, good to high precision anywhere along the positive real axis, was found particularly useful.

In the limit of $\rho \to 0$ it is seen that I_1, I_2, and I_3 all vanish; however, in the magnetic field expression (6.77) which uses these values ρ appears in denominators taken to various powers, and it turns out that this expression does not vanish in this limit. Referring to the

expansions (6.83), (6.84), and (6.85), we insert them into (6.77) and discard any resulting terms in positive powers of ρ, to get

$$\lim_{\rho\to 0}\vec{B}_A(\vec{x}) = -\frac{A\alpha^2\mu_0\sigma_0 E_0}{4}\left[\frac{xy}{4\rho^4}S_3(\rho,z,\alpha),\ \frac{y^2}{4\rho^4}S_3(\rho,z,\alpha)-\frac{S_1(\rho,z,\alpha)}{\rho^2},\right. \tag{6.92}$$

$$\left.\frac{y}{\rho^3}S_2(\rho,z,\alpha)\right],$$

where the indicated powers of ρ in the denominators cancel the ρ-dependences of the accompanying S_n (sec (6.81)); since x and y will vanish with ρ, this reduces further to

$$\lim_{\rho\to 0}\vec{B}_A(\vec{x}) = \frac{A\mu_0\sigma_0 E_0}{4}\left\{1-\sqrt{\frac{\pi}{2}}\left(\frac{z}{\alpha}\right)\exp\left[\frac{z^2}{2\alpha^2}\right]erfc\left(\frac{z}{\sqrt{2}\alpha}\right)\right\}\hat{y}\ . \tag{6.93}$$

At the other extreme, where $\rho >> \alpha$, the value of the Gaussian is still close to unity by the time that ν is large enough to make the Bessel functions for practical purposes vanish; in this case we expand the Gaussian in a power series about zero, and integrate termwise. The basic integral is

$$L_{n,m}(\vec{x}) = \int_0^\infty \nu^n \exp\left[-\frac{z}{\rho}\nu\right]J_m(\nu)\,d\nu\ , \tag{6.94}$$

which for n and m both nonnegative integers and $n \geq m$ is

$$L_{n,m}(\vec{x}) = (-1)^m\frac{(n-m)!}{\beta^{n+1}}P_n^m\left[\frac{1}{\beta}\frac{z}{\rho}\right]\ , \tag{6.95}$$

$$\beta = \left[1+\frac{z^2}{\rho^2}\right]^{1/2} \tag{6.96}$$

(Erde'lyi et al., 1954, v. 2, sec. 8.6, eq. 6, p. 29 and Erde'lyi et al., 1955, v. 1, sec. 3.4, eq. 17, p.144), where the $P_n^m(x)$ are Legendre functions of integer degree n and integer order m (ibid., sec. 3.4, p. 143). The Gaussian series expansion is

$$\exp\left[-\frac{\alpha^2}{\rho^2}\frac{\nu^2}{2}\right] = \sum_{n=0}^{\infty}\frac{(-1)^n}{2^n\,n!}\left(\frac{\alpha}{\rho}\right)^{2n}x^{2n}\ , \tag{6.97}$$

giving for I_1, I_2, and I_3

$$I_1(\rho,z,\alpha) = \sum_{k=0}^{\infty}\frac{(-1)^k}{2^k\,(k!)}\left(\frac{\alpha}{\rho}\right)^{2k}L_{2k,1}(\rho,z)\ , \tag{6.98}$$

$$I_2(\rho,z,\alpha) = \sum_{k=0}^{\infty} \frac{(-1)^k}{2^k\,(k!)} \left(\frac{\alpha}{\rho}\right)^{2k} L_{2k+1,1}(\rho,z) \quad , \tag{6.99}$$

and

$$I_3(\rho,z,\alpha) = \sum_{k=0}^{\infty} \frac{(-1)^k}{2^k\,(k!)} \left(\frac{\alpha}{\rho}\right)^{2k} L_{2k+1,2}(\rho,z) \quad . \tag{6.100}$$

Expressions for $L_{0,1}$ and $L_{1,2}$ are required by (6.98) and (6.100) respectively, but are not given by (6.95); from integral tables, these are

$$L_{0,1}(\rho,z) = 1 - \frac{1}{\beta}\,\frac{z}{\rho} \tag{6.101}$$

(Erde'lyi et al., 1954, v. 2, sec. 8.4, eq. 6, p. 19) and

$$L_{1,2}(\rho,z) = \left(2 + \frac{1}{\beta}\,\frac{z}{\rho}\right)\left(1 - \frac{1}{\beta}\,\frac{z}{\rho}\right)^2 \quad . \tag{6.102}$$

(Erde'lyi et al., 1954, v. 1, sec. 4.14, eq. 2, p. 182), where β is as given by (6.96).

Useful recurrence relations and bootstrap functions for computing the Legendre functions required by (6.95) are

$$(n-m+1)\,P_{n+1}^m(x) = (2n+1)\,x\,P_n^m(x) - (n+m)\,P_{n-1}^m(x) \tag{6.103}$$

and

$$(1-x^2)^{1/2}\,P_n^{m+1}(x) = (n-m)\,x\,P_n^m(x) - (n+m)\,P_{n-1}^m(x) \tag{6.104}$$

(Erde'lyi et al., 1955, v. 1, sec. 3.8, eqs. 12 and 17, p. 161), and

$$P_0^0(x) = 1 \tag{6.105}$$

and

$$P_1^0(x) = x \tag{6.106}$$

(Abramowitz and Stegun, eqs. 8.4.1 and 8.4.3, p. 333). Note that $P_n^m(x) \equiv 0$ for $m > n$. Additional useful functions are

$$P_1^1(x) = -(1-x^2)^{1/2} \quad , \tag{6.107}$$

$$P_2^0(x) = \tfrac{1}{2}(3x^2-1) \quad , \tag{6.108}$$

$$P_2^1(x) = -3x\,(1-x^2)^{1/2} \quad , \tag{6.109}$$

and

$$P_2^2(x) = 3(1-x^2) \quad . \tag{6.110}$$

Reference to (6.95), (6.103), and (6.104) gives the recurrence relations for $L_{n,m}(\rho,z)$

$$\beta^2 L_{n,1}(\rho,z) = (2n-1)(z/\rho) L_{n-1,1}(\rho,z) - n(n-2) L_{n-2,1} \tag{6.111}$$

and

$$L_{n,2}(\rho,z) = (n+1) L_{n-1,1}(\rho,z) - (z/\rho) L_{n,1}(\rho,z) \quad , \tag{6.112}$$

and some useful bootstrap functions, from (6.95) and the previously listed Legendre functions, are

$$L_{1,1}(\rho,z) = \frac{1}{\beta^3} \tag{6.113}$$

and

$$L_{2,1}(\rho,z) = \frac{3}{\beta^5}\frac{z}{\rho} \quad ; \tag{6.114}$$

note that the recurrence relations (6.111) and (6.112) are invalid with the use of bootstrap functions for which $m>n$, making it improper to use either (6.101) or (6.102) to start them off.

In the limit of $\rho\to\infty$, the integrals (6.78), (6.79), and (6.80) reduce to

$$I_1 = \int_0^\infty J_1(v)\,dv = 1 \quad , \tag{6.115}$$

$$I_2 = \int_0^\infty v\,J_1(v)\,dv = 1 \quad , \tag{6.116}$$

and

$$I_3 = \int_0^\infty v\,J_2(v)\,dv = 2 \quad ; \tag{6.117}$$

these integrals are special cases of $L_{0,1}$, $L_{1,1}$, and $L_{1,2}$, and their values were derived from the appropriate expressions in the text (expressions (6.101), (6.113), and (6.102) respectively) by taking the appropriate limits. Substitution of these values into (6.77) gives

$$\lim_{\rho\to\infty} \vec{B}_A(\vec{x}) = -\frac{\mu_0 r_0 E_0 A \alpha^2}{2\rho^2}\left[\frac{2xy}{\rho^2}, \frac{2y^2}{\rho^2}-1, \frac{y}{\rho}\right] \quad . \tag{6.118}$$

Computation of the elements of the tensor gradient of the anomalous magnetic field is expedited by the fact that spatial derivatives of the members of the sets of the S_n and the $L_{n,m}$ are also members of the respective sets; from the integral expressions (6.81) and (6.94) we have

$$\frac{\partial}{\partial\rho} S_n(\rho,z,\alpha) = \frac{z}{\rho^2} S_{n+1}(\rho,z,\alpha) + \frac{\alpha^2}{\rho^3} S_{n+2}(\rho,z,\alpha) \quad , \tag{6.119}$$

$$\frac{\partial}{\partial z} S_n(\rho,z,\alpha) = -\frac{1}{\rho} S_{n+1}(\rho,z,\alpha) \quad , \tag{6.120}$$

$$\frac{\partial}{\partial\rho} L_{n,m}(\rho,z,\alpha) = \frac{z}{\rho^2} L_{n+1,m}(\rho,z,\alpha) \quad , \tag{6.121}$$

and

$$\frac{\partial}{\partial z} L_{n,m}(\rho,z,\alpha) = -\frac{1}{\rho} L_{n+1,m}(\rho,z,\alpha) \quad . \tag{6.122}$$

Modification of the routines used to calculate I_1, I_2, and I_3 for the calculation of their spatial derivatives should be fairly straightforward.

A practical problem in the use of the recurrence relations (6.89) and (6.111) in the calculation of I_1, I_2, and I_3 is that for many choices of ρ, z, and α the series diverge, apparently as a result of numerical instability; where this occurred, investigation of the problem showed that successive terms in the expansions for I_1, I_2, and I_3 first decreased in magnitude to values very small in comparison to the magnitude of the first term in the series, and then increased without bound. It was found that if the expansions were truncated just before the point of divergence was reached, the agreement between the equivalent series in the S_n and the $L_{n,m}$ in their areas of mutual validity was good to several significant places, suggesting that this procedure is a workable solution to the divergence problem. However, in many cases it will be desirable to get at least a rough estimate of the number of terms actually required for a result of a given level of accuracy, either to avoid computing unnecessary terms or to determine whether or not a series expansion is invalid due to divergence before the requisite number is reached. Both methods are based on the series expansion in ascending powers of its argument of a factor in the integrand of an integral, the justification being that another factor in the integrand will have effectively vanished before the argument of the expanded function becomes large enough to invalidate its series expansion. To produce a series truncation error estimate for a given choice of ρ, z, and α, one first truncates the integration at a selected cutoff point, and estimates the error introduced by disregarding the remainder of the integral; then, one calculates the difference at this cutoff point between the value of the factor to be expanded and

the value of its expansion, truncated after the specified number of terms. A reasonably reliable upper limit on the error produced by the series truncation may be arrived at by making the conservative assumption that the percentage discrepancy between the factor value and the value of its expansion is the same over the entire range of integration from zero up to the cutoff point, and the total error is calculated by multiplying this percentage error by the value of the truncated integral based on the truncated series expansion and adding the result to the estimated error from the truncation of the integral. This process involves some tradeoff decisions, in that selecting a greater cutoff point will decrease the integration truncation error but increase the series truncation error unless a larger number of terms is used in the expansion.

As an example, we consider the case of a Gaussian hill 20 meters high and of width such that $\alpha = 80$ meters, rising from an otherwise level ocean floor 100 meters below the surface. The magnetic field is computed at the points of a 5×5 horizontal grid at the ocean surface, centered directly over the peak of the hill and with a grid spacing of 160 meters, with faces parallel to the direction of the inducing EMF. The water depth is not untypical of a continental shelf, and underwater features such as a reef, a dune, or a highly eroded submerged island might have dimensions on the order of this Gaussian hill. A uniform inducing electric field of $1.0\,\mu V/m$ in the $\hat{x}$ direction is assumed, and the ocean's electrical conductivity is taken to be a uniform 3.3 S/m. Note that most of the points on the grid are in the intermediate region between $\rho << \alpha$ and $\rho >> \alpha$; in this region both of the series expansion schemes given above should be usable, and in fact for this problem there was a narrow range of values of ρ where they gave the same values for I_1, I_2, and I_3 to several significant places. However, difficulties encountered suggest that, as a safety precaution, for computations with any given combination of α and z one should compare the outputs of the two algorithms over the range of ρ with which one is concerned, in order to establish whether there is in fact a range of equivalent output, and, if so, exactly where it is. The results of the calculations are presented in table 2.3.

The scaling rules discussed toward the end of section 3 may be used with these results to derive the magnetic values at the ocean surface for any situation where the relative dimensions of ocean depth, hill height, hill width, and grid spacing are the same as in this example. Also, the field values are directly proportional to both the strength of the inducing EMF and the electrical conductivity of the seawater. According to equation (6.77), the field values are directly proportional to the height of the hill, but it should be recalled that this equation loses its validity if the height of the hill approaches either half of the ocean depth or the width of the hill.

	x	-320.0 m	-160.0 m	0.0 m	160.0 m	320.0 m
$y = 320.0m$	B_x	0.850	0.926	0.000	-0.926	-0.850
	B_y	0.153	-0.377	-0.851	-0.377	0.153
	B_z	-0.884	-1.732	-2.357	-1.732	-0.884
$y = 160.0m$	B_x	0.926	1.548	0.000	-1.548	-0.926
	B_y	1.011	1.205	1.044	1.205	1.011
	B_z	-0.866	-2.666	-4.720	-2.666	-0.866
$y = 0.0m$	B_x	0.000	0.000	0.000	0.000	0.000
	B_y	1.748	3.788	9.569	3.788	1.748
	B_z	0.000	0.000	0.000	0.000	0.000
$y = -160.0m$	B_x	-0.926	-1.548	0.000	1.548	0.926
	B_y	1.011	1.205	1.044	1.205	1.011
	B_z	0.866	2.666	4.720	2.666	0.866
$y = -320.0m$	B_x	-0.850	-0.926	0.000	0.926	0.850
	B_y	0.153	-0.377	-0.851	-0.377	0.153
	B_z	0.884	1.732	2.357	1.732	0.884

TABLE 2.3

Field values at the ocean surface over a submerged Gaussian hill as described in the text on page 67. The field values are in units of 10^{-12} *tesla*, and the origin of the coordinate system for position on the surface is on the vertical axis of symmetry of the hill. In the absence of the hill the uniform field at and above the surface would be $\vec{B} = -2.07 \times 10^{-10} \hat{y}$ *tesla*.

7. Interaction with the Earth's magnetic field of seawater current flow

An electric current will be generated by the flow of seawater through the Earth's magnetic field, and this electrical current will in turn generate a magnetic field of its own. As well as the magnetic anomalies associated with the flow of tides and steady ocean currents and with turbulent water motion, which are outside of the scope of this study, there will also be anomalies associated with the diversion of water flow over the ocean bottom by topographical features of the ocean floor. Unfortunately, the flow patterns of real, viscous water about even very simple shapes are difficult to model, and the subject has in general not been well studied; accordingly, even though this effect is probably significant in comparison with the others discussed in this report, it cannot be covered here because the available data is insufficient even to estimate orders of magnitude. For some examples see Cox and Sandstrom, 1962, and Osborne, 1980.

Chapter III

Magnetic Anomalies Induced by Fronts within the Ocean

1. Introduction

Oceanic fronts are regions where dissimilar water types abut one another, and they can exist as stable conditions because the electrical conductivity of seawater increases both with increasing temperature and increasing salinity, whereas the density of seawater increases with increasing salinity but *decreasing* temperature. As a result of this, two bodies of water can lie adjoining each other without a density contrast but with appreciable contrast in electrical conductivity, and fronts with their main contrast in the vertical may have density as well as conductivity jumps. The causes of temperature and salinity variations lie ultimately in air-sea processes such as precipitation, evaporation, insolation, and long wave back radiation, but the actual distribution of water types within the ocean results from dynamic processes which transport regions of water that have been subjected to these influences in different proportions.

Some of the more common of these dynamical processes derive from gravity waves. In this instance, we regard the redistribution of water types in these so-called internal waves as a form of "frontal" creation; these fronts have time scales in the range from the inertial period to the Vaisala period (Eckart, 1960). Other processes - currents and turbulence - can lead to longer time scales. Internal waves are ubiquitous in the ocean but have local intensification in shallow water (Gordon, 1977). Since the vertical structure of the ocean is always one of increasing density with depth (usually caused by decreasing temperature), internal wave fronts are always present. The more persistent fronts where density remains almost constant demand the close proximity of contrasting salinity/temperature water types.

This chapter deals with the calculation of the magnetic anomalies associated with the electrical conductivity properties of oceanic fronts. Section 2 uses a perturbation approach to derive equations describing the alteration of the electric field within the ocean by the presence of a front, and discusses the calculation of the magnetic effects of the front by use of the solutions to these equations. Section 3 deals with solutions to the electric field equations for a special case of particular interest, section 4 illustrates the practical use of the work of section 3, and section 5 gives two different methods for a general solution for the electric fields in the perturbation limit, one being the more convenient for analysis of Fourier transformed data and the other being the more suitable for the study of localized fronts in real space.

2. Basic equations

2.1 The oceanic electric field

We start by supposing that the front exists as a steady state condition, making the magnetic field associated with it constant in time. From Maxwell's equations we then have for $\vec{E}$ the electric field within the ocean

$$\nabla \times \vec{E} = 0 \quad , \tag{2.1}$$

which implies that $\vec{E}$ may be expressed as the gradient of some scalar function ϕ:

$$\vec{E} = \nabla \phi \quad . \tag{2.2}$$

For $\vec{J}$ the electrical current density distribution within the ocean we have

$$\vec{J} = \sigma \vec{E} \quad , \tag{2.3}$$

where σ is the electrical conductivity distribution of the seawater, and

$$\nabla \cdot \vec{J} = 0 \quad , \tag{2.4}$$

another consequence of the steady state assumption. Combining (2.2), (2.3), and (2.4) gives

$$\nabla \cdot (\sigma \nabla \phi) = 0 \quad , \tag{2.5}$$

or

$$\sigma \nabla^2 \phi + (\nabla \sigma) \cdot (\nabla \phi) = 0 \quad . \tag{2.6}$$

For fronts in the ocean, the variations from the mean electrical conductivity of the frontal region are seldom more than a few percent of the mean conductivity, suggesting the use of perturbation methods in solving (2.6). Accordingly, we write σ, which we may take as a given, in the form

$$\sigma(\vec{x}) = \sigma_0(z) + \epsilon \sigma_1(\vec{x}) \tag{2.7}$$

and ϕ in the form

$$\phi(\vec{x}) = \phi_0(\vec{x}) + \epsilon \phi_1(\vec{x}) + \epsilon^2 \phi_2(\vec{x}) + \cdots \quad , \tag{2.8}$$

where ϵ is a perturbation parameter that will eventually be set to unity, and σ_1 is a small perturbation on the mean conductivity σ_0, which is taken for mathematical convenience to be horizontally stratified. Substitution of (2.7) and (2.8) into (2.6) gives

$$\sigma_0 \nabla^2\phi_0 + (\nabla\sigma_0)\cdot(\nabla\phi_0) \tag{2.9}$$

$$+ \epsilon \{\sigma_0 \nabla^2\phi_1 + \sigma_1 \nabla^2\phi_0 + (\nabla\sigma_0)\cdot(\nabla\phi_1) + (\nabla\sigma_1)\cdot(\nabla\phi_0)\}$$

$$+ \epsilon^2 \{\sigma_0 \nabla^2\phi_2 + \sigma_1 \nabla^2\phi_1 + (\nabla\sigma_0)\cdot(\nabla\phi_2) + (\nabla\sigma_1)\cdot(\nabla\phi_1)\}$$

$$+ \cdots = 0 \ .$$

Requiring that (2.9) hold for all choices of the value of ϵ yields

$$\sigma_0 \nabla^2\phi_0 + (\nabla\sigma_0)\cdot(\nabla\phi_0) = 0 \ , \tag{2.10}$$

$$\sigma_0 \nabla^2\phi_1 + (\nabla\sigma_0)\cdot(\nabla\phi_1) + \sigma_1 \nabla^2\phi_0 + (\nabla\sigma_1)\cdot(\nabla\phi_0) = 0 \ , \tag{2.11}$$

$$\sigma_0 \nabla^2\phi_2 + (\nabla\sigma_0)\cdot(\nabla\phi_2) + \sigma_1 \nabla^2\phi_1 + (\nabla\sigma_1)\cdot(\nabla\phi_1) = 0 \ , \tag{2.12}$$

and, for higher orders,

$$\sigma_0 \nabla^2\phi_n + (\nabla\sigma_0)\cdot(\nabla\phi_n) + \sigma_1 \nabla^2\phi_{n-1} + (\nabla\sigma_1)\cdot(\nabla\phi_{n-1}) = 0 \ . \tag{2.13}$$

Making the definition

$$f(z) = \frac{1}{\sigma_0(z)} \frac{d\sigma_0(z)}{dz} \tag{2.14}$$

gives from this

$$\nabla^2\phi_0 + f(z)\,\hat{z}\cdot\nabla\phi_0 = 0 \ , \tag{2.15}$$

$$\nabla^2\phi_1 + f(z)\,\hat{z}\cdot\nabla\phi_1 = p_1(\vec{x}) \tag{2.16}$$

where

$$p_1(\vec{x}) = \frac{\{\sigma_1(\vec{x})\, f(z)\,\hat{z} - \nabla\sigma_1(\vec{x})\}\cdot\nabla\phi_0}{\sigma_0(z)} \ , \tag{2.17}$$

$$\nabla^2\phi_2 + f(z)\,\hat{z}\cdot\nabla\phi_2 = p_2(\vec{x}) \tag{2.18}$$

where

$$p_2(\vec{x}) = \frac{\{\sigma_1(\vec{x})\, f(z)\,\hat{z} - \nabla\sigma_1(\vec{x})\}\cdot\nabla\phi_1}{\sigma_0(z)} - \frac{\sigma_1(\vec{x})}{\sigma_0(z)}\, p_1(\vec{x}) \ , \tag{2.19}$$

and

$$\nabla^2\phi_n + f(z)\,\hat{z}\cdot\nabla\phi_n = p_n(\vec{x}) \tag{2.20}$$

$$p_n(\vec{x}) = \frac{[\sigma_1(\vec{x})\, f(z)\, \hat{z} - \nabla\sigma_1(\vec{x})] \cdot \nabla\phi_{n-1}}{\sigma_0(z)} - \frac{\sigma_1(\vec{x})}{\sigma_0(z)}\, p_{n-1}(\vec{x}) \quad . \tag{2.21}$$

Setting ϵ to 1, we have

$$\sigma(\vec{x}) = \sigma_0(z) + \sigma_1(\vec{x}) \tag{2.22}$$

and

$$\phi(\vec{x}) = \phi_0(\vec{x}) + \phi_1(\vec{x}) + \phi_2(\vec{x}) + \cdots \quad . \tag{2.23}$$

As $|\phi_2|$ will be smaller than $|\phi_1|$ by something on the order of magnitude of the ratio of $\{\max |\sigma_1|\}$ to $|\sigma_0|$, it will generally be practical to ignore all terms beyond ϕ_1 in (2.23).

As an important special case, we suppose that

$$\phi_0(\vec{x}) = E_0 x \quad , \tag{2.24}$$

which is seen to be a valid solution to (2.15); then, since $\phi = \phi_0$ if σ_1 is uniformly equal to zero, in the absence of a front the electric field $\vec{E}$ throughout the ocean is

$$\vec{E} = \nabla\phi_0 = E_0\, \hat{x} \quad , \tag{2.25}$$

which we may take to be induced by some outside source of EMF. If σ_1 is nonzero, then we have for ϕ_1 from (2.16) and (2.17)

$$\nabla^2\phi_1(\vec{x}) + f(z)\, \frac{\partial\phi_1(\vec{x})}{\partial z} = p_1(\vec{x}) \tag{2.26}$$

$$p_1(\vec{x}) = -\frac{E_0}{\sigma_0(z)}\, \frac{\partial\sigma_1(\vec{x})}{\partial x} \quad . \tag{2.27}$$

The choice (2.24) for ϕ_0 is appropriate for virtually all cases of practical interest dealing with fronts near the surface of an ocean.

2.2 The Fourier transformed magnetic field

The Biot-Savart expression for the magnetic field $\vec{B}$ due to a steady state electrical current density field $\vec{J}$ is

$$\vec{B}(\vec{x_0}) = \frac{\mu_0}{4\pi} \int_V \frac{\vec{J}(\vec{x}) \times (\vec{x_0}-\vec{x})}{|\vec{x_0}-\vec{x}|^3} \, d\vec{x} \quad ; \tag{2.28}$$

if we define

$$\vec{P}(\vec{x}) = \frac{\mu_0}{4\pi} \frac{\vec{x}}{|\vec{x}|^3} \quad , \tag{2.29}$$

we note that (2.28) becomes a convolution integral of the form

$$\vec{B}(\vec{x_0}) = \int_V \vec{J}(\vec{x}) \times \vec{P}(\vec{x_0}-\vec{x}) \, d\vec{x} \quad . \tag{2.30}$$

Defining the Fourier transforms $\vec{C}(\vec{k})$, $\vec{K}(\vec{k})$, and $\vec{Q}(\vec{k})$,

$$\vec{B}(\vec{x}) = \int \vec{C}(\vec{k}) \, e^{i\vec{k}\cdot\vec{x}} \, d\vec{k} \quad , \tag{2.31}$$

$$\vec{J}(\vec{x}) = \int \vec{K}(\vec{k}) \, e^{i\vec{k}\cdot\vec{x}} \, d\vec{k} \quad , \tag{2.32}$$

and

$$\vec{P}(\vec{x}) = \int \vec{Q}(\vec{k}) \, e^{i\vec{k}\cdot\vec{x}} \, d\vec{k} \quad , \tag{2.33}$$

we find that (2.30) is equivalent to

$$\vec{C}(\vec{k}) = (2\pi)^3 \, \vec{K}(\vec{k}) \times \vec{Q}(\vec{k}) \quad . \tag{2.34}$$

The current density field $\vec{J}$ has the form

$$\vec{J}(\vec{x}) = \sigma(\vec{x}) \, \nabla\phi(\vec{x}) \quad ; \tag{2.35}$$

if we make the definitions

$$\sigma(\vec{x}) = \int \Sigma(\vec{k}) \, e^{i\vec{k}\cdot\vec{x}} \, d\vec{k} \tag{2.36}$$

and

$$\phi(\vec{x}) = \int \Phi(\vec{k}) \, e^{i\vec{k}\cdot\vec{x}} \, d\vec{k} \quad , \tag{2.37}$$

we find that (2.35) is equivalent to

$$\vec{K}(\vec{k}) = \int i\vec{k}' \, \Sigma(\vec{k}-\vec{k}') \, \Phi(\vec{k}') \, d\vec{k}' \quad . \tag{2.38}$$

An equivalent expression to (2.29) for $\vec{P}(\vec{x})$ is

$$\vec{P}(\vec{x}) = -\frac{\mu_0}{4\pi} \nabla\left[\frac{1}{r}\right] \quad , \quad r^2 = \vec{x}\cdot\vec{x} \quad ; \tag{2.39}$$

some work with this expression shows that

$$\vec{Q}(\vec{k}) = -\frac{\mu_0}{4\pi} (2\pi)^{-3} i\vec{k}\, U(\vec{k}) \quad , \tag{2.40}$$

where

$$U(\vec{k}) = \int \frac{1}{r} e^{-i\vec{k}\cdot\vec{x}}\, d\vec{x} \quad , \tag{2.41}$$

giving for (2.34)

$$\vec{C}(\vec{k}) = \frac{\mu_0}{4\pi} U(\vec{k})\, \vec{L}(\vec{k}) \quad , \tag{2.42}$$

where

$$\vec{L}(\vec{k}) = i\,\vec{k}\times\vec{K}(\vec{k}) \tag{2.43}$$

$$= \int (\vec{k}'\times\vec{k})\, \Sigma(\vec{k}-\vec{k}')\, \Phi(\vec{k}')\, d\vec{k}' \quad .$$

If expression (2.41) is written in Cartesian coordinates, then use of symmetry about the origin reduces it to three sequential cosine transforms, which are given in Erde'lyi et al., 1954, v. 1 (sec. 1.3, eq. 7, p. 11, sec. 1.13, eq. 43, p. 56, and sec. 1.4, eq. 1, p. 14); the result is

$$U(\vec{k}) = \frac{4\pi}{\vec{k}\cdot\vec{k}} \quad . \tag{2.44}$$

The current density distribution $\vec{J}_1$ up to the first order is given by

$$\vec{J}_1(\vec{x}) = \sigma_0(z)\, \nabla\phi_0(\vec{x}) + \vec{J}_A \quad , \tag{2.45}$$

where

$$\vec{J}_A(\vec{x}) = \sigma_1(\vec{x})\, \nabla\phi_0(\vec{x}) + \sigma_0(z)\, \nabla\phi_1(\vec{x}) \quad ; \tag{2.46}$$

the first term of (2.45) is unaffected if σ_1 is set uniformly equal to zero, whereas $\vec{J}_A$ vanishes, thereby identifying itself as the anomalous part of the distribution. The Fourier transform $\vec{C}(\vec{k})$ of the magnetic field resulting from $\vec{J}_A(\vec{x})$ is

$$\vec{C}(\vec{k}) = \frac{\mu_0}{4\pi} U(\vec{k})\, \vec{L}_A(\vec{k}) \quad , \tag{2.47}$$

$$\mathcal{L}_A(\vec{k}) = \int (\vec{k}' \times \vec{k}) \{\Sigma_1(\vec{k}-\vec{k}')\Phi_0(\vec{k}') + \Sigma_0(\vec{k}-\vec{k}')\Phi_1(\vec{k}')\}\, d\vec{k}' \quad , \tag{2.48}$$

where

$$\sigma_0(z) = \int \Sigma_0(\vec{k})\, e^{i\vec{k}\cdot\vec{x}}\, d\vec{k} \quad , \tag{2.49}$$

$$\sigma_1(\vec{x}) = \int \Sigma_1(\vec{k})\, e^{i\vec{k}\cdot\vec{x}}\, d\vec{k} \quad , \tag{2.50}$$

$$\phi_0(\vec{x}) = \int \Phi_0(\vec{k})\, e^{i\vec{k}\cdot\vec{x}}\, d\vec{k} \quad , \tag{2.51}$$

and

$$\phi_1(\vec{x}) = \int \Phi_1(\vec{k})\, e^{i\vec{k}\cdot\vec{x}}\, d\vec{k} \quad . \tag{2.52}$$

3. Exponential decline of the lateral mean electrical conductivity with depth

Let us suppose that $\sigma_0(z)$ the unperturbed electrical conductivity distribution of the ocean goes as

$$\frac{1}{\sigma_0(z)} \frac{d\sigma_0(z)}{dz} = \lambda \quad , \quad \lambda \geq 0 \quad , \tag{3.1}$$

where λ is a constant, giving an exponential decline in σ_0 with depth. Then (2.15) becomes

$$\nabla^2 \phi_0 + \lambda \frac{\partial \phi_0}{\partial z} = 0 \quad , \tag{3.2}$$

for which (2.24) is still a solution, and (2.16) and (2.17) become

$$\nabla^2 \phi_1 + \lambda \frac{\partial \phi_1}{\partial z} = p_1 \quad , \tag{3.3}$$

where

$$p_1(\vec{x}) = \frac{(\sigma_1 \lambda \hat{z} - \nabla \sigma_1) \cdot \nabla \phi_0}{\sigma_0} \tag{3.4}$$

within the ocean and is undefined elsewhere. In this special case, if ϕ_0 and σ_1 are provided, then an analytical solution to (3.3) is possible.

Going to the Fourier transform domain, we define

$$\phi_1(\vec{x}) = \int \Phi_1(\vec{k})\, e^{i\vec{k}\cdot\vec{x}}\, d\vec{k} \tag{3.5}$$

and

$$p_1(\vec{x}) = \int P_1(\vec{k})\, e^{i\vec{k}\cdot\vec{x}}\, d\vec{k} \quad ; \tag{3.6}$$

to avoid ambiguity in the Fourier transform of $p_1(\vec{x})$, we set it to zero outside of the ocean. Making these substitutions into (3.3) gives

$$Q(\vec{k})\, \Phi_1(\vec{k}) = P_1(\vec{k}) \quad , \tag{3.7}$$

where

$$Q(\vec{k}) = -\vec{k}\cdot\vec{k} + i\lambda\, \vec{k}\cdot\hat{z} \quad . \tag{3.8}$$

From (3.7) we have

$$\Phi_{1P}(\vec{k}) = \frac{P_1(\vec{k})}{Q(\vec{k})} \quad , \tag{3.9}$$

whose inverse Fourier transform $\phi_{1P}(\vec{x})$ is a particular solution to equation (3.3). Equation (3.3) with p_1 set uniformly equal to zero is solved by any term of the form $e^{i\vec{k}\cdot\vec{x}}$ for which $\vec{k}$ is such that $Q(\vec{k})=0$. If we write $\vec{k}$ in the form

$$\vec{k} = (k_x, k_y, ik) \quad , \tag{3.10}$$

then (3.8) becomes

$$Q(\vec{k}) = k^2 - \lambda k - k_\beta^2 \quad , \tag{3.11}$$

where

$$k_\beta^2 = k_x^2 + k_y^2 \quad ; \tag{3.12}$$

setting $Q(\vec{k})$ uniformly equal to zero gives for k

$$k = \frac{\lambda}{2} \pm \sqrt{\frac{\lambda^2}{4} + k_\beta^2} \quad . \tag{3.13}$$

Accordingly, we have for the general solution to equation (3.3)

$$\begin{aligned} \phi_1(\vec{x}) &= \phi_{1P}(\vec{x}) \\ &+ \int_{-\infty}^{\infty}\int_{-\infty}^{\infty} A(k_x,k_y)\, \exp\{i(k_x x + k_y y) - k_A z\}\, dk_x\, dk_y \\ &+ \int_{-\infty}^{\infty}\int_{-\infty}^{\infty} B(k_x,k_y)\, \exp\{i(k_x x + k_y y) - k_B z\}\, dk_x\, dk_y \quad , \end{aligned} \tag{3.14}$$

where k_A is the larger of the two roots (3.13) and k_B is the smaller; the integral term in A is downward-increasing, whereas the integral term in B is downward-decreasing.

If we suppose that λ has the same value everywhere from the ocean floor to the surface, then the boundary conditions on any solution to (3.3) are that $\hat{z}\cdot\nabla\phi_1=0$ both at the ocean bottom and the ocean surface, which is equivalent to saying that there is no flow of electrical current through either bottom or surface. This approximation is usually valid because the conductivity of the seafloor, while variable, is usually far smaller than that of the seawater above. From (3.14) we have that

$$\hat{z}\cdot\nabla\phi_1(\vec{x}) = \int_{-\infty}^{\infty}\int_{-\infty}^{\infty} V(k_x,k_y,z)\, \exp\{i(k_x x + k_y y)\}\, dk_x\, dk_y \quad , \tag{3.15}$$

$$V(k_x,k_y,z) = R(k_x,k_y,z) - k_A e^{-k_A z} A(k_x,k_y) - k_B e^{-k_B z} B(k_x,k_y) \quad , \tag{3.16}$$

where

$$R(k_x,k_y,z) = \int_{-\infty}^{\infty} ik_z\, \Phi_{1P}(\vec{k})\, e^{ik_z z}\, dk_z \quad . \tag{3.17}$$

The boundary conditions at surface and bottom are seen to be equivalent to

$$V(k_x,k_y,z_S) = V(k_x,k_y,z_B) = 0 \quad , \tag{3.18}$$

where z_S and z_B are the altitudes of the surface and the bottom respectively. These represent two equations in A and B, which may be solved simultaneously for A and B in terms of R at the two altitudes.

In some cases it may prove convenient to minimize the maximum value of $|\sigma_1|$ by constructing σ_0 from two different exponential curved joined together at some depth within the ocean. If this is done, then then the conditions (3.18) still apply, and there are additional conditions at the interfacing depth, derived from the requirement that the electrical current density distribution be continuous across the interface; provided that σ_0 is continuous across the interface, this is equivalent to saying that $\nabla\phi_1$ is continuous across the interface. We already have in equation (3.15) an expression for the vertical component of the gradient; from equation (3.14) we have for the horizontal components

$$\nabla_H\phi_1(\vec{x}) = \int_{-\infty}^{\infty}\int_{-\infty}^{\infty} i(k_x,k_y,0)\, H(k_x,k_y,z)\, \exp\{i(k_x x+k_y y)\}\, dk_x\, dk_y \quad , \tag{3.19}$$

$$H(k_x,k_y,z) = S(k_x,k_y,z) + e^{-k_A z} A(k_x,k_y) + e^{-k_B z} B(k_x,k_y) \quad , \tag{3.20}$$

where

$$S(k_x,k_y,z) = \int_{-\infty}^{\infty} \Phi_{1P}(\vec{k})\, e^{ik_z z}\, dk_z \quad . \tag{3.21}$$

Let the lower region be called region 1, and the upper region be called region 2, with their interface being at the altitude z_I; our object is to find ϕ_1 in the two regions by solving for A_1 and B_1 in the lower region and A_2 and B_2 in the upper region. For boundary conditions we have

$$V_1(k_x,k_y,z_B) = 0 \quad , \tag{3.22}$$

$$V_1(k_x,k_y,z_I) = V_2(k_x,k_y,z_I) \quad , \tag{3.23}$$

$$H_1(k_x,k_y,z_I) = H_2(k_x,k_y,z_I) \quad , \tag{3.24}$$

and

$$V_2(k_x, k_y, z_S) = 0 \quad , \tag{3.25}$$

giving one equation in A_1 and B_1, one equation in A_2 and B_2, and two equations in all four parameters. Although the process is cumbersome, these conditions are sufficient for the unique simultaneous solutions for A_1, B_1, A_2, and B_2.

4. Practical use of the method of section 3

The basic approach used here will be to first compute the magnetic anomaly field associated with a unit point variation from the mean electrical conductivity distribution σ_0, and then use this as a Green's function to get the field for an arbitrary variation distribution. Drawing upon section 2.2, we have that if $\vec{B_V}$ is the magnetic field associated with a variation distribution σ_1, then its Fourier transform $\vec{C_V}$ is given by

$$\vec{C_V}(\vec{k}) = -\frac{\mu_0}{4\pi}\, U(\vec{k})\, \vec{L_V}(\vec{k}) \quad , \tag{4.1}$$

$$U(\vec{k}) = \frac{4\pi}{\vec{k}\cdot\vec{k}} \quad , \tag{4.2}$$

$$\vec{L_V}(\vec{k}) = i\, \vec{k} \times \vec{K_V}(\vec{k}) \quad , \tag{4.3}$$

where $\vec{K_V}$ is the Fourier transform of $\vec{J_V}$, the anomalous electrical current density distribution associated with the variation distribution;

$$\vec{J_V}(\vec{x}) = \int \vec{K_V}(\vec{k})\, e^{i\vec{k}\cdot\vec{x}}\, d\vec{k} \quad . \tag{4.4}$$

From equation (2.46) we have that

$$\vec{J_V}(\vec{x}) = \vec{J_{V1}}(\vec{x}) + \vec{J_{V2}}(\vec{x}) \quad , \tag{4.5}$$

where

$$\vec{J_{V1}}(\vec{x}) = \sigma_1(\vec{x})\, \nabla\phi_0(\vec{x}) \tag{4.6}$$

and

$$\vec{J_{V2}}(\vec{x}) = \sigma_0(\vec{x})\, \nabla\phi_1(\vec{x}) \quad , \tag{4.7}$$

with the 0*th* and 1*st* order electric field potentials ϕ_0 and ϕ_1 as defined in section 2.1. We assume that ϕ_0 is given by

$$\phi_0(\vec{x}) = E_0\, x \quad , \tag{4.8}$$

so as to give a uniform electric field of $E_0\, \hat{x}$ within the ocean in the absence of a variation distribution, and that the mean distribution σ_0 is given by

$$\sigma_0(z) = W(z)\, \sigma_0(z_S)\, \exp[\lambda\,(z_S - z)] \quad , \tag{4.9}$$

$$W(z) = \begin{cases} 1 \ , & z_B \leq z \leq z_S \\ 0 \ , & otherwise \end{cases} \quad , \tag{4.10}$$

where λ is a constant greater than or equal to zero, z_S is the altitude of the surface of the ocean, and z_B is the altitude of the ocean bottom. Assuming for the moment that

$$\iota_1(\vec{x}) = \delta(\vec{x}-\vec{x_0}) \quad , \tag{4.11}$$

where δ is the Dirac delta distribution, written as

$$\delta(\vec{x}) = \frac{1}{(2\pi)^3} \int_{-\infty}^{\infty} dk_x \int_{-\infty}^{\infty} dk_y \int_{-\infty}^{\infty} dk_z \; exp(-i\vec{k}\cdot\vec{x}) \quad , \tag{4.12}$$

we immediately have for $\vec{K_{V1}}$

$$\vec{K_{V1}}(\vec{k}) = \hat{x} \frac{E_0}{(2\pi)^3} exp(-i\vec{k}\cdot\vec{x_0}) \quad , \tag{4.13}$$

and hence

$$\vec{L_{V1}}(\vec{k}) = i\,(\vec{k}\times\hat{x}) \frac{E_0}{(2\pi)^3} exp(-i\vec{k}\cdot\vec{x_0}) \quad . \tag{4.14}$$

For $\vec{K_{V2}}$ we have that

$$\vec{K_{V2}}(\vec{k}) = \frac{1}{(2\pi)^3} \int_{-\infty}^{\infty} dx \int_{-\infty}^{\infty} dy \int_{-\infty}^{\infty} dz \; exp(-i\vec{k}\cdot\vec{x}) \tag{4.15}$$

$$\times\; W(z)\sigma_0(z_S)\exp\{\lambda(z_S-z)\}\,\nabla\phi_1(\vec{x}) \quad ;$$

if $\Phi_1(\vec{k})$ is the Fourier transform of $\phi_1(\vec{x})$, then this becomes

$$\vec{K_{V2}}(\vec{k}) = \frac{\sigma_0(z_S)exp(-\lambda z_S)}{2\pi} \int_{-\infty}^{\infty} (k_x,k_y,k_z')\,\Phi_1(k_x,k_y,k_z') \tag{4.16}$$

$$\times \left[\frac{\exp\{i(k_z'-k_z-i\lambda)z_S\} - \exp\{i(k_z'-k_z-i\lambda)z_B\}}{k_z'-k_z-i\lambda} \right] \quad ,$$

from which we have

$$\vec{L_{V2}}(\vec{k}) = i\,\frac{\sigma_0(z_S)exp(-\lambda z_S)}{2\pi}\,(\vec{k}\times\hat{z}) \int_{-\infty}^{\infty} (k_z-k_z')\,\Phi_1(k_x,k_y,k_z') \tag{4.17}$$

$$\times \left[\frac{\exp\{i(k_z'-k_z-i\lambda)z_S\} - \exp\{i(k_z'-k_z-i\lambda)z_B\}}{k_z'-k_z-i\lambda} \right] \quad ,$$

To determine Φ_1, we refer to section 3. From equation (3.14) we have that

$$\Phi_1(\vec{k}) = \Phi_{1P}(\vec{k}) + A(k_x,k_y)\,\delta(k_z - ik_A) + B(k_x,k_y)\,\delta(k_z - ik_B) \quad , \tag{4.18}$$

where

$$k_A = \alpha + \beta \quad , \tag{4.19}$$

$$k_B = \alpha - \beta \quad , \tag{4.20}$$

$$\alpha = \frac{\lambda}{2} \quad , \tag{4.21}$$

and

$$\beta = \sqrt{\frac{\lambda^2}{4} + k_0^2} \quad , \; \beta \Rightarrow 0 \quad , \tag{4.22}$$

where

$$k_0^2 = k_x^2 + k_y^2 \quad . \tag{4.23}$$

$\Phi_1(\vec{k})$ is given by

$$\Phi_1(\vec{k}) = \frac{P_1(\vec{k})}{Q(\vec{k})} \quad , \tag{4.24}$$

where

$$Q(\vec{k}) = -(k_z - ik_A)(k_z - ik_B) \tag{4.25}$$

and $P_1(\vec{k})$ is the Fourier transform of $p_1(\vec{x})$ as given by equation (3.4), which in this case is

$$p_1(\vec{x}) = -E_0 \frac{W(z)\,\hat{x}\cdot\nabla\phi_1(\vec{x})}{\sigma_0(z_S)\exp[\lambda(z_S - z)]} \quad ; \tag{4.26}$$

accordingly, we have, assuming (4.11) for σ_1,

$$P_1(\vec{k}) = -i\frac{E_0 exp(\lambda z_S)}{(2\pi)^3\sigma_0(z_S)}\,\hat{x}\cdot\vec{k}\;W(z_0)\;exp(-\lambda z_0)\;exp(-i\vec{k}\cdot\vec{x_0}) \tag{4.27}$$

and

$$\Phi_1(\vec{k}) = i\frac{E_0 exp(\lambda z_S)}{(2\pi)^3\sigma_0(z_S)}\,\hat{x}\cdot\vec{k}\;W(z_0)\;exp(-\lambda z_0)\;\frac{exp(-i\vec{k}\cdot\vec{x_0})}{(k_z - ik_A)(k_z - ik_B)} \quad . \tag{4.28}$$

Reference to the boundary conditions (3.18) shows that $A(k_x,k_y)$ and $B(k_x,k_y)$ are related to

Φ_1 through the matrix expression

$$\begin{bmatrix} A(k_x,k_y) \\ B(k_x,k_y) \end{bmatrix} = \bar{N} \begin{bmatrix} R(k_x,k_y,z_S) \\ R(k_x,k_y,z_B) \end{bmatrix} , \tag{4.29}$$

where

$$\bar{N} = \frac{1}{D} \begin{bmatrix} k_B \exp(-k_B z_B) & -k_B \exp(-k_B z_S) \\ -k_A \exp(-k_A z_B) & k_A \exp(-k_A z_S) \end{bmatrix} \tag{4.30}$$

with

$$D = 2 k_0^2 \exp(-\lambda z_S) \exp(\alpha d) \sinh(\beta d) , \tag{4.31}$$

$$d = z_S - z_B \tag{4.32}$$

and

$$R(k_x,k_y,z) = \int_{-\infty}^{\infty} ik_z \Phi_{1P}(\vec{k}) \exp(ik_z z)\, dk_z . \tag{4.33}$$

If we make the separation

$$\vec{L}_{V2}(\vec{k}) = \vec{L}_P(\vec{k}) + \vec{L}_A(\vec{k}) + \vec{L}_B(\vec{k}) , \tag{4.34}$$

where the terms on the right side are, respectively, the terms on the right side of equation (4.18) substituted individually into expression (4.17), we see that

$$\vec{K}_A(\vec{k}) = i \frac{\sigma_0(z_S)\exp(-\lambda z_S)}{2\pi} (\vec{k} \times \hat{z}) \frac{k_z - ik_A}{k_z + ik_B} \tag{4.35}$$

$$\times \left[\exp\{-i(k_z+ik_B)z_S\} - \exp\{-i(k_z+ik_B)z_B\}\right] A(k_x,k_y)$$

and

$$\vec{K}_B(\vec{k}) = i \frac{\sigma_0(z_S)\exp(-\lambda z_S)}{2\pi} (\vec{k} \times \hat{z}) \frac{k_z - ik_B}{k_z + ik_A} \tag{4.36}$$

$$\times \left[\exp\{-i(k_z+ik_A)z_S\} - \exp\{-i(k_z+ik_A)z_B\}\right] B(k_x,k_y) .$$

The remaining integrals are easily evaluated by contour integration, giving

$$\vec{L}_P(\vec{k}) = \frac{E_0}{(2\pi)_3} \hat{x}\cdot\vec{k}\ (\vec{k} \times \hat{z}) \exp\{-i(k_x x_0 + k_y y_0)\}\ W(z_0) \left[\frac{\lambda \exp(-ik_z z_0)}{(k_z + ik_A)(k_z + ik_B)} \right. \tag{4.37}$$

$$- \frac{(k_z - ik_A)\exp\{-i(k_z + ik_B)z_S\}}{2\beta(k_z + ik_B)} \exp(-k_B z_0)$$

$$+ \frac{(k_z - ik_B)\exp\{-i(k_z + ik_A)z_B\}}{2\beta(k_z + ik_A)} \exp(-k_A z_0) \Bigg] \quad ,$$

$$\vec{L_A}(\vec{k}) = \frac{E_0}{2\pi} \hat{x}\cdot\vec{k}\ (\vec{k}\times\hat{z}) \frac{(k_z - ik_A)}{2\beta(k_z + ik_B)} [\exp\{-i(k_z+ik_B)z_S\} - \exp\{-i(k_z + ik_B)z_B\}] \tag{4.38}$$

$$\times \exp\{-i(k_x x_0+k_y y_0)\}\ W(z_0)\ Y_A(k_x, k_y, z_0) \quad ,$$

and

$$\vec{L_B}(\vec{k}) = \frac{E_0}{2\pi} \hat{x}\cdot\vec{k}\ (\vec{k}\times\hat{z}) \frac{(k_z - ik_B)}{2\beta(k_z + ik_A)} \tag{4.39}$$

$$\times [\exp\{-i(k_z+ik_A)z_S\} - \exp\{-i(k_z + ik_A)z_B\}]$$

$$\times \exp\{-i(k_x x_0+k_y y_0)\}\ W(z_0)\ Y_B(k_x, k_y, z_0) \quad ,$$

where

$$\begin{bmatrix} Y_A(k_x, k_y, z_0) \\ Y_B(k_x, k_y, z_0) \end{bmatrix} = \bar{N} \begin{bmatrix} k_A \exp(-k_A z_S)\exp(-k_B z_0) \\ k_B \exp(-k_B z_B)\exp(-k_A z_0) \end{bmatrix} \quad . \tag{4.40}$$

We now integrate the terms of $\vec{L_V}$ derived above against $\sigma_1(\vec{x_0})$ over all $\vec{x_0}$ within the ocean to get an expression for $\vec{L_V}$ for arbitrary σ_1. If we define the transforms

$$T_F(\vec{k}) = \frac{1}{(2\pi)^3} \int_{-\infty}^{\infty} dx \int_{-\infty}^{\infty} dy \int_{-\infty}^{\infty} dz\ \sigma_1(\vec{x})\ W(z) \exp(-i\vec{k}\cdot\vec{x}) \quad , \tag{4.41}$$

$$T_A(k_x, k_y) = \frac{1}{(2\pi)^3} \int_{-\infty}^{\infty} dx \int_{-\infty}^{\infty} dy \int_{-\infty}^{\infty} dz\ [\sigma_1(\vec{x})\ W(z) \tag{4.42}$$

$$\times \exp\{-i(k_x x+k_y y)\} \exp(-k_A z\ ] \quad ,$$

and

$$T_B(k_x, k_y) = \frac{1}{(2\pi)^3} \int_{-\infty}^{\infty} dx \int_{-\infty}^{\infty} dy \int_{-\infty}^{\infty} dz\ [\sigma_1(\vec{x})\ W(z) \tag{4.43}$$

$$\times \exp\{-i(k_x x + k_y y)\} \exp(-k_B z)\ ] \quad ,$$

we find that the equivalents of (4.14), (4.37), (4.38), and (4.39) are

$$\vec{L_{V1}}(\vec{k}) = i\,(\vec{k}\times\hat{x})\,\frac{E_0}{(2\pi)^3}\,T_F(\vec{k}) \quad , \tag{4.44}$$

$$\vec{L_P}(\vec{k}) = E_0\,\hat{x}\cdot\vec{k}\;(\vec{k}\times\hat{z})\left[\frac{\lambda\;T_F(\vec{k})}{(k_z+ik_A)(k_z+ik_B)}\right. \tag{4.45}$$

$$-\frac{(k_z-ik_A)\exp\{-i(k_z+ik_B)z_S\}}{2\beta(k_z+ik_B)}\;T_B(k_x,k_y)$$

$$\left.+\frac{(k_z-ik_B)\exp\{-i(k_z+ik_A)z_B\}}{2\beta(k_z+ik_A)}\;T_A(k_x,k_y)\right] \quad ,$$

$$\vec{L_A}(\vec{k}) = E_0\,\hat{x}\cdot\vec{k}\;(\vec{k}\times\hat{z})\,\frac{(k_z-ik_A)}{2\beta(k_z+ik_B)} \tag{4.46}$$

$$\times\ [\exp\{-i(k_z+ik_B)z_S\} - \exp\{-i(k_z+ik_B)z_B\}]\;Z_A(k_x,k_y) \quad ,$$

and

$$\vec{L_B}(\vec{k}) = E_0\,\hat{x}\cdot\vec{k}\;(\vec{k}\times\hat{z})\,\frac{(k_z-ik_B)}{2\beta(k_z+ik_A)}\;[\tag{4.47}$$

$$\times\ [\exp\{-i(k_z+ik_A)z_S\} - \exp\{-i(k_z+ik_A)z_B\}]\;Z_B(k_x,k_y) \quad ,$$

where

$$\begin{bmatrix} Z_A(k_x,k_y) \\ Z_B(k_x,k_y) \end{bmatrix} = \bar{N}\begin{bmatrix} k_A\exp(-k_A z_S)\;T_B(k_x,k_y) \\ k_B\exp(-k_B z_B)\;T_A(k_x,k_y) \end{bmatrix} \quad . \tag{4.48}$$

Note that T_F is just an inverse Fourier transform.

5. Two different methods for a general solution

5.1 The solution in rectilinear coordinates

This method is based on the separation of variables in a rectilinear coordinate system, and its final stages make use of partial Fourier transforms. The final result is presented in the form of a partial Fourier transform, and is somewhat easier to convert into a full Fourier transform than into the untransformed equivalent; for this reason, this method is recommended over the other if one wishes to calculate the magnetic effects associated with a front, as it interfaces more cleanly into the mathematics of section 2.2 than does the other method.

We start with the homogeneous equation for any order,

$$\nabla^2\phi(\vec{x}) + f(z)\,\frac{\partial\phi(\vec{x})}{\partial z} = 0 \quad , \tag{5.1}$$

and assume that ϕ separates as

$$\phi(\vec{x}) = V(z)\,H(x,y) \quad . \tag{5.2}$$

Some work then gives the equations

$$\frac{d^2V(z)}{dz^2} + f(z)\,\frac{dV(z)}{dz} - k^2\,V(z) = 0 \tag{5.3}$$

and

$$\nabla_h^2 H(x,y) + k^2\,H(x,y) = 0 \quad , \tag{5.4}$$

where k^2 and $V(z)$ are an eigenvalue and the associated eigenfunction of equation (5.3) under the boundary conditions

$$\left.\frac{dV(z)}{dz}\right|_{z=z_B} = \left.\frac{dV(z)}{dz}\right|_{z=z_S} = 0 \quad , \tag{5.5}$$

derived from the criteria that for all orders $\hat{z}\cdot\nabla\phi$ must be zero at the ocean bottom at z_B and the ocean surface at z_S. For convenience of notation we label the *nth* eigenvalue and its associated functions k_n^2, $V_n(z)$, and $H_n(x,y)$. If orthogonality can be demonstrated for the V_n, then they may be used in the construction of the final solution; that the other requirement of completeness is satisfied is suggested by the observation that equation (5.1) under the boundary conditions (5.5) should have an infinite number of discrete solutions, which should form a complete set if they are orthogonal to each other.

To demonstrate the mutual orthogonality of the $V_n(z)$, we first note that, according to the definition of f(z) in section 2.1,

$$\frac{d\sigma_0(z)}{dz} = f(z)\,\sigma_0(z) \quad . \tag{5.6}$$

Letting a prime denote differentiation with respect to z, we observe that

$$\begin{aligned} \frac{d}{dz}\,(V_m\sigma_0 V_n') &= V_m'\sigma_0 V_n' + fV_m\sigma_0 V_n' + V_m\sigma_0 V_n'' \\ &= V_m'\sigma_0 V_n' + V_m\sigma_0\,(V_n'' + fV_n') \\ &= V_m'\sigma_0 V_n' + k_n^2\,V_m\sigma_0 V_n \end{aligned} \tag{5.7}$$

by (5.3); given this, we then have that

$$\frac{d}{dz}\,(V_m\sigma_0 V_n' - V_m'\sigma_0 V_n) = (k_n^2 - k_m^2)\,V_m\sigma_0 V_n \quad , \tag{5.8}$$

and hence

$$(k_n^2 - k_m^2)\int_{z_B}^{z_S} \sigma_0(z)V_m(z)V_n(z)\,dz = \sigma_0(z)\,[V_m(z)V_n'(z) - V_m'(z)v_n(z)]\,\Big|_{z_B}^{z_S} = 0 \tag{5.9}$$

by (5.5). Therefore, we have that

$$\int_{z_B}^{z_S} \sigma_0(z)V_m(z)V_n(z)\,dz = \delta_{mn}\,I_n \quad , \tag{5.10}$$

where δ_{mn} is in this case the Kronecker delta, and

$$I_n = \int_{z_B}^{z_S} \sigma_0(z)V_n^2(z)\,dz \quad . \tag{5.11}$$

We now turn to the nonhomogeneous equation,

$$\nabla^2\phi(\vec{r}) + f(z)\,\frac{\partial\phi(\vec{r})}{\partial z} = p(\vec{r}) \quad . \tag{5.12}$$

If we define the partial Fourier transforms

$$\phi(\vec{r}) = \int_{-\infty}^{\infty} dk_x \int_{-\infty}^{\infty} dk_y\; F(k_x,k_y,z)\,\exp[i(k_x x + k_y y)] \tag{5.13}$$

and

$$p(\vec{x}) = \int_{-\infty}^{\infty} dk_x \int_{-\infty}^{\infty} dk_y \; P(k_x, k_y, z) \exp\{i(k_x x + k_y y)\} \quad , \tag{5.14}$$

then equation (5.12) is transformed into

$$\frac{\partial^2 F}{\partial z^2} + f(z) \frac{\partial F}{\partial z} - k^2 F = P \quad , \tag{5.15}$$

where

$$k^2 = k_x^2 + k_y^2 \quad ; \tag{5.16}$$

equation (5.15) may be solved through the construction and use of a Green's function G such that

$$F(k_x, k_y, z) = \int_{z_B}^{z_T} G(z, z', k) \; P(k_x, k_y, z') \, dz' \quad . \tag{5.17}$$

The appropriate equation for G is

$$\frac{\partial^2}{\partial z^2} G(z, z', k) + f(z) \frac{\partial}{\partial z} G(z, z', k) - k^2 G(z, z', k) = \delta(z - z') \quad ; \tag{5.18}$$

following a line of reasoning similar to that used to demonstrate the mutual orthogonality of the V_n, we observe that

$$\frac{\partial}{\partial z} (V_n \sigma_0 G' - V_n' \sigma_0 G) = V_n(z) \, \sigma_0(z) \, G(z, z', k) \, (k^2 - k_n^2) \tag{5.19}$$

$$- V_n(z) \, \sigma_0(z) \, \delta(z - z') \quad ,$$

where a prime again denotes differentiation with respect to z, and hence

$$0 = (k^2 - k_n^2) \int_{z_B}^{z_T} \sigma_0(z) V_n(z) G(z, z', k) \, dz + \sigma_0(z') V_n(z') \quad , \tag{5.20}$$

which has the solution

$$G(z, z', k) = \frac{1}{(k_n^2 - k^2)} \frac{V_n(z)}{I_n} \sigma_0(z') V_n(z') + C(z, z', k) \quad , \tag{5.21}$$

where C is any function orthogonal to $V_n(z)$. On the basis of symmetry we guess that

$$G(z,z',k) = \sum_{n=0}^{\infty} \frac{1}{(k_n^2 - k^2)} \frac{V_n(z)}{I_n} \sigma_0(z') V_n(z') \quad , \tag{5.22}$$

and test this by substituting it back into equation (5.18) to get

$$\sum_{n=0}^{\infty} \frac{\sigma_0(z') V_n(z') V_n(z)}{I_n} = \delta(z-z') \quad ; \tag{5.23}$$

this is in fact the expression that one gets by using (5.10) to do a series expansion of $\delta(z-z')$ in the $V_n(z)$, indicating that (5.22) is the correct expression for G.

Accordingly, we have from (5.17) that

$$F(k_x,k_y,z) = \sum_{n=0}^{\infty} \frac{V_n(z)}{(k_n^2 - k^2) I_n} Q_n(k_x,k_y) \quad , \tag{5.24}$$

where

$$Q_n(k_x,k_y) = \int_{z_B}^{z_S} \sigma_0(z) V_n(z) P(k_x,k_y,z)\, dz \quad . \tag{5.25}$$

If $\Phi(\vec{k})$ is the full Fourier transform of $\phi(\vec{r})$, then we have that

$$\Phi(\vec{k}) = \int_{-\infty}^{\infty} F(k_x,k_y,z)\, e^{ik_z z}\, dz \quad , \tag{5.26}$$

the evaluation of which amounts to replacing the $V_n(z)$ in (5.24) with their Fourier transforms. If we calculate $\phi(\vec{r})$ from (5.24) by a two-dimensional inverse Fourier transform of F, we get

$$\phi(\vec{r}) = \sum_{n=0}^{\infty} \frac{V_n(z)}{I_n} K_n(x,y) \quad , \tag{5.27}$$

$$K_n(x,y) = \int_{-\infty}^{\infty} dx' \int_{-\infty}^{\infty} dy' \int_{z_B}^{z_S} dz'\, \sigma_0(z') V_n(z') L_n(x'-x, y'-y)\, p(x',y',z') \quad , \tag{5.28}$$

$$L_n(x,y) = \frac{1}{(2\pi)^2} \int_{-\infty}^{\infty} dk_x \int_{-\infty}^{\infty} dk_y \frac{\exp[i(k_x x + k_y y)]}{k_n^2 - k_x^2 - k_y^2} \tag{5.29}$$

$$= M(k_n x, k_n y) \quad ,$$

where

$$M(x,y) = \frac{1}{(2\pi)^2} \int_{-\infty}^{\infty} du \int_{-\infty}^{\infty} dv \frac{\exp[i(ux+vy)]}{1-u^2-v^2} \quad , \tag{5.30}$$

which reduces, with transformation to polar coordinates followed by integration over all angles, to

$$M(x,y) = \frac{1}{2\pi} \int_0^\infty \frac{k}{1-k^2} J_0(k\rho)\, dk \quad , \tag{5.31}$$

where

$$\rho^2 = x^2 + y^2 \quad . \tag{5.32}$$

Making use of the identities

$$H_n^{(1)}(-z) = -(-1)^n H_n^{(2)}(z) \tag{5.33}$$

$$H_n^{(2)}(-z) = -(-1)^n H_n^{(1)}(z) \quad , \tag{5.34}$$

where

$$H_n^{(1)}(z) = J_n(z) + i N_n(z) \tag{5.35}$$

$$H_n^{(2)}(z) = J_n(z) - i N_n(z) \quad , \tag{5.36}$$

we find that

$$\int_{-\infty}^{\infty} \frac{k}{1-k^2} H_0^{(2)}(k\rho)\, dk = 2 \int_0^\infty \frac{k}{1-k^2} J_n(k\rho)\, dk \quad , \tag{5.37}$$

giving from equation (5.31)

$$M(x,y) = \frac{1}{4\pi} \int_{-\infty}^{\infty} \frac{k}{1-k^2} H_0^{(2)}(k\rho)\, dk \quad ; \tag{5.38}$$

this may be evaluated by contour integration, closing the contour in the lower half plane and excluding the pole at the origin as a nonphysical mathematical artifact, to give

$$M(x,y) = -1/4\, N_0(\rho) \quad . \tag{5.39}$$

The calculation of $\phi(\vec{x})$ from F is somewhat more tedious than the calculation of $\Phi(\vec{k})$, involving two-dimensional convolution integrals as opposed to one-dimensional Fourier transforms.

5.2 The solution in cylindrical coordinates

This method is based on separation of variables in a cylindrical coordinate system, and makes heavy use of Bessel transforms. For the final result, $\phi(\vec{r})$ is presented, in cylindrical coordinates, as a series of Bessel functions of the second kind. Disadvantages of this method are that it is practically suited only for electrical conductivity perturbation distributions localized about the origin, since an extended distribution requires more terms in the series expansion than does a localized one, that large numbers of terms are necessary to adequately describe the electric field close to the origin, since successively higher order terms in the expansion for ϕ tend to be progressively more concerned with the field in the neighborhood of the origin and less with the field at great distances, and that using this method to calculate magnetic effects is more involved than using the method discussed in the last section; balanced against this is the availability of numerically swift algorithms for computing Bessel transforms (Anderson, 1979; Chave, 1983). Accordingly, this method is at its best in computing the electric field associated with a localized electrical conductivity variation, particularly the field at large distances from this variation.

We start by assuming the separation

$$\phi(\rho,\theta,z) = V(z)\, H(\rho,\theta) \quad , \tag{5.40}$$

which, when substituted into the homogeneous equation (5.1) yields for V and H

$$\frac{d^2V(z)}{dz^2} + f(z)\,\frac{dV(z)}{dz} - k^2\, V(z) = 0 \tag{5.41}$$

and

$$\nabla_h^2 H(\rho,\theta) + k^2\, H(\rho,\theta) = 0 \quad ; \tag{5.42}$$

the boundary conditions on ϕ, that $\hat{z}\cdot\nabla\phi=0$ at the ocean bottom at z_B and the ocean surface at z_S, give that

$$\left.\frac{dV(z)}{dz}\right|_{z=z_B} = \left.\frac{dV(z)}{dz}\right|_{z=z_S} = 0 \quad , \tag{5.43}$$

serving to restrict solutions of (5.41) to discrete eigenvalues k_n^2 and associated eigenvalues $V_n(z)$. We observe that (5.41) and (5.43) are identical in form to (5.3) and (5.5) respectively in the previous section, indicating that the eigenfunction orthogonality arguments made there can be extended to the work of this section.

We then define the transforms

$$\phi(\rho,\theta,z) = \sum_{m=0}^{\infty} \int_0^{\infty} k\, dk\, F_m(z,k)\, e^{im\theta}\, J_m(k\rho) \tag{5.44}$$

and

$$p(\rho,\theta,z) = \sum_{m=0}^{\infty} \int_0^{\infty} k\, dk\, P_m(z,k)\, e^{im\theta}\, J_m(k\rho) \tag{5.45}$$

and their inverse transforms

$$F_m(z,k) = \frac{1}{2\pi} \int_0^{\infty} \rho\, d\rho \int_0^{2\pi} d\theta\, \phi(\rho,\theta,z)\, e^{-im\theta}\, J_m(k\rho) \tag{5.46}$$

and

$$P_m(z,k) = \frac{1}{2\pi} \int_0^{\infty} \rho\, d\rho \int_0^{2\pi} d\theta\, p(\rho,\theta,z)\, e^{-im\theta}\, J_m(k\rho) \quad , \tag{5.47}$$

where ϕ and p are as in equation (5.12). Substituting expressions (5.44) and (5.45) into equation (5.12) and using the identity

$$\nabla_h^2\, e^{im\theta} J_m(k\rho) = -\, k^2\, e^{im\theta} J_m(k\rho) \tag{5.48}$$

gives the equation

$$\frac{\partial^2}{\partial z^2} F_m(z,k) + f(z)\, \frac{\partial}{\partial z} F_m(z,k) - k^2\, F_m(z,k) = P_m(z,k) \quad , \tag{5.49}$$

which is seen to have the same form as equation (5.15) in the previous section.

Because of the observed similarities between the work of this section and that of section 4.1, we can immediately write

$$F_m(z,k) = \int_{z_B}^{z_S} G(z,z',k)\, P_m(z',k\, dz') \quad , \tag{5.50}$$

where G is as given by equation (5.22), and hence

$$F_m(z,k) = \sum_{n=0}^{\infty} \frac{1}{(k_n^2 - k^2)}\, \frac{V_n(z)}{I_n}\, K_{nm}(k) \quad , \tag{5.51}$$

where

$$K_{nm}(k) = \int_{z_B}^{z_S} \sigma_0(z)\, V_n(z)\, P_n(z,k)\, dz \quad . \tag{5.52}$$

Substituting (5.51) back into the transform (5.44) then gives

$$\phi(\rho,\theta,z) = \sum_{m=0}^{\infty} \sum_{n=0}^{\infty} \frac{V_n(z)}{I_n} e^{im\theta} L_{nm}(\rho) \tag{5.53}$$

where

$$L_{nm}(\rho) = \int_0^{\infty} k\, dk\, \frac{K_{nm}(k)}{k_n^2 - k^2} J_m(k\rho) \quad . \tag{5.54}$$

We can use the identities (5.33) through (5.36) in section 4.1 together with the observation that

$$K_{nm}(-k) = (-1)^m K_{nm}(k) \tag{5.55}$$

to demonstrate that

$$L_{nm}(\rho) = \tfrac{1}{2} \int_{-\infty}^{\infty} k\, dk\, \frac{K_{nm}(k)}{k_n^2 - k^2} H_m^{(2)}(k\rho) \quad , \tag{5.56}$$

which may be evaluated by contour integration, closing the contour in the lower half plane and detouring the section along the real axis below the origin, to get

$$L_{nm}(\rho) = -\pi K_{nm}(k_n) N_m(k_n\rho) \quad . \tag{5.57}$$

Note that each of the K_{nm} need be evaluated for only a single value of k in these calculations.

References

Abramowitz, M., and I. R. Stegun, *Handbook of Mathematical Functions*, Dover Publications, New York, 1965.

Anderson, W. L., "Numerical integration of related Hankel transforms of orders 0 and 1 by adaptive digital filtering", Geophysics, 44, 1287-1305, 1979.

Chave, A., "Numerical integration of related Hankel transforms by quadrature and continued fraction expansion", Geophysics (in press, to be released in December 1983).

Cox, C. S., J. H. Filloux, and J. C. Larson, "Electromagnetic studies of ocean currents and electrical conductivity below the ocean-floor", *The Sea*, v. 4, pt. 1, Maxwell (ed.), Wiley-Interscience, 1970.

Cox, C. S., and H. Sandstrom, "Coupling of internal and surface waves in water of variable depth", J. Oceano. Soc. Japan, 20*th* Anniv. Vol., 499-513, 1962.

CRC (The Chemical Rubber Company), *Standard Mathematical Tables*, 14*th* Edition, The Chemical Rubber Company, 1965.

Crews, A., and J. Futterman, "Geomagnetic micropulsations due to the motion of ocean waves", J. Geophys. Res., 67, 299-306, 1962.

Eckart, C. H., *Hydrodynamics of Oceans and Atmospheres*, Permagon Press, New York, 290 pp., 1960.

Erdélyi, A., W. Magnus, F. Oberhettinger, and F. G. Tricomi (editors), *Tables of Integral Transforms* (2 volumes), Mc Graw-Hill Book Company, Inc., 1954.

Erdélyi, A., W. Magnus, F. Oberhettinger, and F. G. Tricomi (editors), *Higher Transcendental Functions* (3 volumes), Mc Graw-Hill Book Company, Inc., 1955.

Forsythe, G. E., and W. R. Wasow, *Finite Difference Methods for Partial Differential Equations*,

Wiley and Sons, New York and London, 444 pp., 1960.

Gordon, R. L., *Internal Wave Climate Near the Coast of Northwest Africa during JOINT 1*, University of California at San Diego, 1977.

Grobner, W. and N. Hofreiter, *Integraltafel*, Part 2, Springer-Verlag, Wein and New York, 1966.

Lamb, H., *Hydrodynamics* (*6th* ed.), Dover Publications, New York, pp. 738, 1945.

Larson, R. L., P. A. Larson, J. D. Mudie, and F. N. Spiess, "Models of near bottom magnetic anomalies on the East Pacific Rise crest at 21°N.", J. Geophys. Res., 79,, 2686-2689, 1974.

Osborne, A. R., "Internal solitons in the Andaman Sea", Science, 208, 451-460, 1980.

Reitz, J. R., and F. J. Milford, *Foundations of Electromagnetic Theory*, Addison-Wesley Publishing Company, 1967.

Sommerfeld, A., *Mechanics of Deformable Bodies*, Academic Press, New York and London, 396 pp., 1971.

Vacquier, V., *Geomagnetism in Marine Geology*, Elsevier Publ. Co., Amsterdam and New York, pp.185, 1972.

Warburton, F., and R. Caminiti, "The induced magnetic field of sea waves", J. Geophys. Res., 69, 4311-4318, 1964.

Weaver, J. T., "Magnetic variations associated with ocean waves and swell", J. Geophys. Res., 70, 1921-1929, 1965.